

MASTER

In-plane stability of non-orthogonal asymmetrical steel frames

Bloemberg, E.S.

Award date:
2011

[Link to publication](#)

Disclaimer

This document contains a student thesis (bachelor's or master's), as authored by a student at Eindhoven University of Technology. Student theses are made available in the TU/e repository upon obtaining the required degree. The grade received is not published on the document as presented in the repository. The required complexity or quality of research of student theses may vary by program, and the required minimum study period may vary in duration.

General rights

Copyright and moral rights for the publications made accessible in the public portal are retained by the authors and/or other copyright owners and it is a condition of accessing publications that users recognise and abide by the legal requirements associated with these rights.

- Users may download and print one copy of any publication from the public portal for the purpose of private study or research.
- You may not further distribute the material or use it for any profit-making activity or commercial gain

IN-PLANE STABILITY OF NON-ORTHOGONAL ASYMMETRICAL STEEL FRAMES

A thesis submitted to the Department of Architecture, Building and
Planning of Eindhoven University of Technology in partial fulfillment of the
requirements for the degree of Master of Science

IN-PLANE STABILITY OF NON-ORTHOGONAL ASYMMETRICAL STEEL FRAMES

Author:

E.S. Bloemberg
0638406

Graduation committee:

prof. ir. H.H. Snijder
prof. dr. ir. J.G.M. Kerstens
dr. ir. J. Maljaars

July 2011

Eindhoven University of Technology
Department: Architecture, Building and Planning
Unit: Structural Design and Construction Technology

Report number: A-2011-12
O-2011-11

Preface

This report has been written to finish my study for the degree of Master of Science at Eindhoven University of Technology. The research involved was carried out at the Faculty of Architecture, Building and Planning for the Unit Structural Design and Construction Technology.

I thank prof.ir. H.H. Snijder, chairman of the graduation committee, for providing this research subject. Furthermore, I thank him for the pleasant supervision during this project and his advice in the field of steel structures and the related Eurocode 3 about the general rules for designing steel structures. His advice was very helpful and gave me more insight in the features of steel and the use of Eurocode 3.

Also, I thank prof.dr.ir. J.G.M. Kerstens for his advice in structural mechanics during this project. Especially his advice in Linear Buckling Analysis was very helpful in the beginning of this project.

Finally I thank dr.ir. J. Maljaars, researcher at TNO Delft and secretary of the Technical Committee 8 of Bouwen met Staal about structural stability in steel, for his enthusiasm and critical remarks during this project.

Eeuwe Bloemberg

Eindhoven, July 2011

Table of contents

Preface	V
Table of contents	VII
Summary	XI
Nomenclature	XV
1. Introduction	1
1.1 Problem definition.....	1
1.2 Assignment.....	2
1.3 Objectives.....	2
1.4 Structure of report	2
2. State of the Art	5
2.1 Critical buckling loads	5
2.1.1 Columns with rotational springs.....	5
2.1.2 Symmetrical pitched-roof frames	7
2.2 Ultimate bearing capacities	13
3. Critical buckling loads of non-orthogonal asymmetrical steel frames.....	15
3.1 Differential equation of equilibrium applied to frame 1	15
3.1.1 Introduction to separate column approach	15
3.1.2 Boundary conditions	17
3.1.3 Influence of compression forces in the beam on the critical buckling load.....	21
3.1.4 Example	23
3.1.5 Discussion.....	25
3.2 Betti's theorem	26
3.2.1 Introduction into Betti's Theorem	26
3.2.2 Application of Betti's theorem to buckling analysis.....	27
3.2.3 Example of a one degree of freedom system.....	29
3.2.4 Example of a more degrees of freedom system.....	30
3.3 Kinematic models	31
3.4 Influence of an axial force in the beam on the critical buckling load.....	33
3.4.1 Decrease in critical buckling load for symmetrical pitched-roof frames.....	33
3.4.2 Approach to determine the decrease in critical buckling load for frame 2.....	36
3.4.3 Applicability of the approach developed for frame 2.....	37
3.4.4 Refinement of the approach for frame 2	38
3.4.5 Approach to determine the decrease in critical buckling load for frame 1	41
3.4.6 Applicability of the approach developed for frame 1.....	41
3.5 Conclusions	48

4.	Ultimate bearing capacities of trapezoidal frames	49
4.1	Analysis overview	49
4.2	Material properties	51
4.3	Imperfections	51
4.4	GMNIA 1 using initial sway and bow imperfections	55
4.5	GMNIA 2 using unique initial sway and bow imperfections	62
4.6	GMNIA results	64
4.6	Discussion and conclusions	66
5.	Stability checks according to Eurocode 3	69
5.1	Overview of checks	69
5.2	Stability checks for non-sway frames	69
5.2.1	Check 1: First order analysis and non-sway buckling lengths	69
5.2.2	Check 2: Second order analysis	69
5.3	Stability checks for sway frames	70
5.3.1	Check 3: First order analysis and sway buckling lengths	70
5.3.2	Check 4: First order analysis with amplified sway moments and non-sway buckling lengths	70
5.3.2	Check 5: Second order analysis and non-sway buckling lengths	70
5.4	Stability checks according to section 6.3 of Eurocode 3	71
5.5	Cross section resistance check according to Eurocode 3	73
5.6	Classification of the considered trapezoidal frames	73
5.7	Overview results	75
5.8	Conclusions	76
6.	Conclusions and recommendations	79
6.1	Conclusions	79
6.1.1	Critical buckling loads	79
6.1.2	Ultimate bearing capacity and stability checks	79
6.2	Recommendations	79
6.2.1	Critical buckling loads	79
6.2.2	Stability checks	80
7.	References	81
	Appendix A – Derivation of the stability criterion for columns with rotational springs	83
	Appendix B - Derivation of the rotational spring stiffness of symmetrical pitched-roof frames	85
	Appendix C – Critical buckling loads according to Silvestre and Camotim	89
	Appendix D – Calculation of a kinematic model with four degrees of freedom	91
	Appendix E - Finite element modeling	95
	E.1 Element type	95

E.2 Cross sections	96
E.3 Linear Buckling Analysis.....	97
E.3.1 Analysis method of FEM software.....	97
E.3.2 Number of elements and mesh density.....	98
E.4 Geometric and Material Non-Linear Analysis	100
E.4.1 Number of elements and mesh density.....	100
E.4.2 Other preprocessing parameters.....	101
E.5 Input files Ansys.....	102
E.5.1 LBA of frame 1.....	102
E.5.2 LBA of frame 2.....	104
E.5.3 Ultimate bearing capacity using sway and bow imperfections.....	106
E.5.3 Ultimate bearing capacity using the buckling shape as a unique sway and bow imperfections.....	109
E.5.5 Second order analysis including initial bow imperfections	112
E.5.6 Second order analysis including initial sway imperfections.....	114
Appendix F – Eurocode 3 checks.....	117

Summary

Introduction

In non-orthogonal asymmetrical steel frames, a compression force will be introduced in the beam due to the load distribution. This compression force causes that the columns will be less supported by the beam. This effect and the geometry of non-orthogonal asymmetrical frames make it hard to determine critical buckling lengths for the members.

This research is focused on 2 objectives. The first objective of this research is to obtain accurate approximations of critical buckling lengths for non-orthogonal asymmetrical frames using Linear Buckling Analysis (LBA). Two frames are investigated for this research. The first frame is an asymmetric pitched-roof frame as shown in figure 1 and the second frame is a non-orthogonal trapezoidal frame as shown in figure 2. Column lengths and beam lengths as well as flexural rigidities are variable for both frames. For LBA the frames will be loaded by a uniformly distributed load over the span.

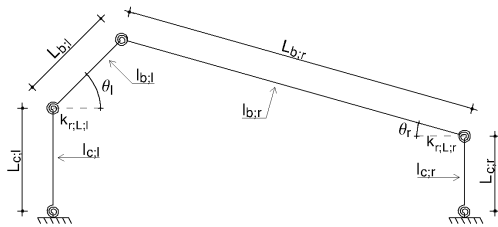


Figure 1: Asymmetric pitched-roof frame

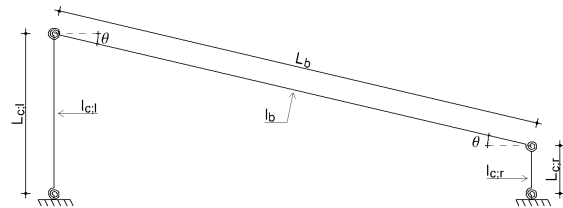


Figure 2: Non-orthogonal trapezoidal frame

The second objective is to verify or falsify the stability checks in Eurocode 3 using Geometric and Material Non-Linear Analyses (GMNIA) for the non-orthogonal trapezoidal frame in figure 2.

Linear Buckling Analysis

Critical buckling loads have been approximated in three different ways. The first method is using the differential equation of equilibrium. This method is applied to asymmetrical pitched-roof frames where each column is analyzed separately (see figure 3). This results in a critical buckling load for the left-hand column and a critical buckling load for the right-hand column. The lowest critical buckling load serves as overall critical buckling load of the columns and give safe results.

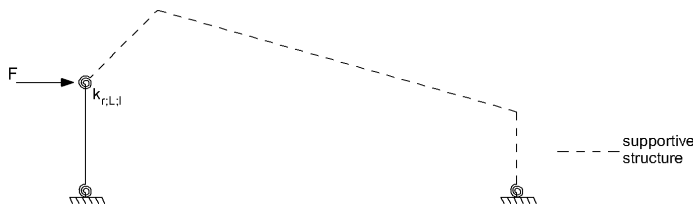


Figure 3: Left-hand column analyzed separately

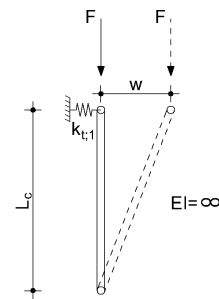


Figure 4: Kinematic model

By varying in geometry it has been concluded that the exchange in stability can not be accurately described using separate column approaches. For the investigated cases the maximum underestimation is 18%. Therefore, more research is recommended to describe the exchange in stability between the left side and the right side of frame more accurately.

The second and third methods for determining critical buckling loads are based on Betti's theorem and kinematic models.

Betti's theorem applied to buckling analysis yields errors that are less than 5% underestimated in critical buckling length [10].

Kinematic models consist of bars with an infinite flexural rigidity, the so called pendulum columns as shown in figure 4. From the equilibrium of these bars, critical buckling loads can be determined with the same accuracy as using Betti's theorem. For both Betti's theorem and kinematic models applies that, the more the buckling mode can be simulated by adding degrees of freedom, the more accurate the critical buckling load can be determined.

Due to compression forces in the beam the column will be less supported by the beam. This results in a decrease in critical buckling load for the columns. Betti's theorem and kinematic models are both methods in which the effects of compression forces in beams will not be taken into account. Therefore approaches have been developed and the accuracy of these approaches has been investigated for the two considered frames. Only cases are considered with hinges at the base and fixed connections between the members.

For the investigated cases of the asymmetrical pitched-roof frames the maximum overestimation in critical buckling load will not be greater than 6%, provided that the critical buckling load without an axial force in the beam is exactly determined. The maximum underestimation will not be greater than 12%. For the non-orthogonal trapezoidal frame, the maximum overestimation is 2% and the maximum underestimation is 3%. More research is recommended to investigate the decrease in critical buckling load for other type connections.

Stability checks according to Eurocode 3

The ultimate bearing capacities for different considered non-orthogonal trapezoidal frames have been calculated using GMNIA for performing stability checks. Imperfections which are modeled using scaling the first order buckling mode give for all cases the lowest ultimate bearing capacity.

According to Eurocode 3, two different analyses exist: analysis according to non-sway frames and analysis according to sway frames.

The non-sway frames are analyzed using two checks.

1. First order elastic analysis and stability checks using non-sway buckling lengths.
2. Second order elastic analysis including initial bow imperfection and no stability check

The sway frames are analyzed using three checks.

3. First order elastic analysis and stability checks using sway buckling lengths
4. First order elastic analysis with amplified sway moments and stability checks using non-sway buckling lengths.
5. Second order elastic analysis including initial sway imperfections and stability checks using non-sway buckling lengths.

Besides the stability checks, the resistance of the cross-section should also be checked according to the requirements of Eurocode 3.

In general, frames which are analyzed as non-sway frames will exceed the cross-section resistance check and not the stability check. For the cases which are defined as sway-frames the checks using sway buckling lengths (check 3) results for all cases in safe but conservative results.

The results of check 4 differ not significantly from the results of check 5. Both checks are based on the same analysis methodology: sway imperfections will be included in the design forces and stability checks are based on non-sway buckling lengths. By increasing the slope of the beam, the results become unsafe.

In Eurocode 3 it is not described if for sway frames with stability checks using non-sway buckling lengths (check 4 and 5), either the equivalent uniform moment factor C_{my} belongs to the definition sway or non-sway buckling modes. For these type of checks, C_{my} is determined twice, once using a non-sway buckling mode and once using a sway buckling mode. From the results it is recommended

to use an equivalent uniform moment factor C_{my} of 0,9 (sway buckling mode). This uniform moment factor gives in general more safe and accurate results especially for the columns.

Nomenclature

A	area of the cross section
A_b	integration constant of the beam
A_c	integration constant of the column
b	width of the cross section
B_b	integration constant of the beam
B_c	integration constant of the column
C	amplification factor
C_b	integration constant of the beam
C_c	integration constant of the column
C_{as}	amplification factor for anti-symmetrical sway
C_{ss}	amplification factor for symmetrical sway
C_{my}	equivalent uniform moment factor
C_{mz}	equivalent uniform moment factor
C_{mLT}	equivalent uniform moment factor
D_b	integration constant of the beam
D_c	integration constant of the column
E	modulus of elasticity
EI	flexural rigidity
EI_b	flexural rigidity of the beam
$EI_{b;l}$	flexural rigidity of the left beam
$EI_{b;r}$	flexural rigidity of the right beam
$EI_{b;m}$	mean flexural rigidity of the beam for asymmetrical pitched-roof frames
$EI_{c;l}$	flexural rigidity of the left column
$EI_{c;r}$	flexural rigidity of the right column
$EI \cdot \eta^{*'}_{cr}$	bending moment due to η_{cr} at the critical cross section
f_y	yield strength
F	force
F_b	beam force
F_c	column force
F_{cr}	critical buckling load
$F_{cr;b}$	critical buckling load of the beam
$F_{cr;c}$	critical buckling load of the column
F_{Ed}	design load
F_p	force which creates a mechanism according to the first order theory of plasticity
F_{ult}	ultimate bearing capacity
h	height of the cross section
h_s	storey height
H	lateral load
H_{Ed}	design value of the horizontal reaction at the bottom of the storey to the horizontal loads and fictitious loads
I_y	moment of inertia about y-y axis
I_b	moment of inertia of the beam
$I_{b;l}$	moment of inertia of the left beam
$I_{b;r}$	moment of inertia of the right beam
I_c	moment of inertia of the column
$I_{c;l}$	moment of inertia of the left column
$I_{c;r}$	moment of inertia of the right column

k	rotational spring stiffness
$k_{r;0}$	rotational spring stiffness at the bottom of the column
$k_{r;b}$	rotational spring stiffness due to the stiffness of the beam
$k_{r;con}$	rotational spring stiffness due to the connection between column and beam
$k_{r;L}$	rotational spring stiffness at the top of the column
$k_{t;b}$	translation spring stiffness at the top of asymmetrical pitched-roof frames
k_{yy}	interaction factor
k_{yz}	interaction factor
k_{zy}	interaction factor
k_{zz}	interaction factor
L_b	beam length
$L_{b;l}$	length of the left beam
$L_{b;r}$	length of the right beam
$L_{b,tot}$	overall length of the beam for asymmetrical pitched-roof frames ($L_{b;l} + L_{b;r}$)
L_c	column length
$L_{c;l}$	length of the left column
$L_{c;r}$	length of the right column
$L_{cr;b}$	critical buckling length of the beam
$L_{cr;c;l}$	critical buckling length of the left column
$L_{cr;c;r}$	critical buckling length of the right column
L_e	element length
L_s	length of the span
L_1	distance for determining $\Delta_{b;2}$
L_2	distance for determining $\Delta_{b;2}$
m	number of columns in a row
M	bending moment
$M_{b;l}$	bending moment in the left beam
$M_{b;r}$	bending moment in the right beam
$M_{c;Rd}$	design resistance for bending
M_{cr}	elastic critical moment for lateral-torsional buckling
M_{ex}	external bending moment
M_{in}	internal bending moment
$M_{N;Rd}$	design plastic moment resistance reduced due to axial forces
$M_{y;Ed}$	design bending moment about y-y axis
$M_{y;Rk}$	characteristic values of resistance to bending moments about y-y axis
$M_{z;Ed}$	design bending moment about z-z axis
$M_{z;Rk}$	characteristic values of resistance to bending moments about z-z axis
n	sample size
N_b	axial force in the beam
$N_{b;l}$	axial force in the left beam
$N_{b;r}$	axial force in the right beam
N_c	axial force in the column
$N_{c;l}$	axial force in the left column
$N_{c;r}$	axial force in the column
$N_{c;Rd}$	design resistance to axial forces
N_{cr}	critical buckling load
$N_{E;b}$	Euler load of the beam
$N_{E;c}$	Euler load of the column
N_{Ed}	design normal force

$N_{pl,Rd}$	design plastic resistance to axial forces
N_{Rk}	characteristic value of resistance to compression
q	uniformly distributed load
Q	load
Q_{cr}	critical buckling load
Q_{ult}	ultimate bearing capacity
s	scale factor
t_f	flange thickness
t_w	web thickness
$V_{b,R}$	reaction force
V_c	shear force in the column
V_e	shear force in element
V_{Ed}	design shear force
$V_{el,Rd}$	elastic design shear resistance
$V_{pl,Rd}$	plastic design shear resistance
w	deflection
w_0	initial deflection
w_b	beam deflection
w_c	column deflection
w_e	element deflection
w_u	deflection belonging to the ultimate elastic-plastic load
$W_{el,y}$	elastic moment of inertia about the y-y axis
$W_{pl,y}$	plastic moment of inertia about the y-y axis
\bar{X}	mean ratio
α	imperfection factor of the buckling curve
α_{cr}	factor by which the design loading would have to be increased to cause elastic instability
α_h	reduction factor for height h applicable to columns
α_m	reduction factor for the number of columns in a row
β	ratio of bending moments in the beam
β_{Δ}	critical buckling length factor for the decrease in critical buckling load for symmetrical pitched-roof frames
β_b	critical buckling length factor of the beam
$\beta_{b,l}$	critical buckling length factor of the left beam
$\beta_{b,r}$	critical buckling length factor of the right beam
β_c	critical buckling length factor of the column
$\beta_{c,l}$	critical buckling length factor of the left column
$\beta_{c,r}$	critical buckling length factor of the right column
γ	Rieckmann factor
γ_{M1}	partial factor for resistance of members to instability
δ	Rieckmann factor
δ_b	bow imperfection for the beam
$\delta_{c,l}$	bow imperfection for the left column
$\delta_{c,r}$	bow imperfection for the right column
$\Delta_{ANSYS,i}$	buckling mode displacement ratio in Ansys
$\Delta_{b,2}$	imperfection at the top of the buckling mode of the beam
$\Delta_{c,l}$	sway imperfection for the left column
$\Delta_{c,r}$	sway imperfection for the right column

ΔF_{cr}	decrease in critical buckling load
$\Delta F_{cr;ANSYS}$	decrease in critical buckling load given by Ansys
$\Delta F_{cr;calc}$	calculated decrease in critical buckling load
$\Delta F_{cr;l}$	calculated decrease in critical buckling load where the properties of the left column are taken into account
$\Delta F_{cr;r}$	calculated decrease in critical buckling load where the properties of the right column are taken into account
$\Delta M_{y,Ed}$	moments due to the shift of the centroidal y-y axis for class 4 sections
$\Delta M_{z,Ed}$	moments due to the shift of the centroidal z-z axis for class 4 sections
ε	strain
η_{cr}	shape of the elastic critical buckling mode
$\eta_{init;b}$	beam amplitude of elastic critical buckling mode
$\eta_{init;c;l}$	left column amplitude of elastic critical buckling mode
$\eta_{init;c;r}$	right column amplitude of elastic critical buckling mode
θ	slope of the beam
λ	multiplier of the compressive forces for obtaining critical buckling loads
$\bar{\lambda}$	inplane non dimensional slenderness calculated for the beam considered as hinged at its ends of the system length measured along the beams
$\bar{\lambda}_{LT}$	non-dimensional slenderness for lateral torsional buckling
σ	stress
φ	angle of rotation
φ_0	basic value for global initial sway imperfections
φ_A	angle of rotation of point A
Φ	value to determine the reduction factor χ
Φ_{LT}	value to determine the reduction factor χ_{LT}
χ	reduction factor for relevant buckling mode
χ_y	reduction factor due to flexural buckling about y-y axis
χ_z	reduction factor due to flexural buckling about z-z axis
χ_{LT}	reduction factor due to lateral torsional buckling
ψ	bending moment ratio

1. Introduction

1.1 Problem definition

In NEN 6770 [1] and NEN-EN 1993-1-1 (Eurocode 3) [2] it is described how to check the stability of steel bars loaded in compression and steel bars loaded in combined bending and compression using critical buckling lengths.

In literature, little information about the determination of critical buckling lengths for non-orthogonal asymmetrical frames is given. Much literature is limited to orthogonal frames and non-orthogonal symmetrical frames. Additional difficulty is that literature which gives possibilities to determine critical buckling lengths for non-orthogonal asymmetrical frames is limited to the case where no compression force in the beam occurs. However, in most cases a compression force will be introduced in the beam due to the load distribution as shown in figure 1.1

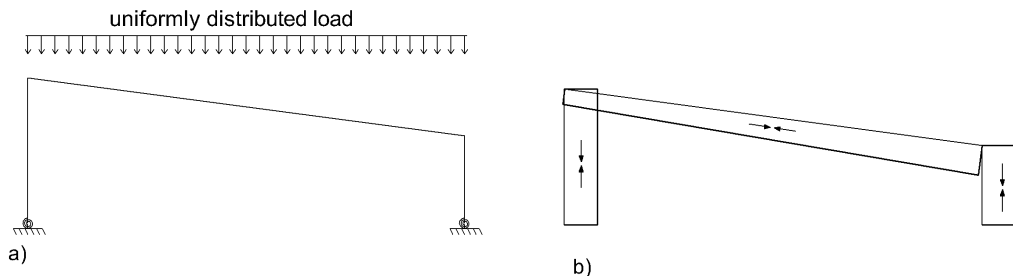


Figure 1.1: a) Non-orthogonal asymmetrical frame loaded by a uniformly distributed load b) Axial force distribution.

This compression force causes that the columns will be less supported by the beam. In mechanical terms the problem can be described as an increase in angle of rotation at the ends of the beam due to this compression force as shown in figure 1.2b. This results in a decrease of the rotational rigidity at the top of the column since the rotational rigidity depends on the bending moment and the angle of rotation as given in Eq. (1.1).

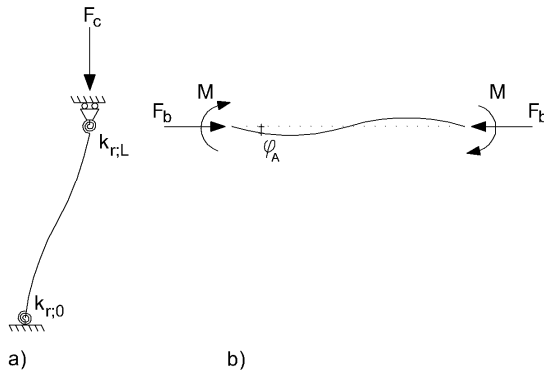


Figure 1.2: a) Buckling mode of a column with rotational springs b) Buckling mode of a beam where the angle of rotations at the ends of the beam are increased due to a compression force.

$$k_{r,L} = \frac{M}{\varphi_A} \tag{1.1}$$

When for buckling analysis the compression force in the beam is ignored, it results in an unsafe approximation due to an underestimation of the critical buckling length.

1.2 Assignment

Two non-orthogonal frames will be considered in this research. The first frame is an asymmetric pitched-roof frame with rotational springs and uniform members as shown in figure 1.3. For this frame, column lengths and beam lengths as well as flexural rigidities are variable.

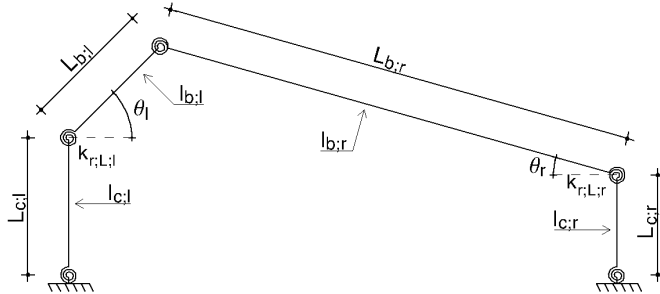


Figure 1.3: Frame 1: Asymmetric pitched-roof frame

The second frame to investigate is a trapezoidal frame with rotational springs and uniform members as shown in figure 1.4. This trapezoidal frame consists of two columns with different lengths and a single beam. Also for this frame, column lengths and beam lengths as well as flexural rigidities are variable.

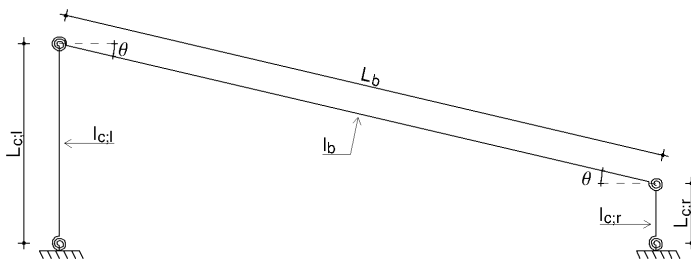


Figure 1.4: Frame 2: Non-orthogonal trapezoidal frame

For these two types of frames, critical buckling lengths will be approximated analytically using Linear Buckling Analyses (LBA). For LBA the frames will be considered as loaded by a uniformly distributed load over the span of the structure only.

Furthermore, the in-plane ultimate bearing capacity of non-orthogonal trapezoidal frames (frame 2) will be determined numerically by means of Geometric and Material Non-Linear Imperfect Analyses (GMNIA) according to the requirements of Eurocode 3. The results of these calculations will verify or falsify the applicability of different stability checks described in Eurocode 3.

1.3 Objectives

The two objectives of this research are:

- Obtaining accurate approximations of critical buckling lengths for the two described non-orthogonal frames using Linear Buckling Analysis (LBA).
- Verify or falsify different stability checks described in Eurocode 3 for trapezoidal frames using Geometric and Material Non-Linear Imperfect Analyses (GMNIA).

1.4 Structure of report

In chapter 2 a State of the Art is given, in which earlier investigations and information with respect to the subjects of this project are briefly described. Chapter 3 describes the analytical methods for approximating critical buckling lengths of both frames using LBA. Chapter 4 covers the determination of ultimate bearing capacities of trapezoidal frames according to Eurocode 3. Using these ultimate

bearing capacities different stability checks of Eurocode 3 will be verified or falsified in chapter 5. Finally, the conclusions and recommendations are given in chapter 6.

2. State of the Art

2.1 Critical buckling loads

Buckling can be described as the loss of structural stability due to compression loads. An analysis with which it is possible to obtain buckling loads is called Linear Buckling Analysis (LBA). In LBA critical buckling loads are determined for perfect structures (i.e. structures without imperfections) with linear elastic material behaviour [3]. An example is the critical buckling load in the case of flexural buckling of a column. By increasing an axial compression force on a perfect column, the deflection of the column changes, at a certain moment, from axial shortening to lateral deflection as shown in figure 2.1. A branching of two equilibrium paths occurs. The intersection point at which this branching occurs is defined as the bifurcation point and the load belonging to this bifurcation point is the critical buckling load (F_{cr}). Prior to the bifurcation point the column is in stable equilibrium and the deflection path is defined as the primary path. By reaching the bifurcation point, the deflection follows the secondary path and the column is in neutral equilibrium.

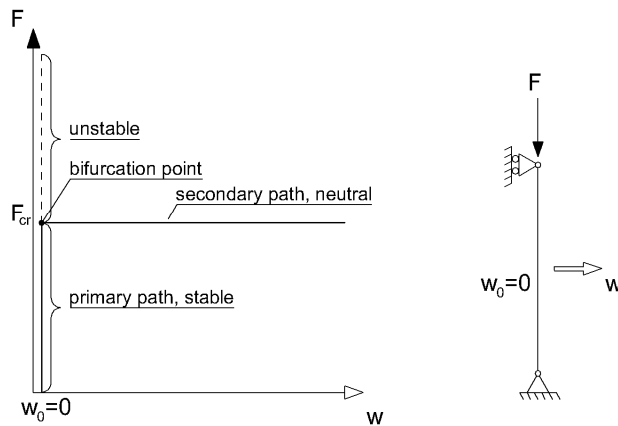


Figure 2.1: Load-deflection diagram of a bifurcation point for a perfect column

2.1.1 Columns with rotational springs

Columns in unbraced frames are typically examples of columns with rotational springs. The connection between column and beam gives rotational spring stiffnesses due to the flexural rigidity of the beam and the rotational rigidity of the connections.

Exact solutions of critical buckling loads for members with different end conditions can be obtained using LBA by deriving the buckling length from the differential equation of equilibrium [3,4]. Table 2.1 gives the stability criterion for columns with rotational springs at both ends and the derivation of this stability criterion (using the differential equation of equilibrium) is given in Appendix A.

This stability criterion gives the critical buckling loads, by solving α_c , expressed in:

$$F_{cr,c} = \alpha_c^2 \cdot EI_c \quad (2.1)$$

Table 2.1: Stability criterion for columns with rotational springs

Buckling shape	
Case	Spring-Spring
Stability criterion	$-\tan(\alpha_c \cdot L_c) + \frac{\zeta_0}{\alpha_c} + \frac{\zeta_L}{\alpha_c} + \frac{\tan(\alpha_c \cdot L_c) \cdot \zeta_0 \cdot \zeta_L}{\alpha_c^2} = 0$ <p>Where:</p> $\zeta_0 = \frac{k_{r,0}}{E I_c}, \quad \zeta_L = \frac{k_{r,L}}{E I_c} \quad \text{and} \quad \alpha_c^2 = \frac{F_c}{E I_c}$

The general critical buckling load formula derived by Euler is:

$$F_{cr;c} = \frac{\pi^2 \cdot E I_c}{(\beta_c \cdot L_c)^2}, \quad (2.2)$$

where β_c is the critical buckling length factor of the column and can be expressed as:

$$\beta_c = \frac{\pi}{\alpha_c \cdot L_c} \quad (2.3)$$

To determine the lowest critical buckling load for the orthogonal unbraced frame given in figure 2.2, the rotational spring stiffness $k_{r,0}$ is zero for a hinged connection and a fixed connection gives an infinite value of $k_{r,0}$.

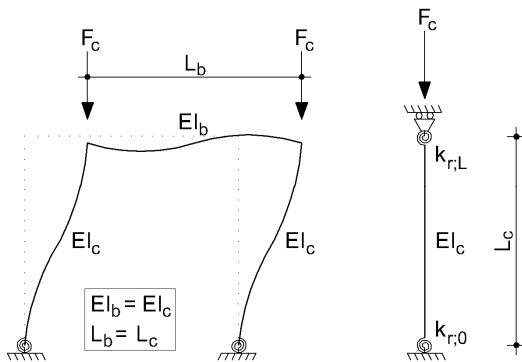


Figure 2.2: Unbraced frame with rotational springs at both ends

The rotational spring stiffness $k_{r,L}$ depends on the buckling shape of the beam. Assuming a rigid connection between column and beam, the angle of rotation at point A of figure 2.3 is:

$$\varphi_A = -\frac{M \cdot L_b}{6 \cdot EI_b} + \frac{M \cdot L_b}{3 \cdot EI_b} = \frac{M \cdot L_b}{6 \cdot EI_b} \quad (2.4)$$

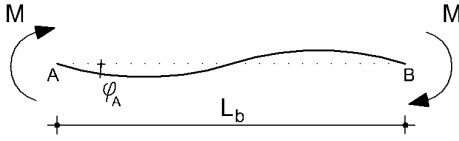


Figure 2.3: Deflected shape of the beam caused by moments

This gives a rotational stiffness $k_{r,L}$ of:

$$k_{r,L} = \frac{M}{\varphi_A} = \frac{6 \cdot EI_b}{L_b} \quad (2.5)$$

By considering a hinged connection at the bottom and a rigid connection between column and beam for the unbraced frame as given in figure 2.2, the values $\zeta_0=0$ and $\zeta_L=6/L_b$ have to be filled in, in the stability criterion of table 2.1. In the cases where the column lengths are equal to the beam length, a smallest root of $2,69911 \cdot 10^{-4}$ yields for α_c , which gives a critical buckling load of:

$$F_{cr;c} = (2,69911 \cdot 10^{-4})^2 \cdot EI_c \quad (2.6)$$

And a critical buckling length factor of:

$$\beta_c = \frac{\pi}{2,69911 \cdot 10^{-4} \cdot 5000} = 2,328 \quad (2.7)$$

The critical buckling load can then be written as:

$$F_{cr;c} = \frac{\pi^2 \cdot EI_c}{(2,328 \cdot L_c)^2} \quad (2.8)$$

2.1.2 Symmetrical pitched-roof frames

The rotational spring stiffness $k_{r,L}$ using Eq. (2.4) and (2.5), is applicable only when no compression force in the beam occurs. Rieckmann [6] developed a method that gives a better approximation of the critical buckling load when a compression force is introduced into the beam. He investigated a symmetric pitched-roof frame with symmetrical loads and hinged connections at the base as shown in figure 2.4. His investigation results in the determination of the parameters δ and γ , which then can be used to determine the critical buckling length factors for beam and column. Where:

$$\delta = \frac{EI_c \cdot L_b}{EI_b \cdot L_c}, \text{ and} \quad (2.9)$$

$$\gamma = \sqrt{\delta \cdot \frac{N_b \cdot L_b}{N_c \cdot L_c}} \quad (2.10)$$

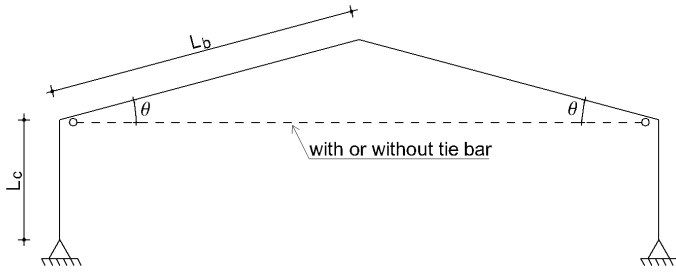


Figure 2.4: Symmetric pitched-roof frame investigated by Rieckmann [6]

Compression forces N_b and N_c can be obtained using a first order elastic analysis, where the average value of the compression force in the beam is decisive for Eq. (2.10).

Table 2.2 gives critical buckling length factors β_c and β_b , which can be determined using δ of Eq. (2.9) and γ of Eq. (2.10).

The critical buckling lengths of the column and beam can be obtained by multiplying the original length by β_c or β_b :

$$L_{cr;c} = \beta_c \cdot L_c \quad (2.11)$$

$$L_{cr;b} = \beta_b \cdot L_b \quad (2.12)$$

The critical buckling load for column and beam is then given by:

$$F_{cr;c} = \frac{\pi^2 \cdot EI_c}{L_{cr;c}^2}, \text{ and} \quad (2.13)$$

$$F_{cr;b} = \frac{\pi^2 \cdot EI_b}{L_{cr;b}^2} \quad (2.14)$$

Table 2.2: Critical buckling length factors

$\delta \backslash \gamma$	0.0000	0.500	1.000	1.500	2.000	2.500	3.000	4.000	6.000	8.000
0.200	2.133	2.138 4.276	2.156 2.156	2.205 1.470	2.347 1.174	2.672 1.069	3.109 1.036	4.064 1.016	6.037 1.006	8.026 1.003
0.600	2.391	2.402 4.805	2.440 2.440	2.522 1.681	2.680 1.340	2.949 1.179	3.316 1.105	4.194 1.048	6.112 1.019	8.080 1.010
1.000	2.635	2.649 5.298	2.695 2.695	2.786 1.858	2.943 1.471	3.185 1.274	3.511 1.170	4.325 1.081	6.188 1.031	8.134 1.017
1.500	2.917	2.933 5.867	2.984 2.984	3.078 2.052	3.229 1.614	3.448 1.379	3.740 1.247	4.489 1.122	6.284 1.047	8.202 1.025
2.000	3.179	3.196 6.391	3.247 3.247	3.341 2.227	3.485 1.742	3.689 1.475	3.956 1.319	4.651 1.163	6.382 1.064	8.271 1.034
2.500	3.423	3.439 6.879	3.491 3.491	3.583 2.388	3.720 1.860	3.912 1.565	4.160 1.387	4.811 1.203	6.481 1.080	8.340 1.043
3.000	3.652	3.668 7.336	3.719 3.719	3.808 2.539	3.940 1.907	4.121 1.649	4.354 1.451	4.968 1.242	6.580 1.097	8.411 1.051
3.500	3.868	3.884 7.768	3.934 3.934	4.020 2.680	4.147 2.074	4.320 1.728	4.540 1.513	5.122 1.281	6.680 1.113	8.481 1.060
4.000	4.073	4.089 8.178	4.137 4.137	4.221 2.814	4.344 2.172	4.509 1.804	4.719 1.573	5.273 1.318	6.781 1.130	8.553 1.069
4.500	4.268	4.284 8.568	4.332 4.332	4.413 2.942	4.531 2.266	4.690 1.876	4.891 1.630	5.421 1.355	6.881 1.147	8.625 1.078
5.000	4.456	4.471 8.942	4.517 4.517	4.597 3.064	4.711 2.356	4.864 1.945	5.057 1.686	5.565 1.391	6.982 1.164	8.697 1.087
5.500	4.636	4.651 9.301	4.696 4.696	4.773 3.182	4.884 2.442	5.031 2.013	5.217 1.739	5.707 1.427	7.082 1.180	8.769 1.096
6.000	4.809	4.824 9.647	4.868 4.868	4.943 3.295	5.051 2.525	5.193 2.077	5.373 1.791	5.846 1.461	7.183 1.197	8.842 1.105
6.500	4.976	4.991 9.981	5.034 5.034	5.107 3.405	5.212 2.606	5.351 2.140	5.525 1.842	5.982 1.495	7.283 1.214	8.915 1.114
7.000	5.138	5.152 10.305	5.195 5.195	5.266 3.511	5.368 2.684	5.503 2.201	5.672 1.891	6.115 1.529	7.382 1.230	8.989 1.124
7.500	5.296	5.309 10.619	5.351 5.351	5.420 3.614	5.520 2.760	5.651 2.260	5.815 1.938	6.246 1.561	7.481 1.247	9.062 1.133
8.000	5.448	5.462 10.923	5.502 5.502	5.570 3.714	5.668 2.834	5.796 2.318	5.955 1.985	6.374 1.593	7.580 1.263	9.136 1.142

Upper value: critical buckling length factor β_c for column
 Lower value: critical buckling length factor β_b for beam

The Dutch foundation 'Bouwen met Staal' (BmS), a national organization for the use of steel in building and bridge engineering, offers a tool on their website to determine the dimensions of the sections for several roof trusses [6]. Also asymmetrical pitched-roof frames are included in this tool where the frame is loaded by a uniformly distributed load with rigid connections in the eaves and hinged connections at the bottom. However the calculations for determining the dimensions of the sections are based on buckling lengths calculated using the method developed by Rieckmann for symmetrical pitched-roof frames. According to the calculation method of BmS, the asymmetric pitched-roof frame is thought to be split up in two independent pitched-roof frames as shown in figure 2.5. Both frames are calculated according to the method of Rieckmann and the decisive critical buckling length of the beam and column are used. This method gives an approximation of the critical buckling length of the members.

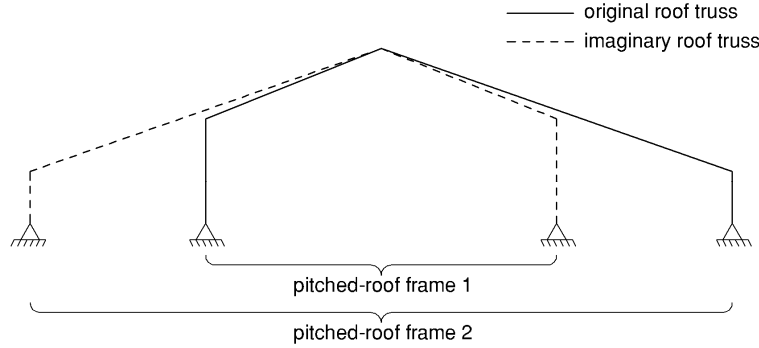


Figure 2.5: Asymmetric pitched-roof frame split up in two independent symmetrical pitched-roof frames.

The method developed by Rieckmann is based on deriving the critical buckling lengths from differential equations of equilibrium. The elastic rotational spring stiffness at the top of the column ($k_{r,L}$) can be determined using a separate differential equation of equilibrium for the beam. In this method, the parameters δ and γ are integrated in the elastic rotational spring stiffness. This method is explained in Appendix B and results in the following rotational spring stiffness:

$$k_{r,L} = \frac{M}{\Phi_b} = \frac{M}{-\left(\frac{M \cdot \cos(\gamma \cdot \alpha_c \cdot L_c) \cdot \delta}{\sin(\gamma \cdot \alpha_c \cdot L_c) \cdot \gamma \cdot \alpha_c \cdot E I_c} - \frac{M \cdot L_b}{(\gamma \cdot \alpha_c \cdot L_c)^2 \cdot E I_b} \right)} \quad (2.15)$$

The frame investigated by Rieckmann has hinged connection at the bottom. Therefore, $\zeta_0=0$ (see table 2.1). This parameter and the rotational spring stiffness should be integrated in the stability criterion of table 2.1 and gives:

$$-\tan(\alpha_c \cdot L_c) + \frac{M}{\alpha_c \cdot \left(\frac{M \cdot \cos(\gamma \cdot \alpha_c \cdot L_c) \cdot \delta}{\sin(\gamma \cdot \alpha_c \cdot L_c) \cdot \gamma \cdot \alpha_c \cdot E I_c} - \frac{M \cdot L_b}{(\gamma \cdot \alpha_c \cdot L_c)^2 \cdot E I_b} \right) \cdot E I_c} = 0 \quad (2.16)$$

Solving α_c gives the critical buckling load of the columns and the beams expressed in:

$$F_{cr,c} = \alpha_c^2 \cdot E I_c, \text{ and} \quad (2.17)$$

$$F_{cr,b} = \frac{\gamma^2 \cdot \alpha_c^2 \cdot E I_b \cdot L_c^2}{L_b^2} \quad (2.18)$$

The above approach of determining critical buckling loads using differential equations of equilibrium for Rieckmann frames is also followed in Sesink [7]. Sesink investigated three different symmetrical pitched-roof frames, which contain many similarities with the frame considered by Rieckmann. The first frame is a symmetric frame with segmented beams and rotational springs as shown in figure 2.6.

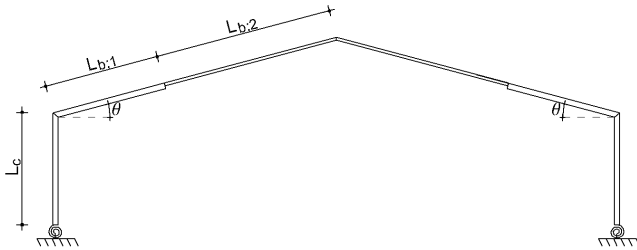


Figure 2.6: Symmetric pitched-roof frame with segmented beams considered by Sesink [7]

The second frame is a symmetric frame with web-tapered columns and beams with rotational springs as shown in figure 2.7.

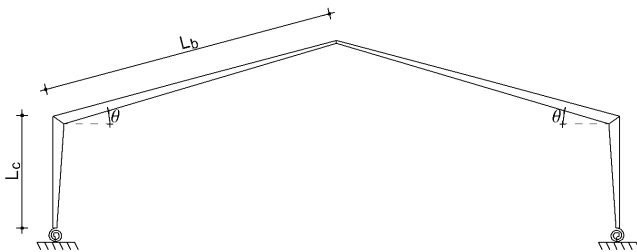


Figure 2.7: Symmetric pitched-roof frame with web-tapered columns and beams considered by Sesink [7]

For these two types of frames critical buckling lengths were determined by means of LBA and GMNIA were executed. The results of this GMNIA were compared with the results of the calculation methods of Eurocode 3 using buckling lengths for determining ultimate bearing capacities.

Besides these two frames, Sesink investigated the symmetric pitched-roof frame considered by Rieckmann extended with rotational springs at the base and the top of the columns as shown in figure 2.8. The rotational spring stiffness at the top of the columns can be obtained by:

$$k_{r,L} = \frac{1}{\frac{1}{k_{r,b}} + \frac{1}{k_{r,con}}} \quad (2.19)$$

Where:

- $k_{r,b}$ is the rotational stiffness due to the stiffness of beam according to Eq. (2.15)
- $k_{r,con}$ is the rotational stiffness due to the connection between column and beam

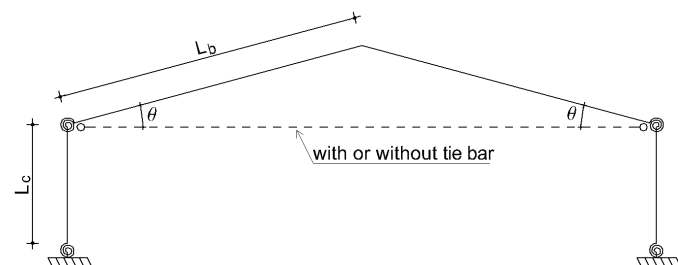


Figure 2.8: Rieckmann frame extended with rotational springs considered by Sesink [7]

The value $k_{r,L}$ of Eq. (2.19) and the rotational stiffness at the base ($k_{r,0}$) have to be filled in, in the stability criteria of table 2.1 and gives the critical buckling loads for this type of frame.

Another investigation with respect to critical buckling lengths of symmetrical pitched-roof frames is conducted by Silvestre and Camotim [8]. They considered symmetrical pitched-roof frames with symmetrical loads and rotational springs at the base as shown in figure 2.9.

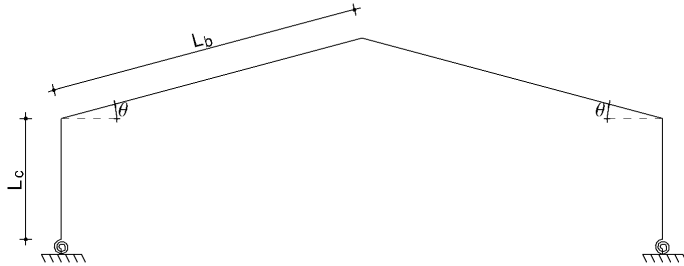


Figure 2.9: Symmetric pitched-roof frame considered by Silvestre and Camotim

In contrast to orthogonal frames, Silvestre and Camotim experienced two global buckling modes for this type of frames: antisymmetrical and symmetrical configurations as shown in figure 2.10. Each buckling mode involves sway displacements and has a corresponding critical buckling load which depends on:

- the ratio of the compression force in the beam and the column, and
- the slope of the beam

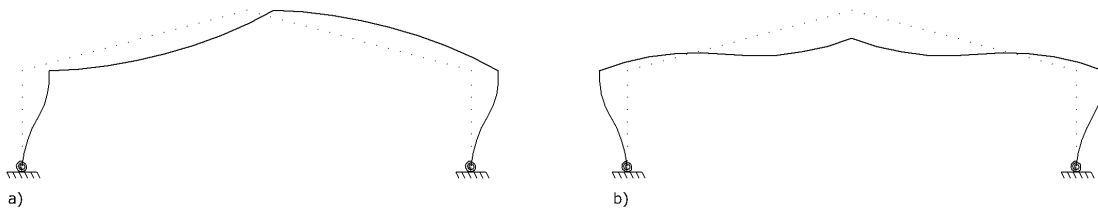


Figure 2.10: a) Antisymmetrical buckling (ASB) mode b) Symmetrical buckling (SB) mode.

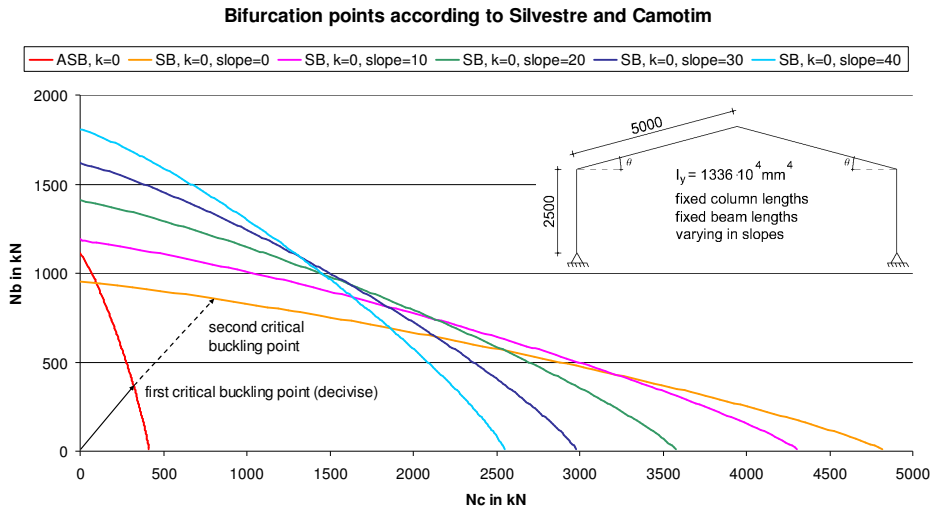
An approximation of the critical buckling loads can be obtained using:

$$\alpha_{cr} = \left[\left(\frac{N_c}{\rho_{c,0} \cdot N_{E,c}} \right)^C + \left(\frac{N_b}{\rho_{b,0} \cdot N_{E,b}} \right)^C \right]^{-1/C} \quad (2.20)$$

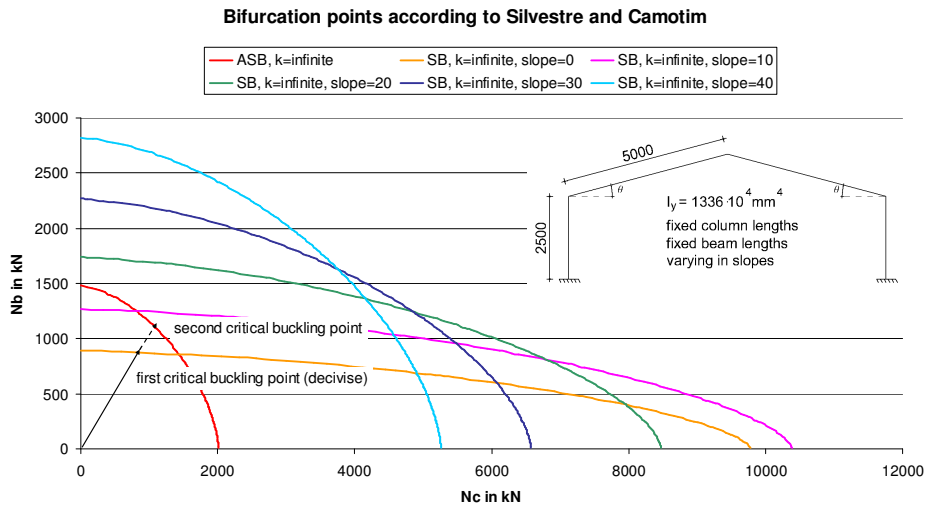
Where α_{cr} is the multiplier of the compression forces for obtaining critical buckling loads

Eq. (2.20) is further explained in Appendix C.

Graph 2.1 and 2.2 gives critical buckling points according to Eq. (2.20) related to antisymmetrical buckling modes and symmetrical buckling modes for frames with beam lengths of 5000mm and column lengths of 2500mm. All members have a moment of inertia of $1336 \cdot 10^4 \text{ mm}^4$ (I_z of a HE200A section). Graph 2.1 shows the cases where the columns are hinged connected to the base. Graph 2.2 shows the cases where the columns are fixed connected to the based. On horizontal x-axis of both graphs the design load in the column is given. On vertical y-axis the design load in the beam is given. The bifurcation load formula show that symmetrical buckling behaviour will be influenced by the slope of the beam (see Appendix C). Therefore five different slopes varying from 0 to 40 degrees are analyzed for symmetrical buckling behaviour.



Graph 2.1: Antisymmetrical and symmetrical bifurcation points according to Silvestre and Camotim for hinged connections at the base.



Graph 2.2: Antisymmetrical and symmetrical bifurcation points according to Silvestre and Camotim for fixed connections at the base.

From both graphs it can be concluded that ASB is always decisive when a relatively large axial force in the column in comparison with the axial force in the beam occurs. On the other hand the slope of the beam is decisive when the axial force in the beam is large in comparison with the axial force in the column.

2.2 Ultimate bearing capacities

By determining ultimate bearing capacities, member imperfections and elastic-plastic material behaviour are to be considered as well [9]. An example is the ultimate bearing capacity in the case of flexural buckling of a column. By increasing the force gradually, the deflection path follows the second order elastic curve and branching off in the direction of the second order plastic curve as shown in figure 2.11. The maximum force at this second order elastic-plastic path is defined as the limit point and gives the ultimate bearing capacity (F_{ult}) of the column.

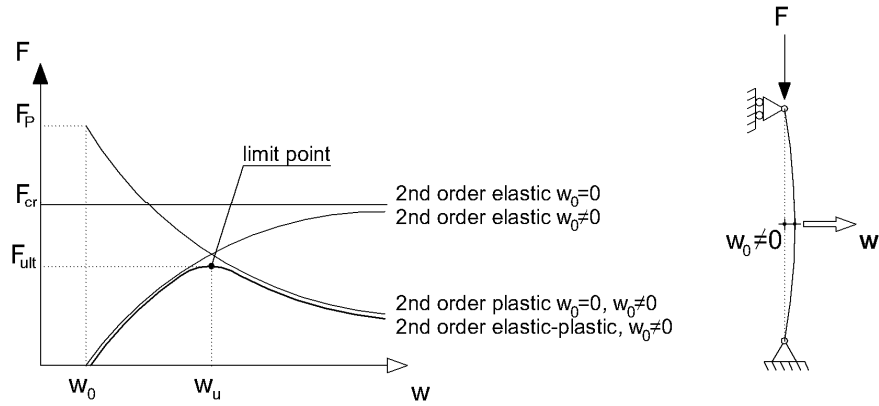


Figure 2.11: Load-deflection diagram of a limit point for an imperfect column

A practical design procedure which allows to predict the ultimate bearing capacity is the Merchant-Rankine approach [9]. According to this approach the ultimate bearing capacity can be predicted using:

$$\frac{1}{F_{ult}} = \frac{1}{F_{cr}} + \frac{1}{F_p} \quad (2.21)$$

or

$$F_{ult} = \frac{F_p}{1 + (F_p / F_{cr})} \quad (2.22)$$

Where F_p is the force that creates a mechanism according to the first order theory of plasticity.

3. Critical buckling loads of non-orthogonal asymmetrical steel frames

In this chapter three different methods will be discussed to determine critical buckling loads analytically. The first method is using the differential equation of equilibrium applied to frame 1, in which each column will be analyzed separately. This method is given in chapter 3.1. Then critical buckling loads for both frames will be determined using Betti's theorem and is given in chapter 3.2. The last method, which will be discussed in chapter 3.3, is the determination of critical buckling loads using kinematic models and this method is applicable for both frames. In contrast to the method using the differential equation of equilibrium, Betti's theorem and kinematic models are both methods in which the influence of a compression force in the beam will not be taking into account. Therefore an approach has been developed where this influence can be determined separately and can be subtracted from the critical buckling loads found by Betti's theorem and kinematic models. This approach will be described and discussed in chapter 3.4. Finally the three methods will be compared and conclusions will be given in chapter 3.5.

3.1 Differential equation of equilibrium applied to frame 1

3.1.1 Introduction to separate column approach

Exact solutions of critical buckling loads can be obtained using the differential equation of equilibrium as described in Appendix A. In contrast to symmetrical frames, critical buckling loads of asymmetrical pitched-roof frames can not be determined using one column analysis due to the asymmetry of the frames. Therefore critical buckling loads of frame 1 are approximate by analyzing each column separately. For analyzing the left-hand column, a concentrated lateral load will be applied at the top of this column. The beams and the right-hand column serve as supportive elements for the left-hand column as shown in figure 3.1. Due to the lateral load at the top of the column, the column displaces and gives an approximation of the buckling mode of the left column.

In the other case, when the right-hand column will be analyzed, the beams and the left-hand column will serve as supportive elements as shown in figure 3.2. The lateral load at the top of column aims to give displacements to the column which approximate the buckling mode of the right-hand column. From both analyses, the lowest critical buckling load of the column will serve as overall critical buckling load for the columns.

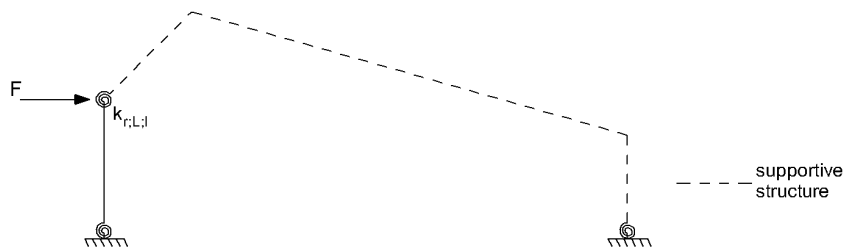


Figure 3.1: Model to determine the critical buckling load of the left-hand column (separate column approach 1)

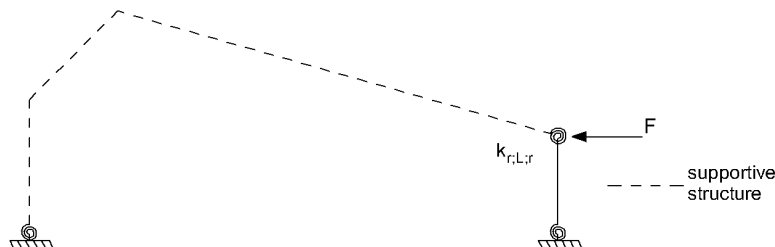


Figure 3.2: Model to determine the critical buckling load of the right-hand column (separate column approach 2)

The rotational spring stiffnesses $k_{r,L,i}$ and $k_{r,L,r}$ at the top of the columns can be obtained using the general formula:

$$k_{r,L,i} = \frac{M_{b,i}}{\varphi_{b,i}} \quad (3.1)$$

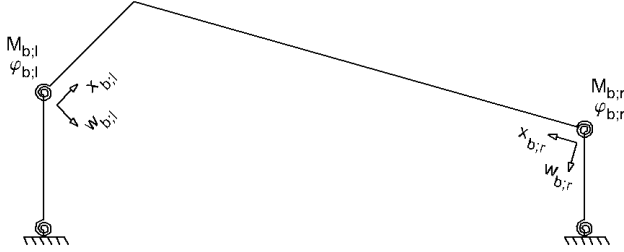


Figure 3.3: Positions $M_{b,i}$ and $\varphi_{b,i}$

The angle of rotation of the beam can be determined using the differential equation of equilibrium for the beam. The differential equation of equilibrium for the beam is:

$$\frac{d^4 w_b}{dx_b^4} + \alpha_b^2 \cdot \frac{d^2 w_b}{dx_b^2} = 0 \quad \text{Where } \alpha_b^2 = \frac{N_b}{EI_b} \quad (3.2)$$

This is a fourth-order homogeneous differential equation, which has as general solution:

$$w_b(x_b) = A_b \cdot \sin(\alpha_b \cdot x_b) + B_b \cdot \cos(\alpha_b \cdot x_b) + C_b \cdot \frac{x_b}{L_b} + D_b \quad (3.3)$$

where A_b , B_b , C_b and D_b are integration constants obtained from boundary conditions. The boundary conditions for non-orthogonal asymmetrical frames differ from the boundary conditions of non-orthogonal symmetrical frames (which are described in Appendix C) and the formulation of these boundary conditions for different non-orthogonal asymmetrical frames will be discussed in later stage of this chapter.

After obtaining the integration constants A_b , B_b , C_b and D_b , the integration constants can be filled in the deflection function of Eq. (3.3). The angle of rotation of the beam can be determined by differentiation of the deflection function, $w_b(x_b)$. The rotational spring stiffness can then be expressed as:

$$k_{r,L,i} = \frac{M_{b,i}}{-w_{b,i}'(0)} \quad (3.4)$$

After determining the rotational spring stiffness at the top and the bottom of the column, the stiffnesses can be substituted in the boundary conditions of Eq. (A.2) and (A.3). The boundary conditions, as given in Eq. (A.1) – (A.4), to determine the integration constants for the column are the same for both columns. So, the matrix of Eq. (A.14) can be written in a matrix for the left-hand column:

$$\begin{pmatrix} 0 & 1 & 0 & 1 \\ \zeta_{0,i} \cdot \alpha_{c,i} & \alpha_{c,i}^2 & \frac{\zeta_{0,i}}{L_{c,i}} & 0 \\ \zeta_{L,i} \cdot \cos(\alpha_{c,i} \cdot L_{c,i}) \cdot \alpha_{c,i} - \sin(\alpha_{c,i} \cdot L_{c,i}) \cdot \alpha_{c,i}^2 & -\zeta_{L,i} \cdot \sin(\alpha_{c,i} \cdot L_{c,i}) \cdot \alpha_{c,i} - \cos(\alpha_{c,i} \cdot L_{c,i}) \cdot \alpha_{c,i}^2 & \frac{\zeta_{L,i}}{L_{c,i}} & 0 \\ 0 & 0 & \frac{\alpha_{c,i}^2}{L_{c,i}} & 0 \end{pmatrix} \cdot \begin{pmatrix} A_c \\ B_c \\ C_c \\ D_c \end{pmatrix} = 0 \quad (3.5)$$

and a matrix for the right-hand column:

$$\begin{pmatrix} 0 & 1 & 0 & 1 \\ \zeta_{0,r} \cdot \alpha_{c,r} & \alpha_{c,r}^2 & \frac{\zeta_{0,r}}{L_{c,r}} & 0 \\ \zeta_{L,r} \cdot \cos(\alpha_{c,r} \cdot L_{c,r}) \cdot \alpha_{c,r} - \sin(\alpha_{c,r} \cdot L_{c,r}) \cdot \alpha_{c,r}^2 - \zeta_{L,r} \cdot \sin(\alpha_{c,r} \cdot L_{c,r}) \cdot \alpha_{c,r} - \cos(\alpha_{c,r} \cdot L_{c,r}) \cdot \alpha_{c,r}^2 & 0 & \frac{\zeta_{L,r}}{L_{c,r}} & 0 \\ 0 & 0 & \frac{\alpha_{c,r}^2}{L_{c,r}} & 0 \end{pmatrix} \cdot \begin{pmatrix} A_c \\ B_c \\ C_c \\ D_c \end{pmatrix} = 0 \quad (3.6)$$

The determinant of matrix (3.5) is:

$$-\tan(\alpha_{c,l} \cdot L_{c,l}) + \frac{\zeta_{0,l}}{\alpha_{c,l}} + \frac{\zeta_{L,l}}{\alpha_{c,l}} + \frac{\tan(\alpha_{c,l} \cdot L_{c,l}) \cdot \zeta_{0,l} \cdot \zeta_{L,l}}{\alpha_{c,l}^2} = 0 \quad (3.7)$$

Eq. (3.7) is the stability criterion for the left-hand column, where $\alpha_{c,l}$ can be solved, which results in the following critical buckling load formula:

$$F_{cr;c,l} = \alpha_{c,l}^2 \cdot EI_{c,l} \quad (3.8)$$

The determinant of matrix (3.6) is:

$$-\tan(\alpha_{c,r} \cdot L_{c,r}) + \frac{\zeta_{0,r}}{\alpha_{c,r}} + \frac{\zeta_{L,r}}{\alpha_{c,r}} + \frac{\tan(\alpha_{c,r} \cdot L_{c,r}) \cdot \zeta_{0,r} \cdot \zeta_{L,r}}{\alpha_{c,r}^2} = 0 \quad (3.9)$$

and results in the following critical buckling load formula for the right-hand column:

$$F_{cr;c,r} = \alpha_{c,r}^2 \cdot EI_{c,r} \quad (3.10)$$

After obtaining both critical buckling loads, the lowest critical buckling load gives an approximation of the overall critical buckling load of the columns. Thereafter, the critical buckling loads of the beams can be determined using:

$$F_{cr;b,j} = F_{cr;c} \cdot \frac{N_{b,j}}{N_c} \quad (3.11)$$

3.1.2 Boundary conditions

The integration constants A_b to D_b of Eq. (3.3) can be determined by developing boundary conditions for the specific properties of the beam considered in its buckling mode. Consider the frame given in figure 3.1. Due to the concentrated lateral load the frame deflects and a moment distribution occurs in the frame. The mechanical model of the left beam and the moment distribution in the left beam is given in figure 3.4.

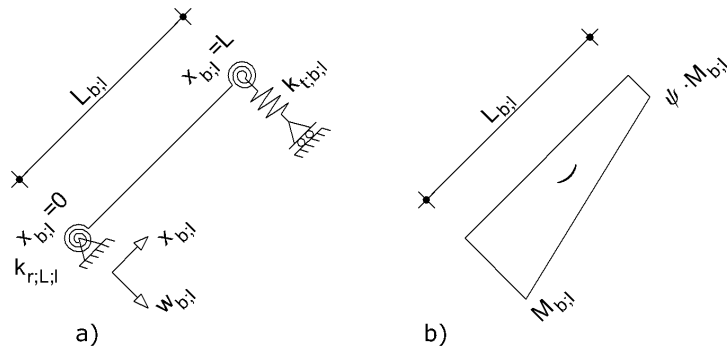


Figure 3.4: a) Left beam b) Moment distribution in the left beam

This model will be used to determine the rotational spring stiffness $k_{r;l;l}$. Due to the connection between beam and column, no displacements occur perpendicular to the left end of the beam ($w_{b;l}$ on position $x_{b;l} = 0$). Therefore, the first boundary condition can be written as:

$$BC.1 \quad w_{b;l}(0) = 0 \quad (3.12)$$

The second and third boundary condition will describe the influence of bending moments. The values of bending moments on position $x_{b;l} = 0$ and position $x_{b;l} = L$ should be determined where the bending moment on position $x_{b;l} = L$ will be expressed as a ratio (ψ) of the bending moment on position $x_{b;l} = 0$, as shown in figure 3.4b. The second and third boundary conditions can be written as:

$$BC.2 \quad w_{b;l}''(0) \cdot EI_{b;l} = M_{b;l} \quad (3.13)$$

$$BC.3 \quad w_{b;l}''(L) \cdot EI_{b;l} = \psi \cdot M_{b;l} \quad (3.14)$$

Due to the geometry of the frame and the applied lateral load, the top of the frame will deflect not only in horizontal way, but also in vertical way. To take into account this vertical displacement, a fictitious translational spring $k_{t;b;l}$ is modeled at the top of the frame. The translational spring stiffness can be obtained using the general formula:

$$k_{t;b;l} = \frac{V_{b;l}(L)}{w_{b;l}(L)} \quad (3.15)$$

where $V_{b;l}(L)$ is the reaction force perpendicular to position $x_{b;l} = L$.

To obtain the reaction force $V_{b;l}(L)$ a roller will be modeled at the top of the frame. Due to the lateral load at the top of the column, reaction force $V_{b;R}$ (shown in figure 3.5) can be found since the hinged connection prevents vertical displacements. This reaction force should be decomposed in a force perpendicular to position $x_{b;l} = L$ and gives $V_{b;l}(L)$.

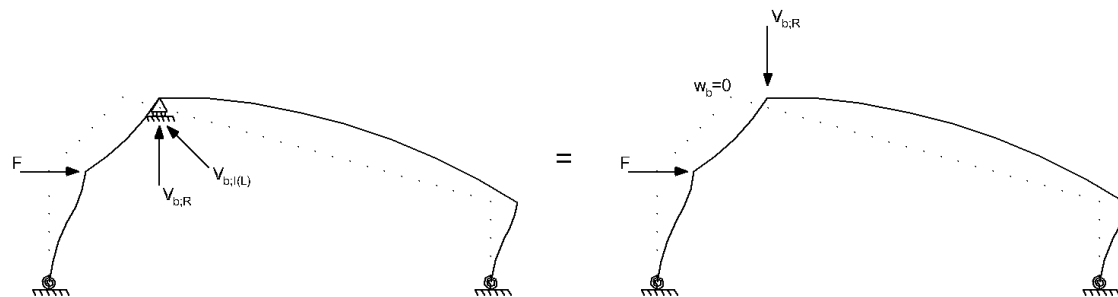


Figure 3.5: Model to determine $V_{b;l}(L)$

To obtain the vertical displacement at the top of the frame, a first order elastic calculation of the frame without a roller connection at the top of the frame will be executed. The vertical displacement w_b , as given in figure 3.6, should be decomposed in a displacement perpendicular to position $x_{b,j} = L$ and gives $w_{b,j}(L)$.

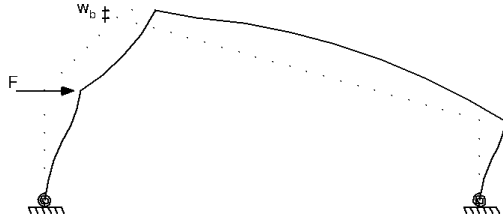


Figure 3.6: Vertical displacement at the top of the frame

$$\text{Note: } k_{t,b,j} = \frac{V_{b,j}(L)}{w_{b,j}(L)} = \frac{V_{b,R} \cdot \cos \theta_l}{w_b \cdot \cos \theta_l} \quad (3.16)$$

So the fourth boundary condition can be written as:

$$\text{BC.4} \quad -\frac{w_{b,j}'''(L) \cdot EI_{b,j}}{k_{t,b}} + w_{b,j}(L) = 0 \quad (3.17)$$

The general solution of the fourth-order homogeneous differential equation as given in Eq. (3.3), should be substituted in the described boundary conditions. The first, second and third derivative of this general solution are respectively (expressed for the left beam):

$$w_{b,j}'(x_{b,j}) = A_{b,j} \cdot \cos(\alpha_{b,j} \cdot x_{b,j}) \cdot \alpha_{b,j} - B_{b,j} \cdot \sin(\alpha_{b,j} \cdot x_{b,j}) \cdot \alpha_{b,j} + \frac{C_{b,j}}{L_{b,j}} \quad (3.18)$$

$$w_{b,j}''(x_{b,j}) = -A_{b,j} \cdot \sin(\alpha_{b,j} \cdot x_{b,j}) \cdot \alpha_{b,j}^2 - B_{b,j} \cdot \cos(\alpha_{b,j} \cdot x_{b,j}) \cdot \alpha_{b,j}^2 \quad (3.19)$$

$$w_{b,j}'''(x_{b,j}) = -A_{b,j} \cdot \cos(\alpha_{b,j} \cdot x_{b,j}) \cdot \alpha_{b,j}^3 + B_{b,j} \cdot \sin(\alpha_{b,j} \cdot x_{b,j}) \cdot \alpha_{b,j}^3 \quad (3.20)$$

Substituting the general solution into the boundary conditions gives:

$$\text{BC.1} \quad w_{b,j}(0) = B_{b,j} + D_{b,j} = 0 \quad (3.21)$$

$$\text{BC.2} \quad w_{b,j}''(0) \cdot EI_{b,j} = -\alpha_{b,j}^2 \cdot B_{b,j} \cdot EI_{b,j} = M_{b,j} \quad (3.22)$$

$$\text{BC.3} \quad w_{b,j}''(L) \cdot EI_{b,j} = -A_{b,j} \cdot \sin(\alpha_{b,j} \cdot L_{b,j}) \cdot \alpha_{b,j}^2 \cdot EI_{b,j} - B_{b,j} \cdot \cos(\alpha_{b,j} \cdot L_{b,j}) \cdot \alpha_{b,j}^2 \cdot EI_{b,j} = \psi \cdot M_{b,j} \quad (3.23)$$

$$\text{BC.4} \quad -\frac{w_{b,j}'''(L) \cdot EI_{b,j}}{k_{t,j}} + w_{b,j}(L) = \frac{A_{b,j} \cdot \cos(\alpha_{b,j} \cdot L_{b,j}) \cdot \alpha_{b,j}^3 \cdot EI_{b,j}}{k_{t,b,j}} - \frac{B_{b,j} \cdot \sin(\alpha_{b,j} \cdot L_{b,j}) \cdot \alpha_{b,j}^3 \cdot EI_{b,j}}{k_{t,b,j}} + A_{b,j} \cdot \sin(\alpha_{b,j} \cdot L_{b,j}) + B_{b,j} \cdot \cos(\alpha_{b,j} \cdot L_{b,j}) + C_{b,j} + D_{b,j} = 0 \quad (3.24)$$

Eq. (3.22) / BC.2 leads to:

$$\boxed{B_{b,j} = -\frac{M_{b,j}}{\alpha_{b,j}^2 \cdot EI_{b,j}}} \quad (3.25)$$

Eq. (3.23) / BC.3 leads to:

$$w_{b,j}''(L) \cdot EI_{b,j} = -A_{b,j} \cdot \sin(\alpha_{b,j} \cdot L_{b,j}) \cdot \alpha_{b,j}^2 \cdot EI_{b,j} + \frac{M_{b,j}}{\alpha_{b,j}^2 \cdot EI_{b,j}} \cdot \cos(\alpha_{b,j} \cdot L_{b,j}) \cdot \alpha_{b,j}^2 \cdot EI_{b,j} = \psi \cdot M_{b,j} \quad (3.26)$$

$$\boxed{A_{b,j} = \frac{-\psi \cdot M_{b,j} + M_{b,j} \cdot \cos(\alpha_{b,j} \cdot L_{b,j})}{\sin(\alpha_{b,j} \cdot L_{b,j}) \cdot \alpha_{b,j}^2 \cdot EI_{b,j}}} \quad (3.27)$$

Eq. (3.21) / BC.1 leads to:

$$w_{b,j}(0) = -\frac{M_{b,j}}{\alpha_{b,j}^2 \cdot EI_{b,j}} + D_{b,j} = 0 \quad (3.28)$$

$$\boxed{D_{b,j} = \frac{M_{b,j}}{\alpha_{b,j}^2 \cdot EI_{b,j}}} \quad (3.29)$$

Eq. (3.24) / BC.4 leads to:

$$\begin{aligned} -\frac{w_{b,j}''''(L) \cdot EI_{b,j}}{k_{t,b,j}} + w_{b,j}(L) &= \frac{\left(\frac{-\psi \cdot M_{b,j} + M_{b,j} \cdot \cos(\alpha_{b,j} \cdot L)}{\sin(\alpha_{b,j} \cdot L_{b,j}) \cdot \alpha_{b,j}^2 \cdot EI_{b,j}} \right) \cdot \cos(\alpha_{b,j} \cdot L_{b,j}) \cdot \alpha_{b,j}^3 \cdot EI_{b,j}}{k_{t,b,j}} + \\ &\frac{\frac{M_{b,j}}{\alpha_{b,j}^2 \cdot EI_{b,j}} \cdot \sin(\alpha_{b,j} \cdot L_{b,j}) \cdot \alpha_{b,j}^3 \cdot EI_{b,j}}{k_{t,b,j}} + \left(\frac{-\psi \cdot M_{b,j} + M_{b,j} \cdot \cos(\alpha_{b,j} \cdot L_{b,j})}{\sin(\alpha_{b,j} \cdot L_{b,j}) \cdot \alpha_{b,j}^2 \cdot EI_{b,j}} \right) \cdot \sin(\alpha_{b,j} \cdot L_{b,j}) - \\ &\frac{M_{b,j}}{\alpha_{b,j}^2 \cdot EI_{b,j}} \cdot \cos(\alpha_{b,j} \cdot L_{b,j}) + C_{b,j} + \frac{M_{b,j}}{\alpha_{b,j}^2 \cdot EI_{b,j}} = 0 \end{aligned} \quad (3.30)$$

And gives:

$$\begin{aligned} C_{b,j} &= \frac{\frac{\psi \cdot M_{b,j} - M_{b,j} \cdot \cos(\alpha_{b,j} \cdot L_{b,j})}{\sin(\alpha_{b,j} \cdot L_{b,j}) \cdot \alpha_{b,j}^2 \cdot EI_{b,j}} \cdot \cos(\alpha_{b,j} \cdot L_{b,j}) \cdot \alpha_{b,j}^3 \cdot EI_{b,j}}{k_{t,b,j}} - \\ &\frac{\frac{M_{b,j}}{\alpha_{b,j}^2 \cdot EI_{b,j}} \cdot \sin(\alpha_{b,j} \cdot L_{b,j}) \cdot \alpha_{b,j}^3 \cdot EI_{b,j}}{k_{t,b,j}} + \frac{\psi \cdot M_{b,j} - M_{b,j} \cdot \cos(\alpha_{b,j} \cdot L_{b,j})}{\alpha_{b,j}^2 \cdot EI_{b,j}} + \\ &\frac{M_{b,j} \cdot \cos(\alpha_{b,j} \cdot L_{b,j})}{\alpha_{b,j}^2 \cdot EI_{b,j}} - \frac{M_{b,j}}{\alpha_{b,j}^2 \cdot EI_{b,j}} \end{aligned} \quad (3.31)$$

Eq. (3.31) simplified gives:

$$C_{b,j} = \frac{\psi \cdot M_{b,j} - M_{b,j}}{\alpha_{b,j}^2 \cdot EI_{b,j}} + \frac{\psi \cdot M_{b,j} \cdot \alpha_{b,j} \cdot \cos(\alpha_{b,j} \cdot L_{b,j}) - M_{b,j} \cdot \alpha_{b,j}}{k_{t,b,j} \cdot \sin(\alpha_{b,j} \cdot L_{b,j})} \quad (3.32)$$

Integration constants $A_{b,j}$ to $D_{b,j}$ substituted into Eq. (3.3) gives:

$$w_{b,j}(x_{b,j}) = \left(\frac{-\psi \cdot M_{b,j} + M_{b,j} \cdot \cos(\alpha_{b,j} \cdot L_{b,j})}{\sin(\alpha_{b,j} \cdot L_{b,j}) \cdot \alpha_{b,j}^2 \cdot EI_{b,j}} \right) \cdot \sin(\alpha_{b,j} \cdot x_{b,j}) - \frac{M_{b,j} \cdot \cos(\alpha_{b,j} \cdot x_{b,j})}{\alpha_{b,j}^2 \cdot EI_{b,j}} + \left(\frac{\psi \cdot M_{b,j} - M_{b,j}}{\alpha_{b,j}^2 \cdot EI_{b,j}} + \frac{\psi \cdot M_{b,j} \cdot \alpha_{b,j} \cdot \cos(\alpha_{b,j} \cdot L_{b,j}) - M_{b,j} \cdot \alpha_{b,j}}{k_{t,b,j} \cdot \sin(\alpha_{b,j} \cdot L_{b,j})} \right) \cdot \frac{x_{b,j}}{L_{b,j}} + \frac{M_{b,j}}{\alpha_{b,j}^2 \cdot EI_{b,j}} \quad (3.33)$$

The first derivative of $w_{b,j}(0)$ is:

$$w_{b,j}'(0) = \left(\frac{-\psi \cdot M_{b,j} + M_{b,j} \cdot \cos(\alpha_{b,j} \cdot L_{b,j})}{\sin(\alpha_{b,j} \cdot L_{b,j}) \cdot \alpha_{b,j} \cdot EI_{b,j}} \right) + \left(\frac{\psi \cdot M_{b,j} - M_{b,j}}{\alpha_{b,j}^2 \cdot EI_{b,j} \cdot L_{b,j}} + \frac{\psi \cdot M_{b,j} \cdot \alpha_{b,j} \cdot \cos(\alpha_{b,j} \cdot L_{b,j}) - M_{b,j} \cdot \alpha_{b,j}}{k_{t,b,j} \cdot \sin(\alpha_{b,j} \cdot L_{b,j}) \cdot L_{b,j}} \right) \quad (3.34)$$

Using Eq. (3.4) the rotational spring stiffness at the top of the left column can be determined and results in:

$$k_{r,L,j} = \frac{M_{b,j}}{\left(\frac{-\psi \cdot M_{b,j} + M_{b,j} \cdot \cos(\alpha_{b,j} \cdot L_{b,j})}{\sin(\alpha_{b,j} \cdot L_{b,j}) \cdot \alpha_{b,j} \cdot EI_{b,j}} \right) + \left(\frac{\psi \cdot M_{b,j} - M_{b,j}}{\alpha_{b,j}^2 \cdot EI_{b,j} \cdot L_{b,j}} + \frac{\psi \cdot M_{b,j} \cdot \alpha_{b,j} \cdot \cos(\alpha_{b,j} \cdot L_{b,j}) - M_{b,j} \cdot \alpha_{b,j}}{k_{t,b,j} \cdot \sin(\alpha_{b,j} \cdot L_{b,j}) \cdot L_{b,j}} \right)} \quad (3.35)$$

3.1.3 Influence of compression forces in the beam on the critical buckling load

Parameters δ and γ developed by Rieckmann should be integrated in the rotational spring stiffness to account for the effects on the stiffness due to compression forces in the beams. Parameter δ (given in Eq. (2.9)) can be integrated in $EI_{b,j}$ and $L_{b,j}$ which results in the following equations:

$$EI_{b,j} = \frac{EI_{c,j} \cdot L_{b,j}}{\delta_1 \cdot L_{c,j}}, \text{ and} \quad (3.36)$$

$$L_{b,j} = \frac{\delta_1 \cdot EI_{b,j} \cdot L_{c,j}}{EI_{c,j}} \quad (3.37)$$

Parameter γ_1 (given in Eq. (2.10)) can be written as:

$$\gamma_1 = \sqrt{\frac{EI_{c,j} \cdot L_{b,j}}{EI_{b,j} \cdot L_{c,j}} \cdot \frac{N_{b,j} \cdot L_{b,j}}{N_{c,j} \cdot L_{c,j}}} = \frac{\alpha_{b,j} \cdot L_{b,j}}{\alpha_{c,j} \cdot L_{c,j}} \quad \text{where } \alpha_{b,j} = \sqrt{\frac{N_{b,j}}{EI_{b,j}}} \text{ and } \alpha_{c,j} = \sqrt{\frac{N_{c,j}}{EI_{c,j}}}, \quad (3.38)$$

and gives:

$$\alpha_{b;l} = \frac{\gamma_l \cdot \alpha_{c;l} \cdot L_{c;l}}{L_{b;l}}, \text{ and} \quad (3.39)$$

$$\alpha_{b;l} \cdot L_{b;l} = \gamma_l \cdot \alpha_{c;l} \cdot L_{c;l} \quad (3.40)$$

Eq. (3.36), (3.37), (3.39) and (3.40) substituted into Eq. (3.35) gives the rotational spring stiffness at the top of the left-hand column for asymmetrical pitched-roof frames:

$$k_{r;l,j} = \frac{M_{b;l}}{\left(\left(\frac{(-\psi \cdot M_{b;l} + M_{b;l} \cdot \cos(\gamma_l \cdot \alpha_{c;l} \cdot L_{c;l})) \cdot \delta_l}{\sin(\gamma_l \cdot \alpha_{c;l} \cdot L_{c;l}) \cdot \gamma_l \cdot \alpha_{c;l} \cdot EI_{c;l}} \right) + \left(\frac{\psi \cdot M_{b;l} \cdot L_{b;l} - M_{b;l} \cdot L_{b;l}}{(\gamma_l \cdot \alpha_{c;l} \cdot L_{c;l})^2 \cdot EI_{b;l}} + \frac{\psi \cdot M_{b;l} \cdot \alpha_{c;l} \cdot \gamma_l \cdot \cos(\gamma_l \cdot \alpha_{c;l} \cdot L_{c;l}) \cdot EI_{c;l} - M_{b;l} \cdot \gamma_l \cdot \alpha_{c;l} \cdot EI_{c;l}}{k_{t;b;l} \cdot \sin(\gamma_l \cdot \alpha_{c;l} \cdot L_{c;l}) \cdot \delta_l \cdot EI_{b;l} \cdot L_{b;l}} \right) \right)} \quad (3.41)$$

Exactly the same method as described in chapter 3.1.2 and this chapter, will be applied to determine the rotational spring stiffness at the top of the right-hand column ($k_{r;l,r}$). Figure 3.7a gives the mechanical model of the right beam and the moment distribution in the beam is given in figure 3.7b.

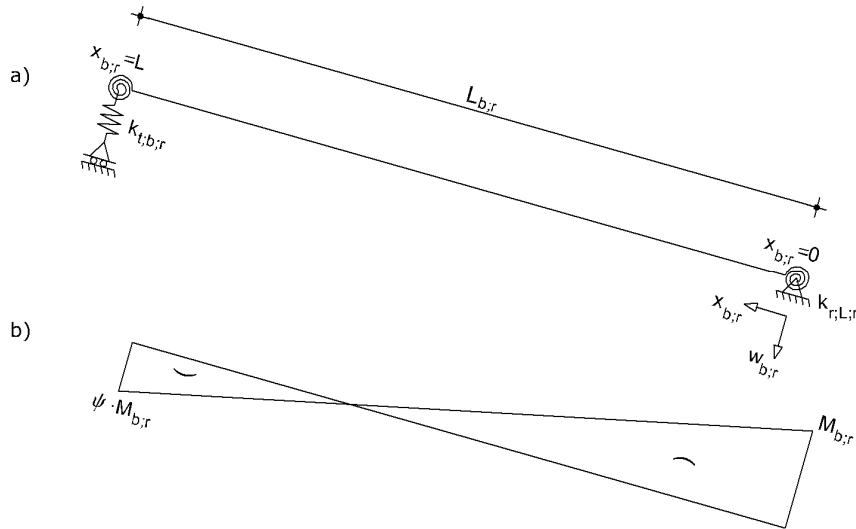


Figure 3.7: a) Right beam b) Moment distribution in the right beam

The rotational spring stiffness $k_{r;l,r}$ can be determined by:

$$k_{r;l,r} = \frac{M_{b;r}}{\left(\left(\frac{(-\psi \cdot M_{b;r} + M_{b;r} \cdot \cos(\gamma_r \cdot \alpha_{c;r} \cdot L_{c;r})) \cdot \delta_r}{\sin(\gamma_r \cdot \alpha_{c;r} \cdot L_{c;r}) \cdot \gamma_r \cdot \alpha_{c;r} \cdot EI_{c;r}} \right) + \left(\frac{\psi \cdot M_{b;r} \cdot L_{b;r} - M_{b;r} \cdot L_{b;r}}{(\gamma_r \cdot \alpha_{c;r} \cdot L_{c;r})^2 \cdot EI_{b;r}} + \frac{\psi \cdot M_{b;r} \cdot \alpha_{c;r} \cdot \gamma_r \cdot \cos(\gamma_r \cdot \alpha_{c;r} \cdot L_{c;r}) \cdot EI_{c;r} - M_{b;r} \cdot \gamma_r \cdot \alpha_{c;r} \cdot EI_{c;r}}{k_{t;b;r} \cdot \sin(\gamma_r \cdot \alpha_{c;r} \cdot L_{c;r}) \cdot \delta_r \cdot EI_{b;r} \cdot L_{b;r}} \right) \right)} \quad (3.42)$$

3.1.4 Example

A two hinged frame is loaded by a uniformly distributed load as given in figure 3.8. The sections of the frame consist of HE100A profiles modeled in Ansys. All properties of these composed HE100A sections are given in table E.1 of Appendix E.

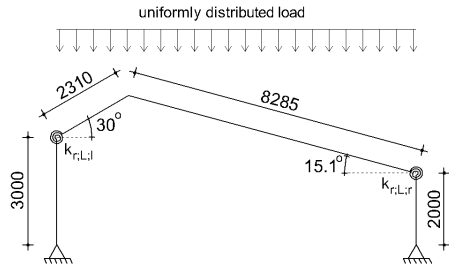


Figure 3.8: Asymmetric pitched-roof frame loaded by a uniformly distributed load.

The δ parameters of Riekmann are:

$$\delta_l = \frac{EI_{c,l} \cdot L_{b,l}}{EI_{b,l} \cdot L_{c,l}} = \frac{2,1 \cdot 10^5 \cdot 3319,5 \cdot 10^3 \cdot 2310}{2,1 \cdot 10^5 \cdot 3319,5 \cdot 10^3 \cdot 3000} = 0,77 \quad (3.43)$$

$$\delta_r = \frac{EI_{c,r} \cdot L_{b,r}}{EI_{b,r} \cdot L_{c,r}} = \frac{2,1 \cdot 10^5 \cdot 3319,5 \cdot 10^3 \cdot 8285}{2,1 \cdot 10^5 \cdot 3319,5 \cdot 10^3 \cdot 2000} = 4,143 \quad (3.44)$$

And using a first order elastic analysis the γ parameters are:

$$\gamma_l = \sqrt{\delta_l \cdot \frac{N_{b,l} \cdot L_{b,l}}{N_{c,l} \cdot L_{c,l}}} = \sqrt{0,77 \cdot 0,806 \cdot \frac{2310}{3000}} = 0,691 \quad (3.45)$$

$$\gamma_r = \sqrt{\delta_r \cdot \frac{N_{b,r} \cdot L_{b,r}}{N_{c,r} \cdot L_{c,r}}} = \sqrt{4,143 \cdot 0,503 \cdot \frac{8285}{2000}} = 2,938 \quad (3.46)$$

One concentrated lateral load of 1 kN has been applied on the top of the left-hand column to determine the rotational spring stiffness $k_{r,L,l}$ (figure 3.9a) and results in the moment distribution of figure 3.9b.

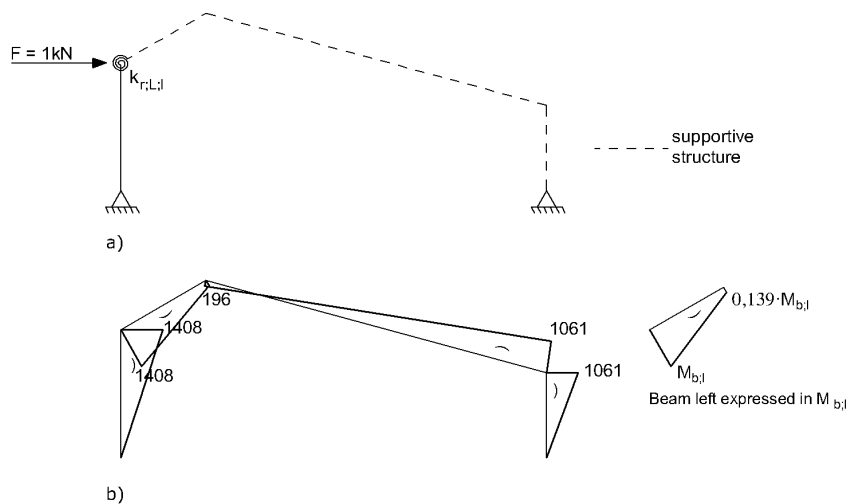


Figure 3.9: a) Model to determine the rotational spring stiffness $k_{r,L,l}$ b) Moment distribution in Nm.

The vertical displacement at the top of the frame is 0,524mm and as given in figure 3.9b, ψ is 0,139. The reaction force $V_{b,R}$ of figure 3.5 is 203N.

The translational spring stiffness $k_{t,b,l}$ of Eq. (3.14) results then in:

$$k_{t,b,l} = \frac{203 \cdot \cos(30)}{0,524 \cdot \cos(30)} = 387 \frac{\text{N}}{\text{mm}} \quad (3.47)$$

All properties are known to determine $k_{r,l,l}$ of Eq. (3.41) and then to solve $\alpha_{c,l}$ of Eq. (3.7). By filling in all properties, $\alpha_{c,l}$ results in:

$$\alpha_{c,l} = 3,80722 \cdot 10^{-4} \quad (3.48)$$

and gives a critical buckling load of:

$$F_{cr;c,l} = \alpha_{c,l}^2 \cdot EI_{c,l} = 101043\text{N} \quad (3.49)$$

To determine the rotational spring stiffness $k_{r,l,r}$, one concentrated lateral load of 1 kN has been applied on the top of the right column and results in the moment distribution of figure 3.10b.

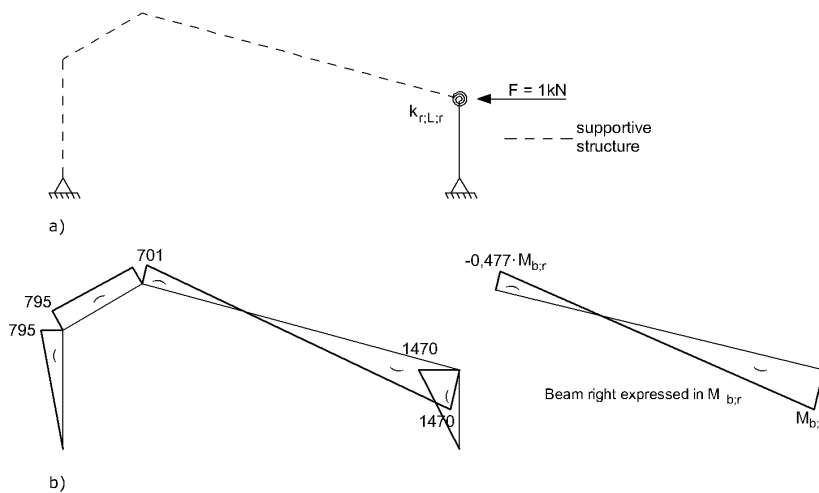


Figure 3.10: a) Model to determine the rotational spring stiffness $k_{r,l,r}$ b) Moment distribution in Nm.

The vertical displacement at the top of the frame is 1,646mm and as given in figure 3.10b ψ is -0,477. The reaction force $V_{b,R}$ is 639N.

The translational spring stiffness $k_{t,b,r}$ is:

$$k_{t,b,r} = \frac{639 \cdot \cos(15,1)}{1,646 \cdot \cos(15,1)} = 387 \frac{\text{N}}{\text{mm}} \quad (3.50)$$

All properties are known to determine $k_{r,l,r}$ of Eq. (3.42) and then to solve $\alpha_{c,r}$ of Eq. (3.9). By filling in all properties, $\alpha_{c,r}$ results in:

$$\alpha_{c,r} = 3,66644 \cdot 10^{-4} \quad (3.51)$$

and gives a critical buckling load of:

$$F_{cr;c,r} = \alpha_{c,r}^2 \cdot EI_{c,r} = 93709\text{N} \quad (3.52)$$

Using LBA in Ansys, which is described in Appendix E.3, an overall critical buckling load for the columns is found of:

$$F_{cr,c;ANSYS} = 96384N \quad (3.53)$$

3.1.5 Discussion

The described method to determine the overall critical buckling load of the columns using two separate column approaches, results in two different critical buckling loads. The lowest critical buckling load can be taken to find a safe approximation for the overall critical buckling of the columns. In the case considered in chapter 3.1.4, the lowest calculated critical buckling load differs about 3% in comparison with the result found by Ansys. This case gives an accurate approximation of the exact critical buckling load.

However, by varying in column lengths the deviation in critical buckling load will not remain constant and result for some cases in inaccurate approximations of the overall critical buckling load. This is determined by investigating the frame of figure 3.8 where the length of the right column varies from 1500mm to 4000mm as presented in figure 3.11. The differences in critical buckling load of the left-hand and the right-hand column compared with the overall critical buckling load found by Ansys are plotted in graph 3.1, with on horizontal x-axis the length of the right column and on the vertical y-axis the error in percents in critical buckling load. An error lower than zero percent implies an underestimation of the critical buckling load and gives a safe approximation. An error higher than zero percent implies an overestimation of the critical buckling load and results in an unsafe approximation. In addition to these analyses, the errors in critical buckling loads according to the method developed by 'Bouwen met Staal' (BmS), which is explained in chapter 2.1.2, are also plotted in graph 3.1.

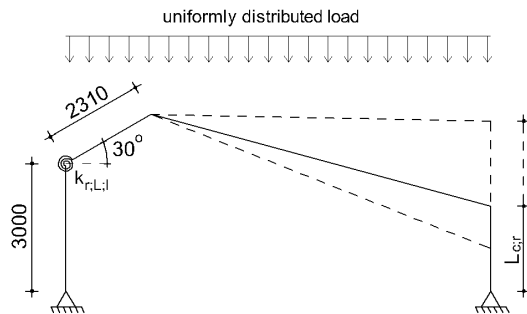
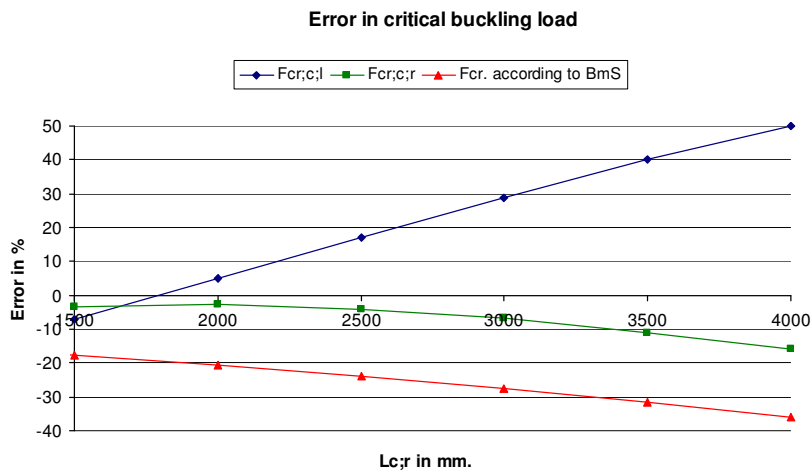


Figure 3.11: Right column varies from 1500mm to 4000mm



Graph 3.1: Error in critical buckling loads for the frame given in figure 3.11

From graph 3.1 it can be seen that the separate column approach with column length between 1500mm and 3000mm for the right-hand column results in errors below the 10 percent when the lowest critical buckling load is taken. The errors between the separate column approach and the method developed by BmS are in most cases between the 15 and 20 percent.

3.2 Betti's theorem

Girgin, Ozmen and Orakdogan [10] developed a simplified procedure for determining approximate values of critical buckling loads of both regular and irregular frames which is based on Betti's theorem. This procedure yields errors that are less than 5% underestimation in critical buckling length [10]. First a theoretical introduction will be given about this theorem which is taken from [11].

3.2.1 Introduction into Betti's Theorem

Consider a structure with a set of coordinates 1, 2, ..., n, n+1, ..., m as shown in figure 3.12a. Two systems of forces act on this structure. The F system of forces acts on coordinates 1 to n, and the Q system of forces acts on the coordinates n+1 to m as shown in figure 3.12b and 3.12c. The displacements which will be caused by F are indicated by $w_{i,F}$ and the displacements which will be caused by Q are indicated by $w_{i,Q}$.

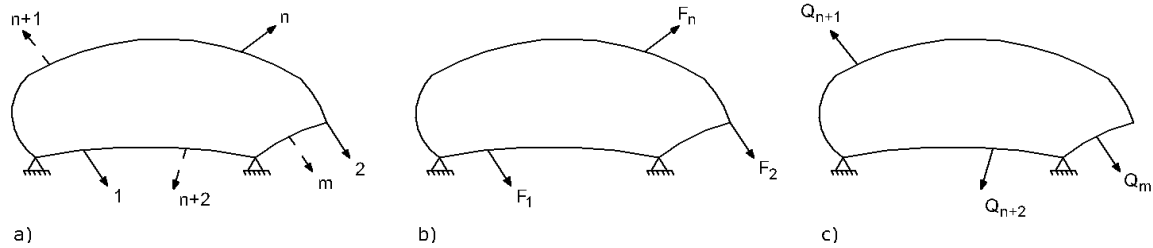


Figure 3.12: Betti's Theorem a) Coordinate system b) F system of forces c) Q system of forces

Suppose that only the F system is applied to the structure and results in displacements (w_F), stresses (σ_F) and strains (ε_F). The internal work is equal to the external work:

$$\frac{1}{2} \cdot \sum_{i=1}^n F_i \cdot w_{i,F} = \frac{1}{2} \cdot \int_x \{\sigma\}_F^T \cdot \{\varepsilon\}_F dx \quad (3.54)$$

Where:

$\{\sigma\}_F^T$ is the transpose stress vector $\{\sigma_x, \sigma_y, \sigma_z, \tau_{xy}, \tau_{xz}, \tau_{yz}\}$ of system F
 $\{\varepsilon\}_F$ is the strain vector $\{\varepsilon_x, \varepsilon_y, \varepsilon_z, \gamma_{xy}, \gamma_{xz}, \gamma_{yz}\}$ of system F

Suppose now that when the F system is being applied to the structure, the Q system is already acting on the structure and causing stresses σ_Q at any point. The external and internal work during the application of the F system are again equal and can be written as:

$$\frac{1}{2} \cdot \sum_{i=1}^n F_i \cdot w_{i,F} + \sum_{i=n+1}^m Q_i \cdot w_{i,F} = \frac{1}{2} \cdot \int_x \{\sigma\}_F^T \cdot \{\varepsilon\}_F dx + \int_x \{\sigma\}_Q^T \cdot \{\varepsilon\}_F dx \quad (3.55)$$

From Eq. (3.54) and (3.55) follows that:

$$\sum_{i=n+1}^m Q_i \cdot w_{i,F} = \int_x \{\sigma\}_Q^T \cdot \{\varepsilon\}_F dx \quad (3.56)$$

When the F system is applied first and the Q system is added subsequently a similar situation will be obtained.

$$\sum_{i=1}^n F_i \cdot w_{iQ} = \int_x \{\sigma\}_F^T \cdot \{\epsilon\}_Q dx \quad (3.57)$$

If the material of the structure obeys Hooke's law, thus:

$$\sigma_Q = E \cdot \epsilon_Q \quad \text{and} \quad \sigma_F = E \cdot \epsilon_F$$

where E is constant and substituting ϵ in Eq (3.56) and (3.57), the right hand sides of these equations are equal. Hence:

$$\sum_{i=1}^n F_i \cdot w_{iQ} = \sum_{i=n+1}^m Q_i \cdot w_{iF} \quad (3.58)$$

Eq. (3.58) is known as Betti's theorem and says that the sum of the products of the forces of the F system and the displacements at the corresponding coordinates caused by the Q system is equal to the sum of the products of the forces of the Q system and the displacements at the corresponding coordinates caused by the F system. In the following chapters, Eq. (3.58) will be written as:

$$W_1 = W_2 \quad (3.59)$$

3.2.2 Application of Betti's theorem to buckling analysis

The practical method to determine approximate values of critical buckling loads of both regular and irregular frames developed by [10] based on Betti's theorem will be given and discussed below. Consider the frame given in figure 3.13. According to [10] it is assumed that the lateral loads given in figure 3.13c result in displacements which are identical to the buckling mode of the frame. Therefore the buckling mode displacements given in figure 3.13b are the same as the displacements given in figure 3.13d.

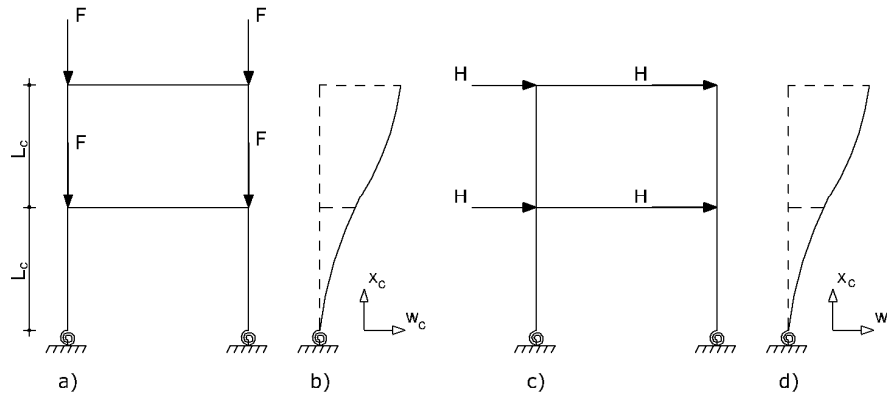


Figure 3.13: Storey frame a) Vertical loaded b) Buckling mode displacements c) Lateral loaded d) Displacements due to H

If the axial deformations are neglected, the virtual work on any column can be obtained from:

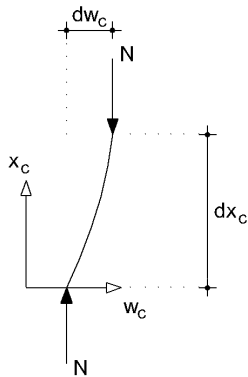
$$w = \int_{x_c=0}^L F \cdot dw_c \cdot \frac{dw_c}{dx_c} \quad (3.60)$$

or

$$w = n \cdot F \int_{x_c=0}^L \left(\frac{dw_c}{dx_c} \right)^2 dx_c \quad (3.61)$$

where L denotes the height of the individual column and n is the number of F which occurs on the individual column. The total virtual work can be expressed as:

$$W_1 = F \cdot \sum n \cdot \int_0^L \left(\frac{dw_c}{dx_c} \right)^2 dx_c \quad (3.62)$$



The bending moment and relative displacement diagrams of an individual column are shown in figure 3.14. The dimensionless coefficient α gives the location of the point of contraflexure and δ gives the relative storey displacement.

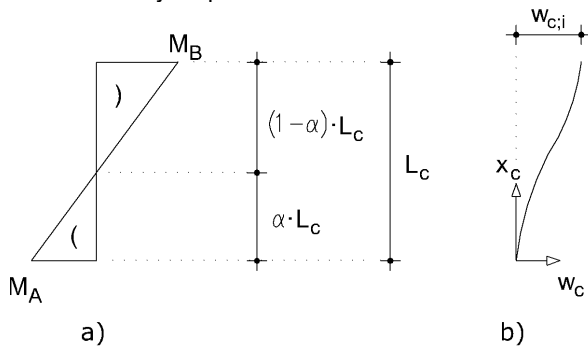


Figure 3.14: a) Bending moments in the column b) Relative displacements in the column

The expression for the degree of curvature of the column is:

$$\frac{d^2 w_c}{dx_c^2} = - \frac{M(x_c)}{EI_c} \quad (3.63)$$

Where $M(x_c)$ can be expressed as:

$$M(x_c) = M_A \cdot \left(1 - \frac{x_c}{\alpha \cdot L_c} \right) \quad (3.64)$$

Substituting Eq. (3.64) into Eq. (3.63) and integrating twice with the boundary conditions:

$$w_c = 0 \text{ for } x_c = 0 \quad \text{and} \\ w_c = w_{c;i} \text{ for } x_c = L_c$$

gives:

$$w_c(x_c) = \left(\frac{w_{c,i}}{L_c} + \frac{M_A \cdot L_c \cdot (3 \cdot \alpha - 1)}{6 \cdot E I_c \cdot \alpha} \right) \cdot x_c + \frac{M_A}{6 \cdot E I_c \cdot \alpha \cdot L_c} \cdot x_c^2 \cdot (x_c - 3 \cdot \alpha \cdot L_c) \quad (3.65)$$

The derivative of Eq. (3.65) is:

$$\frac{dw_c}{dx_c} = \frac{w_{c,i}}{L_c} + \frac{M_A \cdot L_c \cdot (3 \cdot \alpha - 1)}{6 \cdot E I_c \cdot \alpha} + \frac{M_A \cdot x_c^2}{6 \cdot E I_c \cdot \alpha \cdot L_c} + \frac{x_c \cdot (x_c - 3 \cdot \alpha \cdot L_c) \cdot M_A}{3 \cdot E I_c \cdot \alpha \cdot L_c} \quad (3.66)$$

and must be integrated in Eq. (3.62). The total virtual work results then in:

$$W_1 = F \cdot \sum n \cdot \frac{w_{c,i}^2}{L_c} \cdot 1 + \left(\frac{M_A \cdot L_c^2}{E I_c \cdot w_{c,i}} \right)^2 \cdot \left(\frac{1}{12} - \frac{1}{12 \cdot \alpha} + \frac{1}{45 \cdot \alpha^2} \right) \quad (3.67)$$

The virtual work of the shear force in the columns in conjunction with the displacements gives W_2 and can be written as:

$$W_2 = \sum (V_c \cdot w_{c,i}) \quad (3.68)$$

Substitute Eq. (3.67) and (3.68) into Betti's theorem, given in Eq. (3.59), and solving F results in the critical buckling load F_{cr} for the frame:

$$F_{cr} = \frac{\sum (V_c \cdot w_{c,i})}{\sum n \cdot \frac{w_{c,i}^2}{L_c} \cdot 1 + \left(\frac{M_A \cdot L_c^2}{E I_c \cdot w_{c,i}} \right)^2 \cdot \left(\frac{1}{12} - \frac{1}{12 \cdot \alpha} + \frac{1}{45 \cdot \alpha^2} \right)} \quad (3.69)$$

3.2.3 Example of a one degree of freedom system

Consider the frame as given in figure 3.15a.

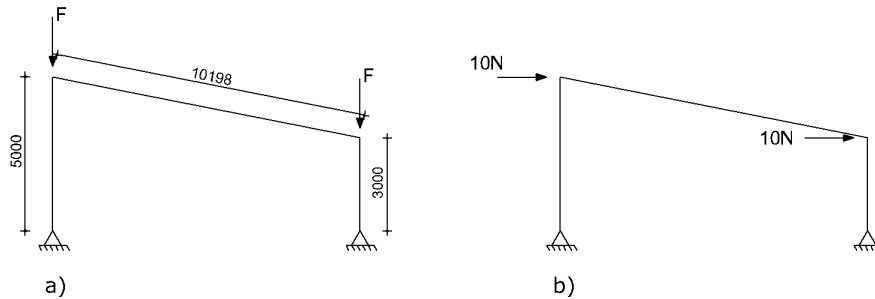


Figure 3.15: a) Non-orthogonal frame b) Lateral loaded

The frame members have a flexural rigidity of $6,97095 \cdot 10^{11}$ Nmm², and no axial force occurs in the beam. Due to lateral loads of 10 Newton on the top of the columns (for example) as given in figure 3.15b the parameters which should be known to solve Eq. (3.69) are given in table 3.1.

Table 3.1. Buckling load parameters of the frame given in figure 3.15

Column	V_c	L_c	$w_{c,i}$	$V_c \cdot w_{c,i}$	$n \cdot (w_{c,i}^2/L_c)$
Left	6	5000	0,577	3,462	$6,6586 \cdot 10^{-5}$
Right	14	3000	0,577	8,078	$1,1098 \cdot 10^{-4}$
Sum				11,54	$1,7756 \cdot 10^{-4}$

This results in a critical buckling load of:

$$F_{cr} = \frac{11,54}{1,7756 \cdot 10^{-4} \cdot 1} = 64991\text{N} \quad (3.70)$$

Ansys gives a critical buckling load of 61937N, so the critical buckling load calculated using Betti's theorem gives an overestimation of 4,9%. This overestimation is caused by the number of displacements in the calculation of Betti's theorem. The displacements of the frame are only determined at the top of the columns, which results that the buckling mode of the frame cannot be simulated accurately. It gives an approximation of the buckling mode and results in a too stiff behaviour of the buckling mode.

3.2.4 Example of a more degrees of freedom system

To simulate the buckling mode more accurately, the number of displacements of the frame can be extended. In the cases with more degrees of freedom for each column, the degrees of freedom will be evenly distributed over the height of the columns. For instance, for a frame with two degrees of freedom for each column, the first degree of freedom will be positioned at the top of the column and the second degree of freedom will be positioned at half column height. The total displacement which occurs in the upper element is w_1 minus the displacement at the top of the lower element w_2 as given in figure 3.16.

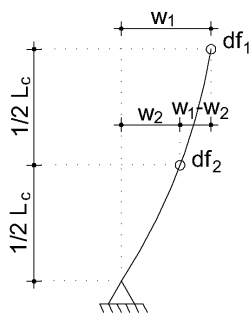


Figure 3.16: Displacements of a column with two degrees of freedom

When the frame of figure 3.15 will be analyzed according to a system with two degrees of freedom for each column, the buckling load parameters which should be known to determine the critical buckling load according to Betti's Theorem are given in table 3.2.

Table 3.2. Buckling load parameters of the frame given in figure 3.15

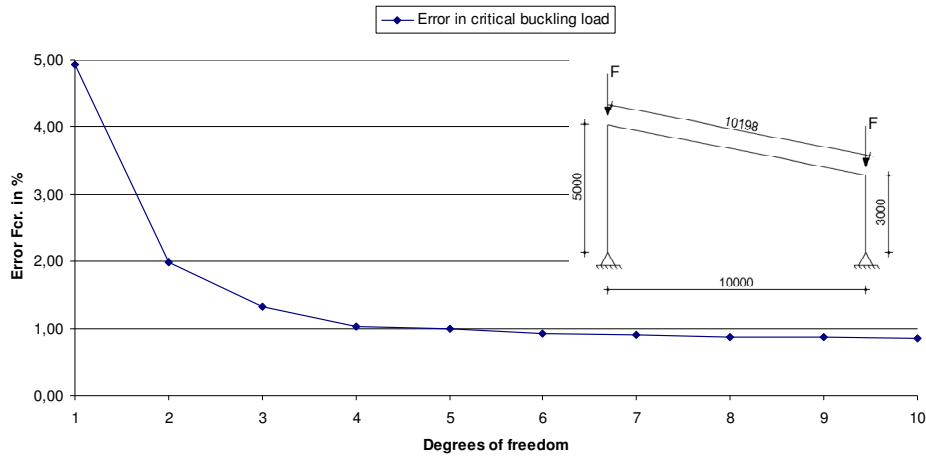
Element	V_e	L_e	$w_{e,i}$	$V_e * w_{e,i}$	$n * (w_{e,i}^2 / L_e)$
Left 1	6	2500	0,221	1,328	$1,9590 * 10^{-5}$
Left 2	6	2500	0,356	2,134	$5,0609 * 10^{-5}$
Right 1	14	1500	0,255	3,563	$4,3180 * 10^{-5}$
Right 2	14	1500	0,322	4,512	$6,9252 * 10^{-5}$
Sum				11,537	$1,8263 * 10^{-4}$

According to Eq. (3.69) the critical buckling load is:

$$F_{cr} = \frac{11,537}{1,8263 \cdot 10^{-4} \cdot 1} = 63171\text{N} \quad (3.70)$$

A critical buckling load of 63171N gives an overestimation of 2% in comparison with Ansys. This example clearly shows that using a two degree of freedom system the buckling mode can be simulated more accurately and results thus in a less stiff behaviour of the buckling mode. Graph 3.2. shows the error in critical buckling load related to the number of degrees of freedom in each column for the frame

given in figure 3.15. In this graph it can be seen that when the number of degrees in freedom increase, an asymptote arise on x-axis.



Graph 3.2: Error in critical buckling load related to the number of degrees of freedom in each column

3.3 Kinematic models

Kinematic models are models from which an accurate approximation of the critical buckling load can be determined and consist of bars with an infinite flexural rigidity, the so called pendulum columns [12]. The nodes between these pendulum columns are laterally supported using translational springs with the exception of the node at the bottom. Kinematic models can exist in one degree of freedom systems or multiple degrees of freedom systems. In the case of figure 3.16b the structure consists of a model with two degrees of freedom, with two displacements required to define its displacement configuration.

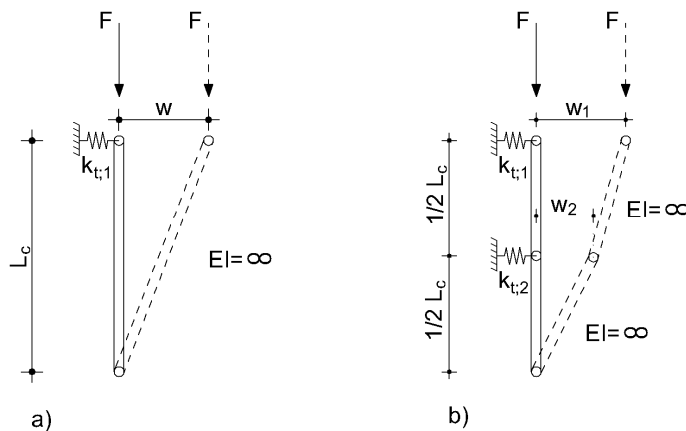


Figure 3.16: a) Model with one degree of freedom b) Model with two degrees of freedom

The translational spring stiffness represents the flexural rigidity of a certain column. To replace a certain column with a flexural rigidity for a kinematic model, the column will be coupled by means of rods with the pendulum columns as shown in figure 3.18. These rods ensure that the degrees of freedom of the pendulum columns displace with the same distance as the position where the rods are coupled with the structure.

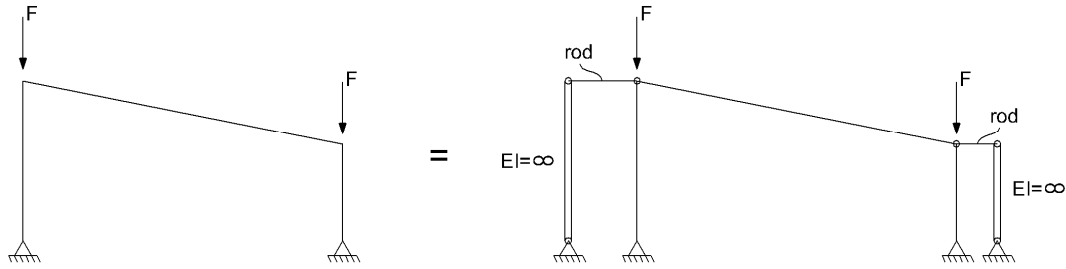


Figure 3.17: Coupling of columns with pendulum columns results in a kinematical model with in this case one degree of freedom for each column.

The non-orthogonal frame of figure 3.15 is modeled as a kinematic model with 2 degrees of freedom (1 degree of freedom for each column) as given in figure 3.18. To obtain displacements which are similar to the buckling mode of the frame, lateral loads have to be applied at the top of the columns which are in proportion to the vertical loads existing at the columns [10].

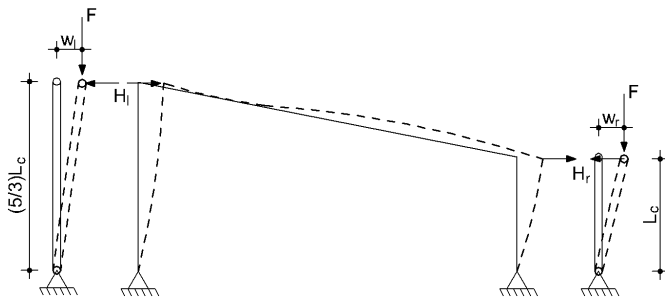


Figure 3.18: Kinematic model of the frame in figure 3.15

From the equilibrium follows:

$$F \cdot w_l = H_l \cdot (5/3) \cdot L_c \quad \rightarrow \quad H_l = \frac{F \cdot w_l}{(5/3) \cdot L_c} \quad (3.71)$$

$$F \cdot w_r = H_r \cdot L_c \quad \rightarrow \quad H_r = \frac{F \cdot w_r}{L_c} \quad (3.72)$$

The displacements at the top of the columns can be written as:

$$w_l = \frac{0.7449 \cdot H_l \cdot L_c^3}{EI_c} + \frac{0.7449 \cdot H_r \cdot L_c^3}{EI_c} \quad (3.73)$$

$$w_r = \frac{0.7449 \cdot H_l \cdot L_c^3}{EI_c} + \frac{0.7449 \cdot H_r \cdot L_c^3}{EI_c} \quad (3.74)$$

Eq. (3.71) and (3.72) substituted in Eq. (3.73) and (3.74) gives:

$$w_l = \frac{0.4469 \cdot F \cdot w_l \cdot L_c^2}{EI_c} + \frac{0.7449 \cdot F \cdot w_r \cdot L_c^2}{EI_c} \quad (3.75)$$

$$w_r = \frac{0.4469 \cdot F \cdot w_l \cdot L_c^2}{EI_c} + \frac{0.7449 \cdot F \cdot w_r \cdot L_c^2}{EI_c} \quad (3.76)$$

and can be written as matrix:

$$\begin{pmatrix} 1 - 0.4469 \cdot \frac{F \cdot L_c^2}{EI_c} & -0.7449 \cdot \frac{F \cdot L_c^2}{EI_c} \\ -0.4469 \cdot \frac{F \cdot L_c^2}{EI_c} & 1 - 0.7449 \cdot \frac{F \cdot L_c^2}{EI_c} \end{pmatrix} \cdot \begin{pmatrix} w_l \\ w_r \end{pmatrix} = 0 \quad (3.77)$$

To find a non-trivial solution the determinant of matrix (3.77) is:

$$\left(1 - 0.4469 \cdot \frac{F \cdot L_c^2}{EI_c}\right) \cdot \left(1 - 0.7449 \cdot \frac{F \cdot L_c^2}{EI_c}\right) - \left(-0.7449 \cdot \frac{F \cdot L_c^2}{EI_c}\right) \cdot \left(-0.4469 \cdot \frac{F \cdot L_c^2}{EI_c}\right) = 0 \quad (3.78)$$

Eq. (3.78) results in a critical buckling load of 64988N. This is an overestimation of 4.9% in comparison with the critical buckling load found by Ansys.

A four degree of freedom system results in a critical buckling load of 62938N (see Appendix D) and is an overestimation of 1.6% in comparison with the critical buckling load found by Ansys. It can be seen that kinematic models result in upper bound solutions and multiple degrees of freedom result in a more accurate approximation of the critical buckling load since the buckling mode of the frame can be simulated more accurately.

3.4 Influence of an axial force in the beam on the critical buckling load

Betti's theorem and the kinematic models as described in chapter 3.2 and 3.3 give critical buckling loads of regular and irregular frames for cases where no axial forces in the beams occur. In this chapter an approach will be given, based on Rieckmanns table, where the influence of an axial force in the beam on the critical buckling load can be taken into account. This approach is analyzed by means of parameter studies.

3.4.1 Decrease in critical buckling load for symmetrical pitched-roof frames

For symmetrical pitched-roof frames, where the beams are loaded in compression due to a uniformly distributed load, Rieckmann developed a table from which the critical buckling load of such frames can be determined (see table 2.2) using the parameters δ and γ .

$$\delta = \frac{EI_c \cdot L_b}{EI_b \cdot L_c}, \text{ and} \quad (3.79)$$

$$\gamma = \sqrt{\delta \cdot \frac{N_b \cdot L_b}{N_c \cdot L_c}} \quad (3.80)$$

This table also enables to determine the critical buckling load for symmetrical pitched-roof frames where no axial force in the beams occurs using the parameters related to $\gamma = 0$.

Due to compression forces in the beam the critical buckling load of the columns decrease. In table 3.3 the table of Rieckmann has been written in the form where the total decrease in critical buckling load of the columns can be determined. Substituting parameter β_Δ in Eq. (3.81) results in the decrease in critical buckling load, ΔF_{cr} .

$$\frac{\pi^2 \cdot EI_c}{(\beta_\Delta \cdot L_c)^2} = \Delta F_{cr} \quad (3.81)$$

The β_Δ parameters are obtained by determining the critical buckling load using Rieckmanns table where no axial force in the beam occurs, minus the critical buckling load using Rieckmanns table where an axial force in the beam is present.

$$\Delta F_{cr} = \frac{\pi^2 \cdot EI_c}{(\beta_{c;\gamma=0} \cdot L_c)^2} - \frac{\pi^2 \cdot EI_c}{(\beta_{c;\gamma \neq 0} \cdot L_c)^2} \quad (3.82)$$

Table 3.3 makes it possible to determine the critical buckling load of symmetrical pitched-roof frames using Betti's theorem and kinematic models where ΔF_{cr} of Eq. (3.82) can be taken into account by subtracting it from the critical buckling loads found using Betti's theorem and kinematic models.

Table 3.3: Parameters β_{Δ} to determine the decrease in critical buckling load of the columns for symmetrical pitched-roof frames.

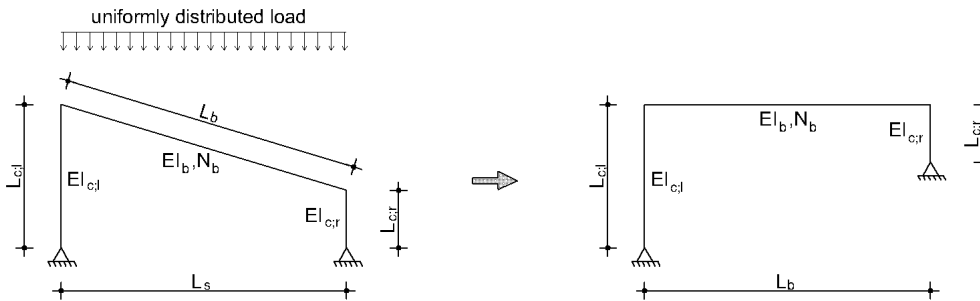
$\delta \backslash \gamma$	0.0000	0.500	1.000	1.500	2.000	2.500	3.000	4.000	6.000	8.000
0.200	∞	31.207	14.642	8.416	5.113	3.541	2.932	2.506	2.280	2.213
0.600	∞	25.012	11.991	7.517	5.292	4.085	3.451	2.910	2.598	2.503
1.000	∞	25.664	12.557	8.114	5.916	4.691	3.987	3.323	2.912	2.785
1.500	∞	27.965	13.843	9.139	6.802	5.471	4.661	3.838	3.293	3.121
2.000	∞	30.863	15.615	10.334	7.758	6.266	5.341	4.355	3.666	3.444
2.500	∞	35.527	17.428	11.584	8.742	7.071	6.023	4.871	4.031	3.754
3.000	∞	39.142	19.327	12.891	9.731	7.882	6.707	5.387	4.390	4.054
3.500	∞	42.658	21.205	14.201	10.727	8.686	7.388	5.901	4.744	4.346
4.000	∞	46.086	23.246	15.517	11.715	9.494	8.065	6.413	5.094	4.632
4.500	∞	49.429	24.922	16.788	12.712	10.295	8.739	6.922	5.441	4.911
5.000	∞	54.444	27.206	18.131	13.730	11.115	9.424	7.439	5.788	5.189
5.500	∞	57.771	29.094	19.490	14.736	11.936	10.109	7.949	6.132	5.462
6.000	∞	61.029	30.982	20.794	15.725	12.743	10.782	8.458	6.474	5.731
6.500	∞	64.230	32.875	22.111	16.726	13.531	11.450	8.965	6.815	5.997
7.000	∞	69.743	34.780	23.446	17.743	14.347	12.130	9.476	7.156	6.262
7.500	∞	75.724	37.033	24.901	18.782	15.181	12.824	9.990	7.498	6.527
8.000	∞	76.140	38.981	26.174	19.746	15.963	13.493	10.495	7.836	6.787

Decrease of the critical buckling load of the column: $\Delta F_{cr} = \frac{\pi^2 \cdot E I_c}{(\beta_{\Delta} \cdot L_c)^2}$

Although this table is particularly developed for symmetrical pitched-roof frames, approaches have been developed to approximate the decrease in critical buckling load for asymmetrical frames loaded by a uniformly distributed load over the length of the span using this table. Firstly frame 2 has been investigated. Below the approach is illustrated.

3.4.2 Approach to determine the decrease in critical buckling load for frame 2

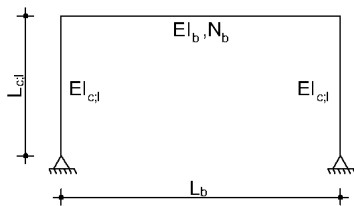
1. Determine the mean compression force in the beam and the compression force in the columns due to the uniformly distributed load.



Note: L_b for Rieckmann parameters δ and γ is $(1/2) \cdot L_b$ of frame 2.

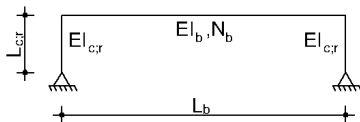
2. Determine the decrease in critical buckling load of the column using table 3.2 for an orthogonal frame where the properties of the left-hand column are taken into account and the properties of the beam with the mean compression force determined in step 1.

$$\Delta F_{cr,l} = \frac{\pi^2 \cdot EI_{c,l}}{(\beta_{\Delta,l} \cdot L_{c,l})^2} \quad (3.83)$$



Determine also the decrease in critical buckling load where the properties of the right-hand column are taken into account and the properties of the beam with the mean compression force determined in step 1.

$$\Delta F_{cr,r} = \frac{\pi^2 \cdot EI_{c,r}}{(\beta_{\Delta,r} \cdot L_{c,r})^2} \quad (3.84)$$



3. From these two decreases, calculated in step 2, determine the mean. This mean gives an approximation of the decrease in critical buckling load for the columns in frame 2.

$$\Delta F_{cr,calc} = \frac{\Delta F_{cr,l} + \Delta F_{cr,r}}{2} \quad (3.85)$$

3.4.3 Applicability of the approach developed for frame 2

A number of frames have been analyzed using this approach, where the following features and boundary conditions have been applied to the frames:

- The left column has a fixed length
- $0.3 \leq \frac{L_{c,r}}{L_{c,l}} \leq 1.0$
- $2.0 \leq \frac{L_s}{L_{c,l}} \leq 4.0$
- $1.0 \leq \frac{EI_c}{EI_b} \leq 7.0$
- $0.5 \leq \gamma \leq 8.0$
- $0.2 \leq \delta \leq 8.0$

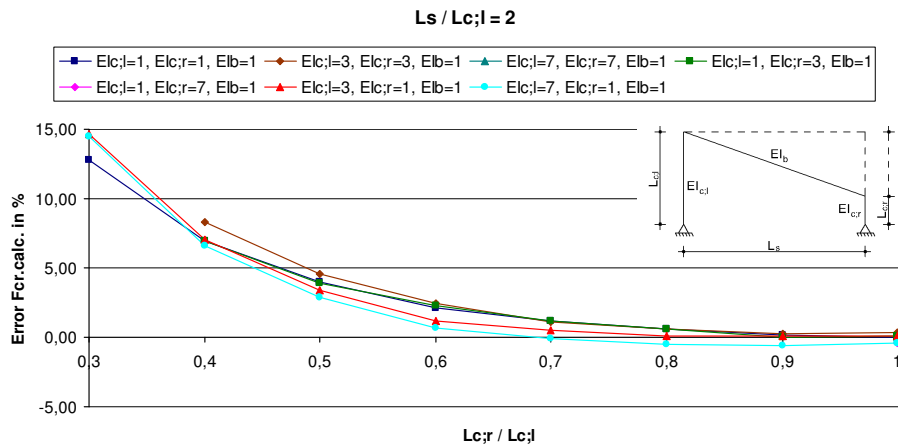
For these analyses, the critical buckling loads of the columns are determined exact using LBA in Ansys without an axial force in the beam ($F_{cr,ANSYS;Nb=0}$) and with an axial force in the beam ($F_{cr,ANSYS}$). Next, the calculated decreases, $\Delta F_{cr,calc}$, as described in the approach are determined and are subtracted from the Ansys results without an axial force in the beam. This results in the 'calculated' critical buckling load.

$$F_{cr,calc} = F_{cr,ANSYS;Nb=0} - \Delta F_{cr,calc} \quad (3.86)$$

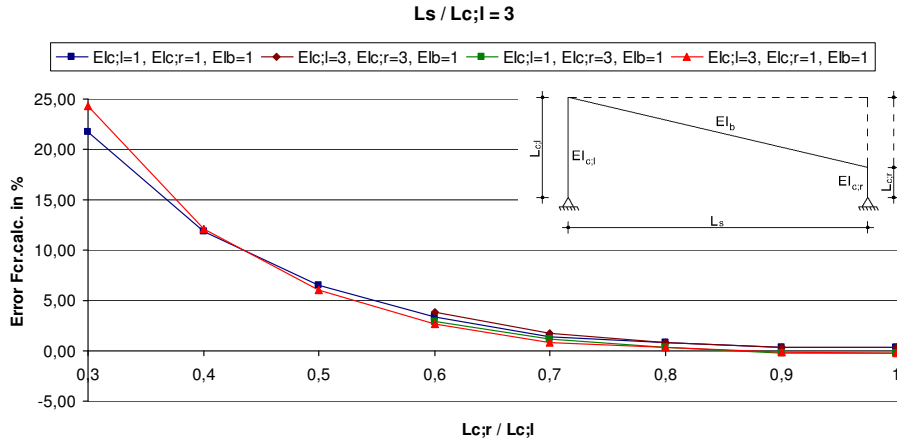
Finally, the errors in percentages for the calculated critical buckling loads have been determined using:

$$\text{Error} = \frac{F_{cr,ANSYS} - F_{cr,calc}}{F_{cr,ANSYS}} \cdot 100\% \quad (3.87)$$

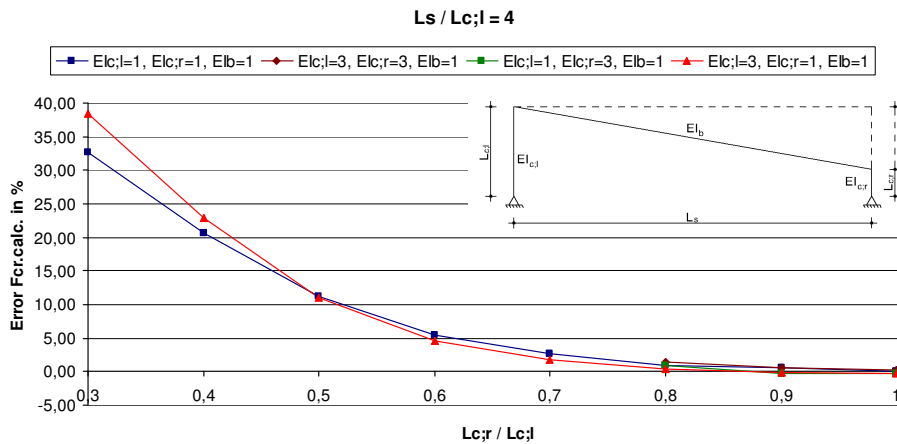
In graphs 3.2 to 3.4, the errors for the calculated critical buckling load are shown in graphs with on horizontal x- axis the ratio between the length of the left-hand column and the right-hand column and on vertical y-axis the error percentage. Errors lower than zero percent imply an underestimation of the calculated critical buckling load and give a safe approximation. A difference greater than zero percent implies an overestimation of the calculated critical buckling load and results thus in an unsafe approximation. The results depend only on the ratio between the flexural rigidity of the members, the ratio between both column lengths and the ratio between the column lengths and the span. Because of this, only ratios are given in the graphs.



Graph 3.2: Error $F_{cr,calc}$ for $\frac{L_s}{L_{c,l}} = 2$



Graph 3.3: Error $F_{cr.calc.}$ for $\frac{L_s}{L_{c;l}} = 3$



Graph 3.4: Error $F_{cr.calc.}$ for $\frac{L_s}{L_{c;l}} = 4$

Most errors show an overestimation in calculated critical buckling load and they show that when the ratio between the column lengths comes closer to zero, the errors in critical buckling load increase. As well as the ratio in column lengths, the ratio between the span and the column lengths influences the error in calculated critical buckling load. By increasing this ratio, the error in critical buckling load will also increase. If the acceptable range in overestimation and underestimation in critical buckling load will be set at 5 percent, most frames with a column length ratio below 0.5 do not fulfill this requirement.

3.4.4 Refinement of the approach for frame 2

To reduce the errors in calculated critical buckling load, the approach has been extended. For this extension, the difference between the exact decrease in critical buckling load, $\Delta F_{cr;ANSYS} = F_{cr;ANSYS;Nb=0} - F_{cr;ANSYS}$, and the calculated decrease in buckling load as given in Eq. (3.85) has been investigated for all analyses. The ratios of the decreases are calculated using:

$$\frac{\Delta F_{cr;ANSYS}}{\Delta F_{cr;calc}} \quad (3.88)$$

Eq. (3.87) results thus in a multiplier/correction factor for the approximate calculated decrease in critical buckling load to obtain the exact decrease in critical buckling load.

As shown in graph 3.2 to 3.4, the errors in calculated critical buckling load will not be strongly influenced by the ratios of the flexural rigidity. Therefore, mean ratios have been determined related to a particular column length ratio and a particular column-span ratio using Eq. (3.89).

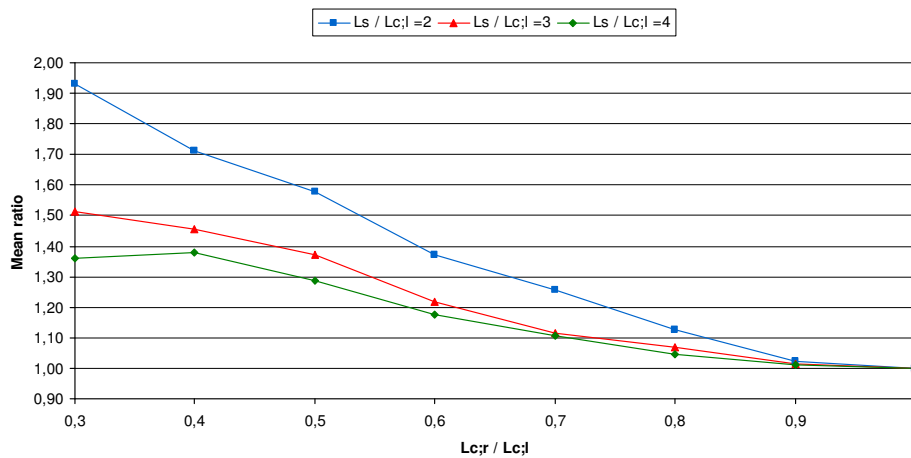
$$\bar{X} = \frac{\sum_{i=1}^n \Delta F_{cr.ANSYS}}{\sum_{i=1}^n \Delta F_{cr.calc.}} \quad (3.89)$$

Where n is the number of analyzed frames related to a particular column length ratio and a particular column-span ratio.

The mean ratios \bar{X} are given in table 3.3 and plotted in graph 3.5.

Table 3.3: Mean ratios \bar{X} between the exact decrease in critical buckling load and the 'calculated' decrease in critical buckling load

$L_s/L_{c,i}$ \ $L_{c,r}/L_{c,i}$	0,3	0,4	0,5	0,6	0,7	0,8	0,9	1,0
2	1,93	1,71	1,58	1,37	1,25	1,12	1,02	1,00
3	1,51	1,45	1,37	1,22	1,11	1,07	1,01	1,00
4	1,36	1,38	1,29	1,18	1,11	1,04	1,01	1,00

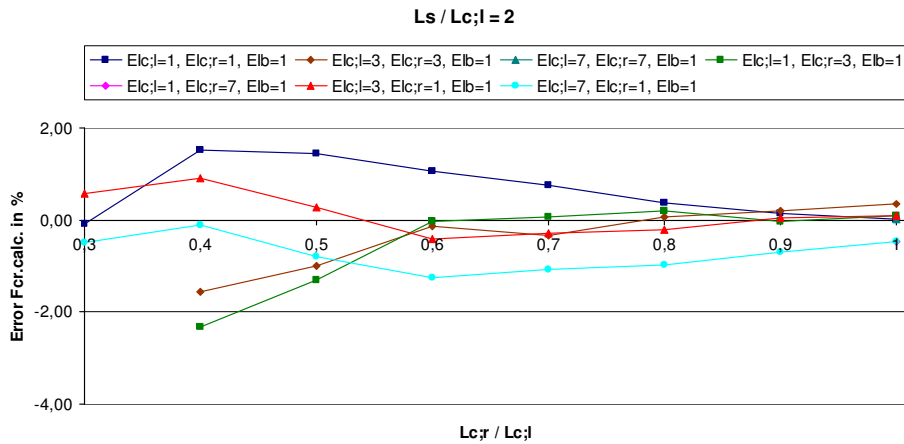


Graph 3.5: Mean ratios \bar{X}

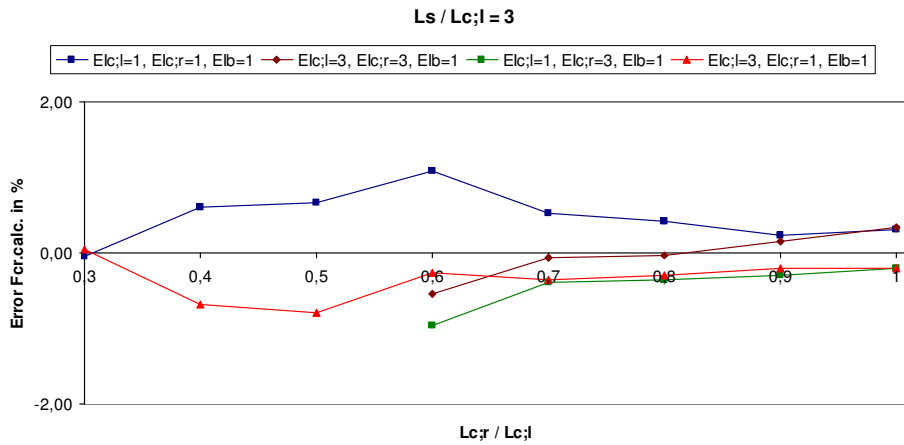
Using these mean ratios, a more accurate approximation of the decrease in critical buckling load can be determined using:

$$\Delta F_{cr.calc.} = \frac{\Delta F_{cr.l} + \Delta F_{cr.r}}{2} \cdot \bar{X} \quad (3.90)$$

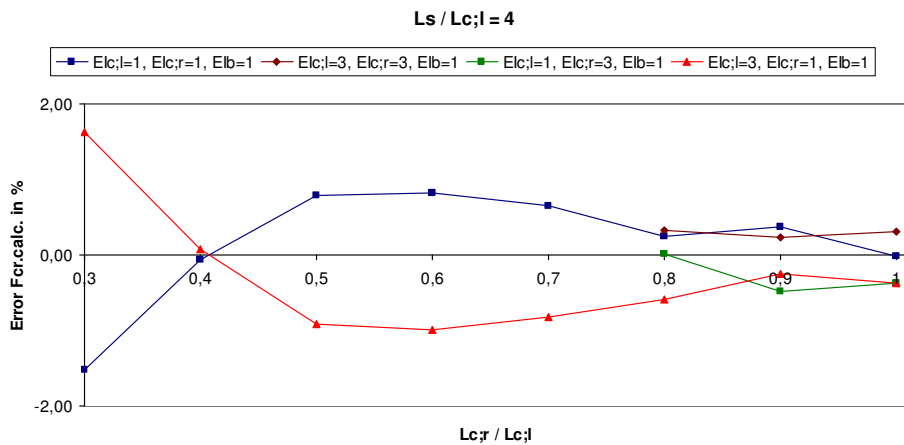
Applying Eq. (3.90) in the analyses of the frames, the errors in critical buckling are much lower and this is shown in the graphs 3.6 to 3.8.



Graph 3.6: Error $F_{cr.calc.}$ for $\frac{L_s}{L_{c_j}} = 2$, in which the mean ratios \bar{X} are taken into consideration



Graph 3.7: Error $F_{cr.calc.}$ for $\frac{L_s}{L_{c_j}} = 3$, in which the mean ratios \bar{X} are taken into consideration

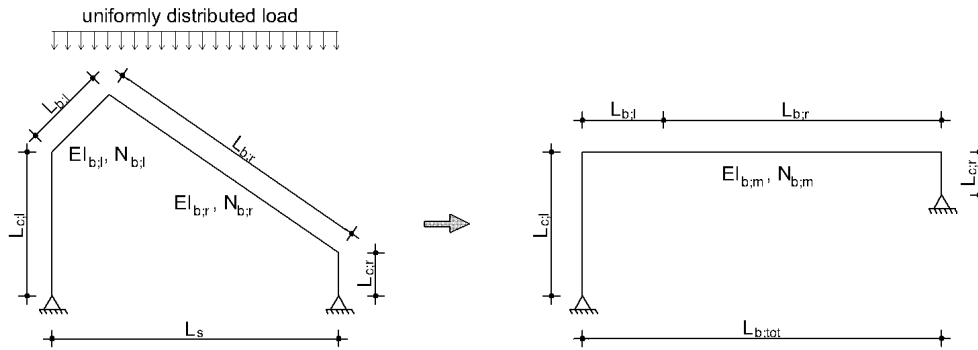


Graph 3.8: Error $F_{cr.calc.}$ for $\frac{L_s}{L_{c_j}} = 4$, in which the mean ratios \bar{X} are taken into consideration

The results shown in graph 3.6 - 3.8 give errors in critical buckling load between the 2 percent overestimation and 3 percent underestimation and are all in the acceptable range.

3.4.5 Approach to determine the decrease in critical buckling load for frame 1

The approach for frame 1 shows many similarities with the approach for frame 2. First of all, the frame will be considered as a frame with a single beam with a mean axial force in the beam and a mean flexural rigidity of the beam.



The mean axial force in the beam can be calculated using the following equation:

$$N_{b,m} = N_{b,l} \cdot \frac{L_{b,l}}{L_{b,tot}} + N_{b,r} \cdot \frac{L_{b,r}}{L_{b,tot}} \quad (3.91)$$

And the mean flexural rigidity of the beam can be calculated using:

$$EI_{b,m} = EI_{b,l} \cdot \frac{L_{b,l}}{L_{b,tot}} + EI_{b,r} \cdot \frac{L_{b,r}}{L_{b,tot}} \quad (3.92)$$

From this considered frame the decrease in buckling load will be determined where the properties of the left column are taken into account for both columns and once with the properties of the right column for both columns, as described in approach step 2 of frame 2. From these both decreases the mean will be determined and results in an approximation of the decrease in critical buckling load.

$$\Delta F_{cr;calc} = \frac{\Delta F_{cr,l} + \Delta F_{cr,r}}{2} \quad (3.93)$$

Note: L_b for Rieckmann parameters δ and γ is $(1/2) \cdot L_{b,tot}$ of frame 1.

3.4.6 Applicability of the approach developed for frame 1

A number of frames have been analyzed according to this approach, where the following features and boundary conditions have been made for the frames:

- The left column has a fixed length
- The left beam has a fixed slope
- The angle between the right beam and right column will be ≥ 90 degrees
- $0.3 \leq \frac{L_{cr}}{L_{c,l}} \leq VAR$

- $2.0 \leq \frac{L_s}{L_{c;l}} \leq 4.0$
- $1.0 \leq \frac{EI_c}{EI_b} \leq 7.0$
- $0.5 \leq \gamma \leq 8.0$
- $0.2 \leq \delta \leq 8.0$

Graphs 3.9 to 3.11 give the results for frames with a slope of the left beam of 25 degrees and the horizontal distance of the apex located at one fifth of the span. This model is given in figure 3.19. The method and the processing of the results in graphs have been executed in exactly the same way as for frame 2.

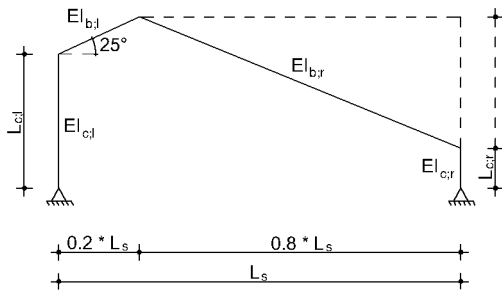
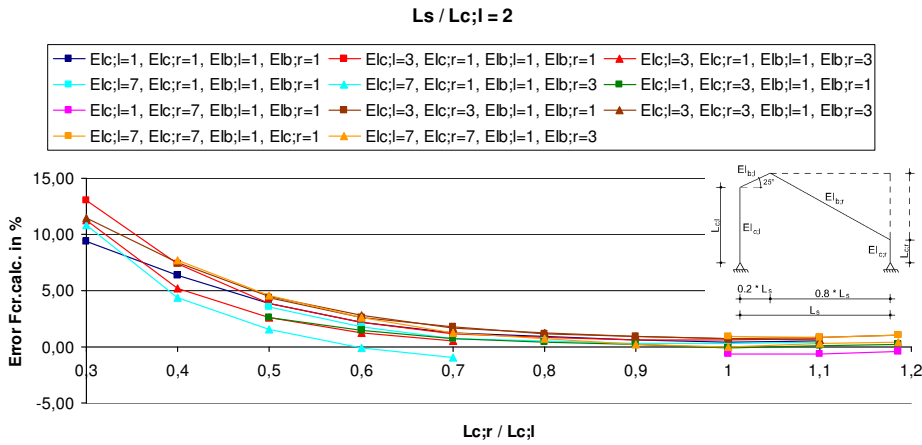
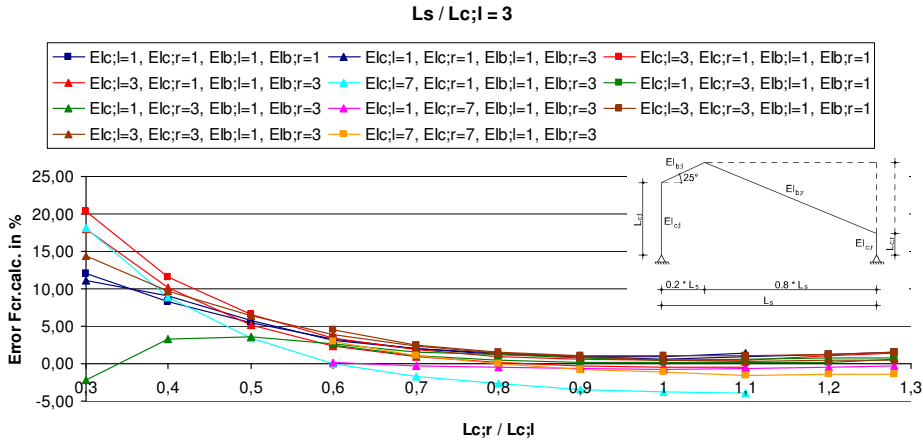


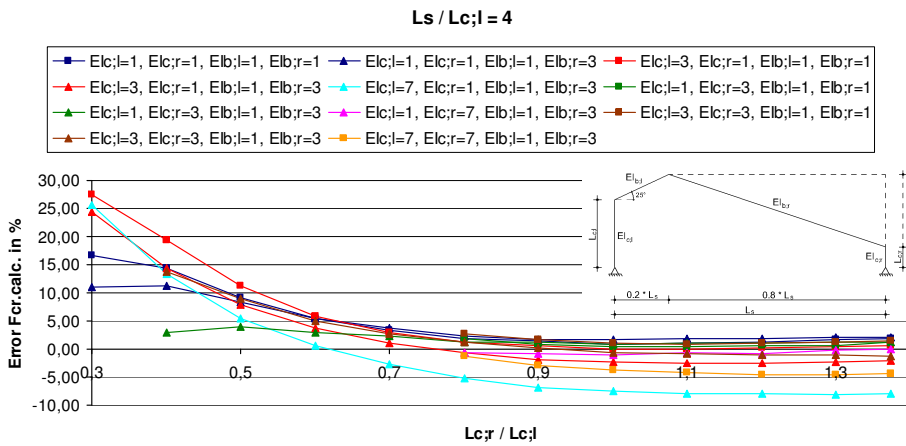
Figure 3.19: Model for the graphs 3.9 to 3.11



Graph 3.9: Error $F_{cr.calc.}$ for $\frac{L_s}{L_{c;l}} = 2$, $\theta_l = 25^\circ$ and the apex on a horizontal distance of $0.2 \cdot L_s$



Graph 3.10: Error $F_{cr.calc.}$ for $\frac{L_s}{L_{c,l}} = 3$, $\theta_1 = 25^\circ$ and the apex on a horizontal distance of $0,2 \cdot L_s$



Graph 3.11: Error $F_{cr.calc.}$ for $\frac{L_s}{L_{c,l}} = 4$, $\theta_1 = 25^\circ$ and the apex on a horizontal distance of $0,2 \cdot L_s$

Graphs 3.12 to 3.14 give the results for frames with a slope of the left beam of 45 degrees and the horizontal distance of the apex located at one fifth of the span. This model is shown in figure 3.20.

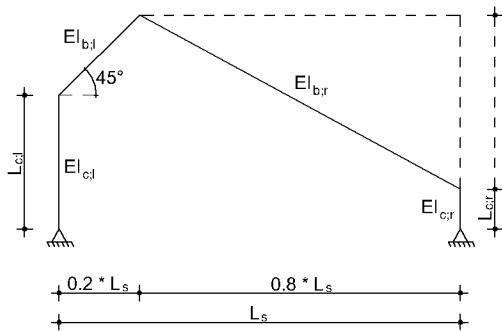
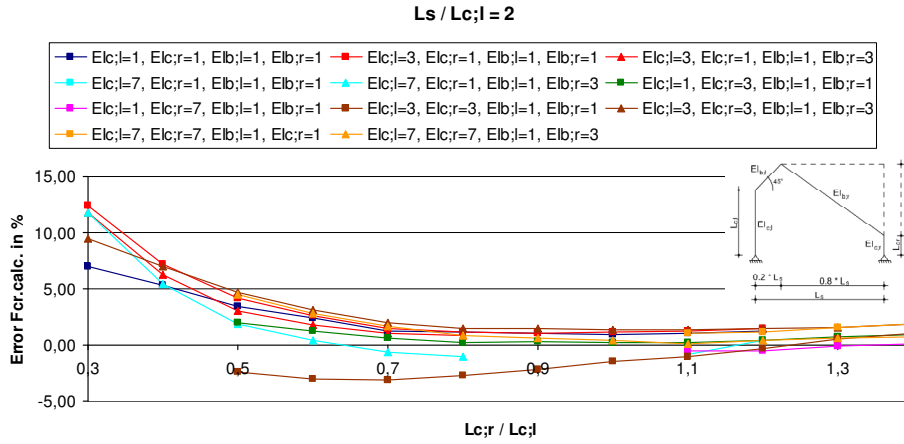
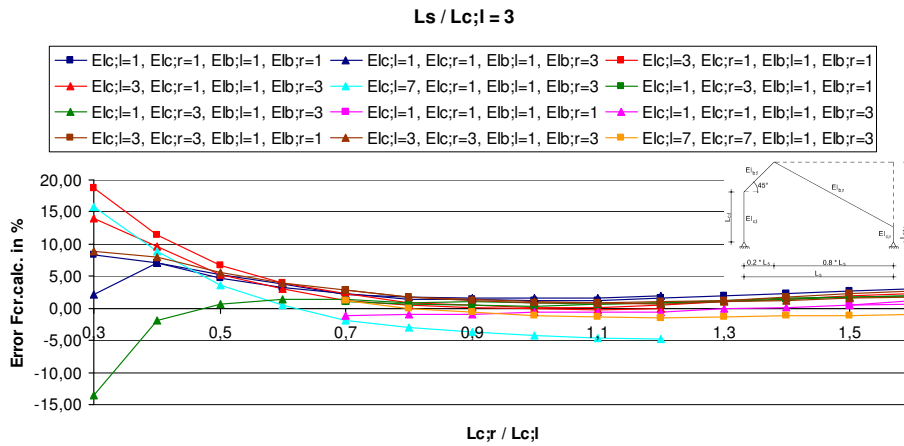


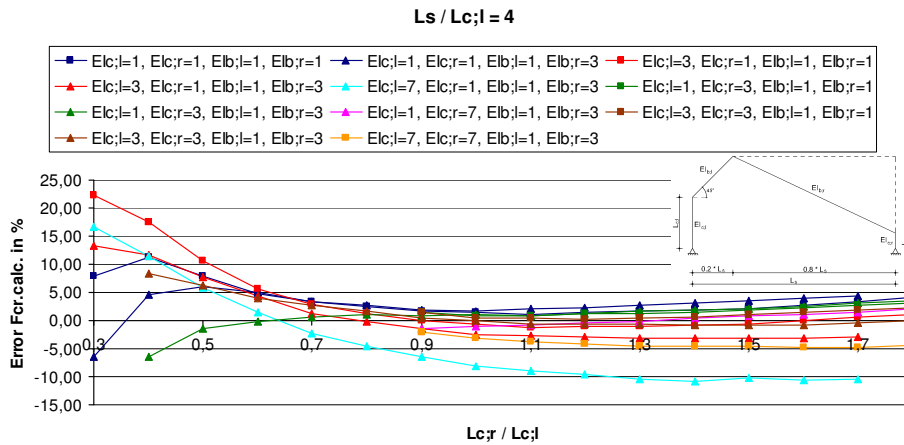
Figure 3.20: Model for the graphs 3.12 to 3.14



Graph 3.12: Error $F_{cr.calc.}$ for $\frac{L_s}{L_{c;l}} = 2$, $\theta_1 = 45^\circ$ and the apex on a horizontal distance of $0,2 \cdot L_s$



Graph 3.13: Error $F_{cr.calc.}$ for $\frac{L_s}{L_{c;l}} = 3$, $\theta_1 = 45^\circ$ and the apex on a horizontal distance of $0,2 \cdot L_s$

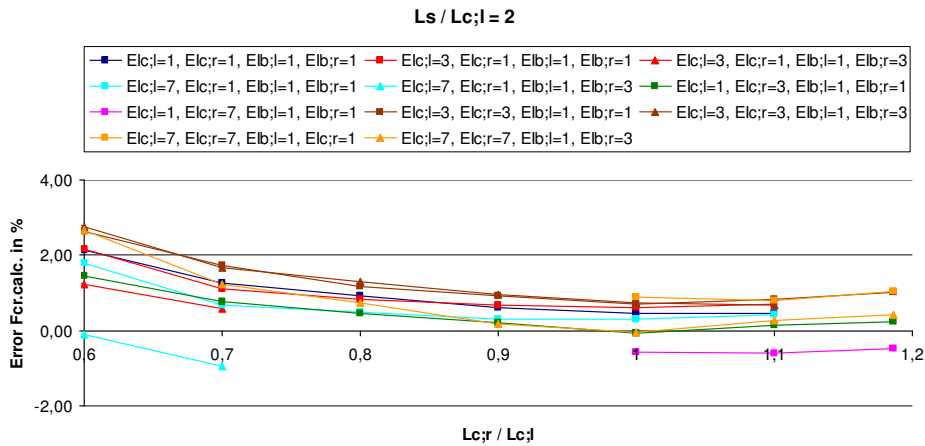


Graph 3.14: Error $F_{cr.calc.}$ for $\frac{L_s}{L_{c;l}} = 4$, $\theta_1 = 45^\circ$ and the apex on a horizontal distance of $0,2 \cdot L_s$

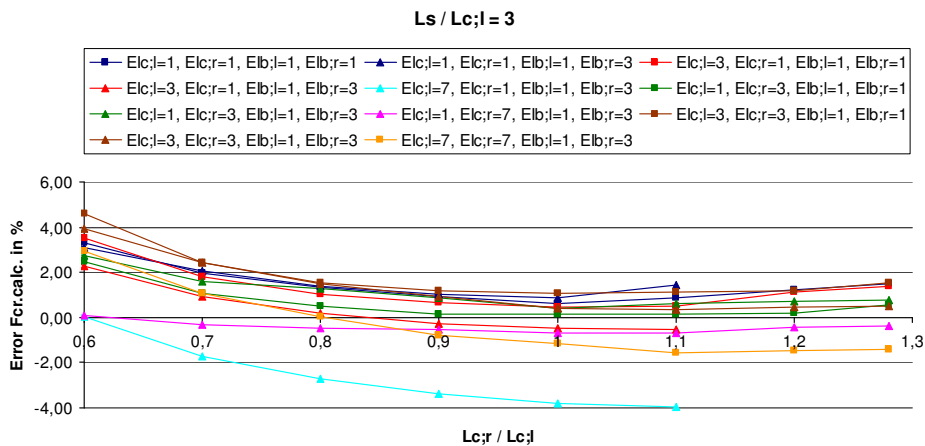
As seen in graphs 3.9 – 3.14 the overestimation in critical buckling load will not be greater than 5 percents by a column ratio of 0.7 or greater. Striking, when the column length ratio will come closer to 0.3 and the span to column ratio will be greater than 2, wide ranges in errors occur. In the cases where the right beam has a flexural rigidity greater than or equal to the right column, the error line will decline and results in some analyses in an underestimation of the critical buckling load. For all other cases, when the ratio comes closer to 0.3, the overestimation increases.

For frame 2, a multiplier/correction factor has been developed to reduce the errors in calculated critical buckling load. This factor has reduced the errors effectively, because the calculated critical buckling loads were all overestimated and were not strongly influenced by the ratios of the flexural rigidity. The analyses of frame 1 show that the error in calculated critical buckling load for a certain span to column ratio are (slightly) underestimated or overestimated. Therefore the application of a multiplier by determining mean ratios using Eq. (3.88) will not result in a significant decrease in error, since the multiplier is close to 1.

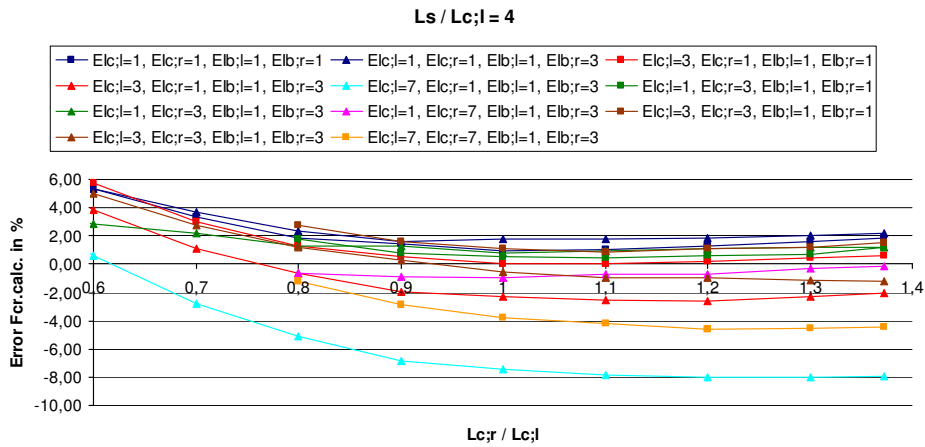
Due to wide range in errors for column length ratios below 0.6, the approach of frame 1 can only be used for column length ratios of 0.6 or greater. The graphs 3.9 to 3.14 have been re-plotted with this boundary condition and are shown in graphs 3.15 to 3.20.



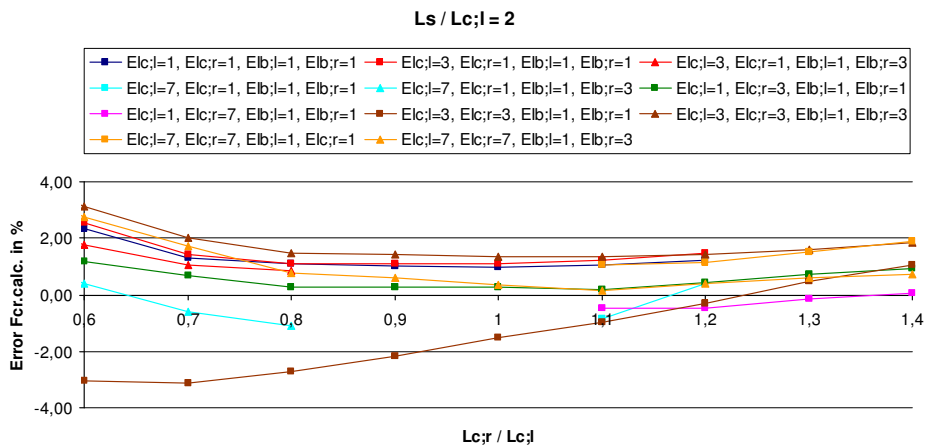
Graph 3.15: Error $F_{cr.calc.}$ for $\frac{L_s}{L_{c_j}} = 2$, $\theta_1 = 25^\circ$ and the apex on a horizontal distance of $0,2 \cdot L_s$



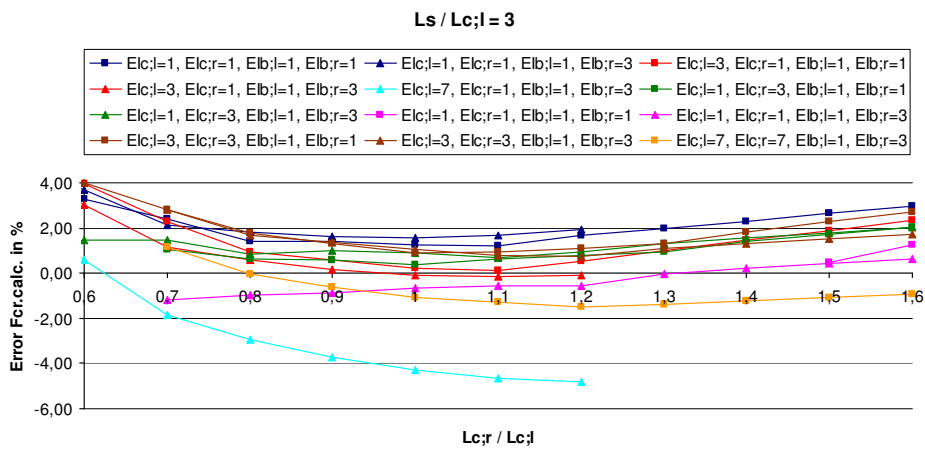
Graph 3.16: Error $F_{cr.calc.}$ for $\frac{L_s}{L_{c_j}} = 3$, $\theta_1 = 25^\circ$ and the apex on a horizontal distance of $0,2 \cdot L_s$



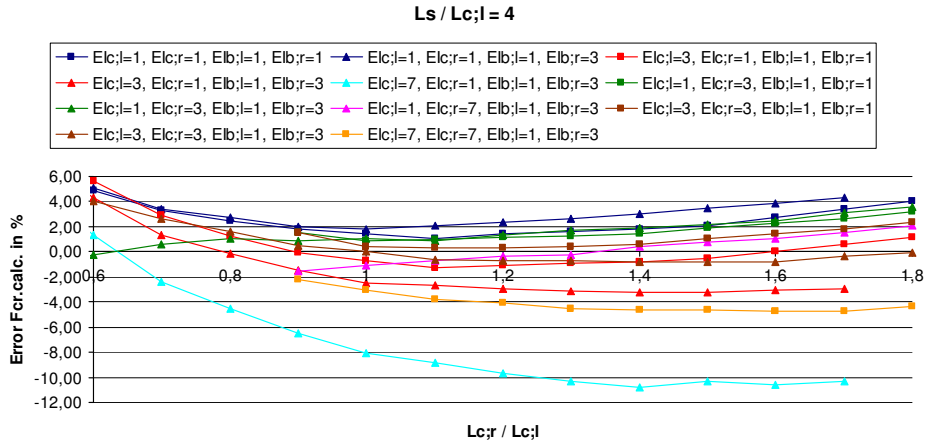
Graph 3.17: Error $F_{cr.calc.}$ for $\frac{L_s}{L_{c;l}} = 4$, $\theta_1 = 25^\circ$ and the apex on a horizontal distance of $0,2 \cdot L_s$



Graph 3.18: Error $F_{cr.calc.}$ for $\frac{L_s}{L_{c;l}} = 2$, $\theta_1 = 45^\circ$ and the apex on a horizontal distance of $0,2 \cdot L_s$



Graph 3.19: Error $F_{cr.calc.}$ for $\frac{L_s}{L_{c;l}} = 3$, $\theta_1 = 45^\circ$ and the apex on a horizontal distance of $0,2 \cdot L_s$



Graph 3.20: Error $F_{cr,calc.}$ for $\frac{L_s}{L_{c,l}} = 4$, $\theta_1 = 45^\circ$ and the apex on a horizontal distance of $0,2 \cdot L_s$

In the previous analyses there has been varied in column lengths, the span to column ratio and the slope of the left beam. In graph 3.14 the errors in calculated critical buckling load have been given for frames where the horizontal distance of the apex is changed from $0,2 \cdot L_s$ to $0,4 \cdot L_s$ for a span to column ratio of 4 and a slope of the left beam of 25 degrees as shown in figure 3.21.

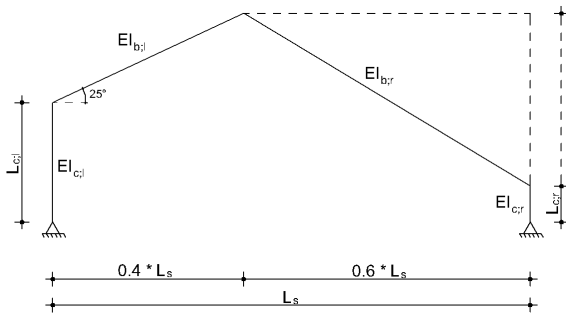
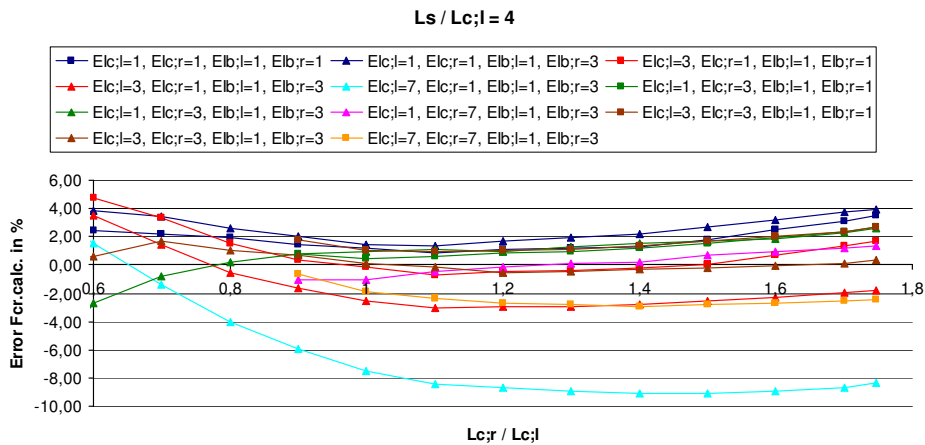


Figure 3.21: Model for graph 3.21



Graph 3.21: Error $F_{cr,calc.}$ by $\frac{L_s}{L_{c,l}} = 4$, $\theta_1 = 25^\circ$ and the apex on a horizontal distance of $0,4 \cdot L_s$

From graph 3.21 it can be seen that the results will not differ significantly from the results of graph 3.17 where the horizontal distance of the apex is located at one fifth of the span.

3.5 Conclusions

In general, the differential equation of equilibrium applied to frame 1 where each column will be analyzed separately, results in safe approximations. Looking at the accuracy of the results, the accuracy differs too much that the exchange of stability between the left-hand column and the right-hand column cannot be described accurately enough using two separate column approaches. However, the critical buckling load of the frame can be determined more accurately than using the approach which is developed by BmS.

Kinematic models and Betti's theorem are two methods in which the critical buckling loads can be determined accurately for frames where the beam is not loaded in compression. The more the buckling mode can be simulated by adding degrees of freedom, the more accurate the critical buckling load can be determined. Using one degree of freedom for each column, critical buckling loads will be found which are about five percent overestimated. In cases with two degrees of freedom the overestimation of the critical buckling loads will be reduced to about two percent.

A disadvantage of kinematic models compared to Betti's theorem is that calculations are very time-consuming, in particular for cases that consist of two or more degrees of freedom for each column. This makes Betti's theorem attractive, since critical buckling loads can be determined using a relatively simple and quick method.

To take the influence of compression forces in the beam(s) into consideration for kinematic models and Betti's theorem, approaches have been developed, based on Rieckmann's table, and the accuracy of these approaches has been investigated for different cases. Because the approaches are based on Rieckmann's table, the connections in all cases were designed as hinged connections at the base and rigid connections between the members.

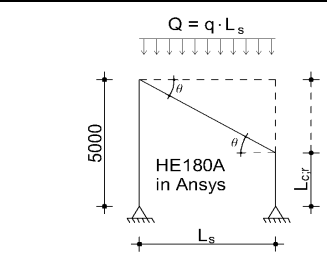
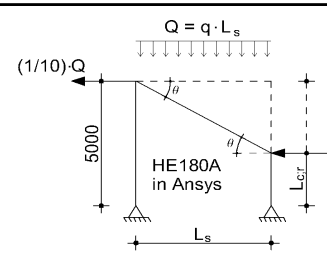
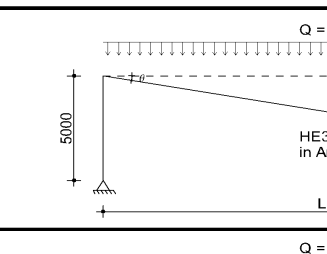
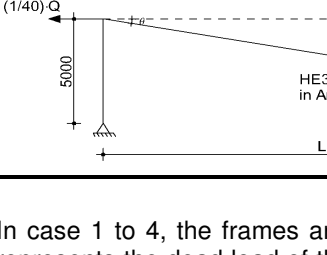
For the investigated cases of frame 1, the maximum overestimation in critical buckling load will not be greater than 6 percent, provided the critical buckling load without an axial force in the beam is exactly determined. The maximum underestimation in critical buckling load will not be greater than 12 percent. For frame 2 the maximum overestimation is 2 percent and the maximum underestimation is 3 percent.

4. Ultimate bearing capacities of trapezoidal frames

4.1 Analysis overview

In this chapter ultimate bearing capacities of trapezoidal frames will be determined for different frame geometries and different load combinations. The frames which will be analyzed are given in table 4.1. To obtain ultimate bearing capacities, imperfections should be modeled which depend on the critical buckling load of the frame. In chapter 3, different methods have been given to obtain accurate approximations of critical buckling loads for trapezoidal frames which are hinged connected at the base and loaded by a uniformly distributed load. Despite the methods give accurate approximations, critical buckling loads for similar cases in table 4.1 will not be determined using the methods of chapter 3. The critical buckling loads will be determined exact in Ansys using LBA. Exact critical buckling loads result in reliable imperfections and therefore in reliable ultimate bearing capacities and reliable stability checks which will be discussed in chapter 5.

Table 4.1: Frame overview

Figure	Case	θ	L_{cr} in mm	L_s in mm	L_b in mm
	1	0	5000	5000	5000
	2	10	4118	5000	5077
	3	20	3180	5000	5321
	4	30	2113	5000	5774
	5	0	5000	5000	5000
	6	10	4118	5000	5077
	7	20	3180	5000	5321
	8	30	2113	5000	5774
	9	0	5000	20000	20000
	10	5	3250	20000	20076
	11	10	1473	20000	20309
	12	0	5000	20000	20000
	13	5	3250	20000	20076
	14	10	1473	20000	20309

In case 1 to 4, the frames are loaded by a uniformly distributed load. The uniformly distributed load represents the dead load of the structure. All members consist of HE180A sections and the properties of these composed Ansys sections are given in table E.2. The span is relatively short in comparison with the column lengths, resulting in a slope of 30 degrees for case 4.

For stability checks in Eurocode 3, each frame should be defined as a sway or a non-sway frame. When a frame is defined as a sway frame, second order effects as a result of horizontal displacements Δ (figure 4.1) of the frame can not be neglected. Eurocode 3 [2] gives information about the application of a second order elastic F- Δ analysis. Second order elastic F- Δ effects can be neglected and a first order elastic analysis for obtaining internal forces suffices only if Eq. (4.1) is satisfied. Frames which satisfy Eq. (4.1) are classified as non-sway frames. In all other cases (i.e. sway frames), a second order elastic F- Δ analysis is required, or a method incorporating these second order effects implicitly.

$$\alpha_{cr} = \frac{F_{cr}}{F_{Ed}} \geq 10 \quad (4.1)$$

Where:

- α_{cr} is the factor by which the design loading would have to be increased to cause elastic instability in a global mode
- F_{cr} is the elastic critical buckling load for global instability mode based on initial elastic stiffnesses
- F_{Ed} is the design load of the structure

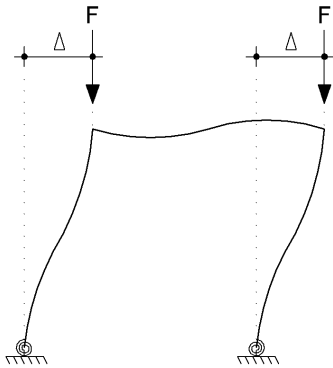


Figure 4.1: Horizontal displacements Δ caused by F

Non-orthogonal frames with roof slopes not steeper than 1:2 (26°), may be analyzed according to Eq. (4.1). For these frames α_{cr} may be calculated using the approximate formula given in Eq. (4.2), provided that the axial compression in the beams may be assumed to be not significant.

$$\alpha_{cr} = \left(\frac{H_{Ed}}{V_{Ed}} \right) \cdot \left(\frac{h_s}{\delta_{H,Ed}} \right) \quad (4.2)$$

Where:

- H_{Ed} is the design value of the horizontal reaction at the bottom of the storey to the horizontal loads and fictitious horizontal loads
- V_{Ed} is the total design vertical load on the structure on the bottom of the storey
- h_s is the storey height
- $\delta_{H,Ed}$ is the horizontal displacement at the top of the storey, relative to the bottom of the storey, when the frame is loaded with horizontal loads and fictitious horizontal loads which are applied at each floor level

The axial compression in the beams is considered significant if:

$$\bar{\lambda} \geq 0,3 \cdot \sqrt{\frac{A \cdot f_y}{N_{Ed}}} \quad (4.3)$$

Where:

- $\bar{\lambda}$ is the inplane non dimensional slenderness calculated for the beam considered as hinged at its ends of the system length measured along the beams.
 N_{Ed} is the design value of the compression force in the beam

The frame in case 4 has a slope of 30 degrees which exceeds the applicability of the approximation formula for α_{cr} given in Eq. (4.2). For this case, Eurocode 3 assumes that the axial force in the beam is significant and Eq. (4.2) may not be used. For all cases, critical buckling loads will be determined exactly, so an approximation of α_{cr} according to Eq. (4.2) need not be performed and all values of α_{cr} will be determined using Eq. (4.1).

The geometry and the members of case 5 to 8 are equal to case 1 to 4, but besides a uniformly distributed load, lateral loads acting on the top of the frame which represent loads due to wind. Different ratios of axial forces arise in the columns due to these lateral loads.

The length of the span for case 9 to 14 is four times as large as the span in case 1 to 8. All members consist of HE320A sections and the properties of these composed sections are given in table E.1. Using these increased spans, a greater axial force will be introduced in the beam compared to the cases where the span is relatively short.

4.2 Material properties

As mentioned in chapter 2.2, imperfections and elastic-plastic material behavior will be considered by determining the ultimate bearing capacity of a frame. When performing a geometric and material non-linear analysis in finite element software a stress-strain relationship with corresponding yield strength has to be described. All geometric and material non-linear analyses in this report are executed using a bi-linear stress-strain relation as shown in figure 4.2. This relation is also called an elastic perfectly plastic model since there is no further increase in stress after initial yielding. Steel grade S235 is taken, which means that the yield stress is 235 N/mm^2 . The Young's modulus is set on $2,1 \cdot 10^5 \text{ N/mm}^2$ and the Poisson ratio on 0.3.

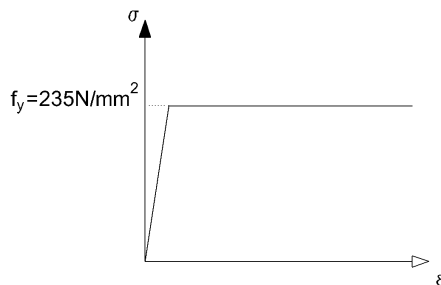


Figure 4.2: Bi-linear stress-strain relationship with a yield strength of 235 N/mm^2

4.3 Imperfections

Eurocode 3 offers several stability checks for frames. Eurocode 3 describes that no stability check for members is necessary if second order effects in individual members and relevant frame imperfections are taken into account in the global analysis of the structure. Imperfections should be incorporated to cover the effects of residual stresses and geometrical imperfections such as lack of verticality, lack of flatness, lack of fit and any minor eccentricities present in joints of the unloaded structure. Eurocode 3 distinguishes two types of imperfections: global and local imperfections. Global imperfections are frame imperfections and affect frame instability using a sway imperfection Δ . Local imperfections are member imperfections and affect member instability using a bow imperfection δ . Both imperfections are shown in figure 4.3. An analysis in which geometric and material second order effects and sway and bow imperfection are taken into account, will be called a Geometric and Material Non-Linear Imperfect Analysis (GMNIA).

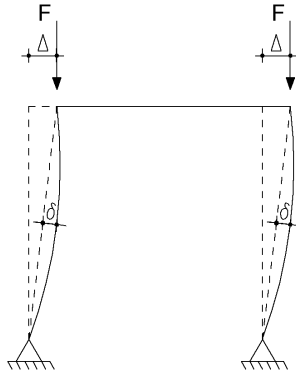


Figure 4.3: Sway imperfections Δ and bow imperfections δ

According to Eurocode 3, the angle of rotation for sway imperfection may be determined from:

$$\varphi = \varphi_0 \cdot \alpha_h \cdot \alpha_m \quad (4.4)$$

Where:

φ_0 is the basic value 1/200
 α_h is the reduction factor for structure height h applicable to columns

$$\alpha_h = \frac{2}{\sqrt{h}}, \text{ but } \frac{2}{3} \leq \alpha_h \leq 1$$

α_m is the reduction factor for the number of columns in a row

$$\alpha_m = \sqrt{0,5 \cdot \left(1 + \frac{1}{m}\right)}$$

m is the number of columns in a row including only these columns which carry a vertical load N_{Ed} not less than 50% of the average value of the column in the vertical plane considered.

In table 5.1 of Eurocode 3 (shown in table 4.2 of this report) a table is given in which the design values of initial local bow imperfections can be determined. According to this table the design value of an initial local bow imperfection depend on the length of the member, the buckling curve and the type of analysis (elastic or plastic).

Table 4.2: Design values of initial local bow imperfections

Buckling curve	elastic analysis	plastic analysis
	δ / L	δ / L
a_0	1 / 350	1 / 300
a	1 / 300	1 / 250
b	1 / 250	1 / 200
c	1 / 200	1 / 150
d	1 / 150	1 / 100

However, according to the Dutch annex the bow imperfection should be determined using Eq. (12.3-9) of NEN 6771 [13] and is given in Eq. (4.5):

$$\delta_i = \alpha \cdot (\bar{\lambda} - 0,2) \cdot \frac{M_{c,Rd}}{N_{c,Rd}} \quad (4.5)$$

Where:

α is the imperfection factor of the buckling curve given in table 5.1
 $\bar{\lambda}$ is the in-plane non-dimensional slenderness factor

$$\bar{\lambda} = \sqrt{\frac{A \cdot f_y}{F_{cr}}}$$

$M_{c,Rd}$ is the design resistance for bending
 $N_{c,Rd}$ is the design resistance to axial forces

As an alternative to sway and bow imperfections, the shape of the elastic critical buckling mode of the structure may be applied as a unique sway and bow imperfection. The amplitude of this imperfection may be determined from:

$$\eta_{init} = \delta_i \cdot \frac{N_{cr}}{EI \cdot \eta''_{cr,max}} \cdot \eta_{cr} \quad (4.6)$$

Where:

δ_i bow imperfection according to Eq. (4.5)
 η_{cr} is the shape of the elastic critical buckling mode
 $EI \cdot \eta''_{cr,max}$ is the bending moment due to η_{cr}

The shape of the elastic critical buckling load η_{cr} in Eq. (4.6) is assumed as displacements due to N_{cr} as shown in figure 4.4. This assumption is based on term: $EI \cdot \eta''_{cr,max} \cdot \eta_{cr,max}$ is interpreted as the second derivative of displacement η_{cr} resulting in a curvature. This curvature multiplied by EI resulting in the internal bending moment due to η_{cr} . N_{cr} multiplied by displacement η_{cr} gives the external bending moment and this moment should be in equilibrium with the internal moment. Therefore Eq. (4.6) can be written as:

$$\eta_{init} = \delta_i \cdot \frac{N_{cr} \cdot \eta_{cr}}{EI \cdot \eta''_{cr,max}} = \delta_i \cdot \frac{M_{ex}}{M_{in}} = \delta_i \cdot 1 = \delta_i \quad (4.7)$$

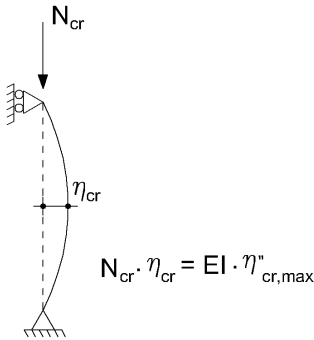


Figure 4.4: η_{cr} assumed as displacement

For each member which is loaded in compression an imperfection should be calculated. The imperfection which causes the greatest scaling of the critical buckling mode and thus the greatest unique sway and bow imperfection should be used as imperfection.

Once the critical buckling lengths and the amplitudes of the imperfections are determined, the minimum imperfections can be determined by considering the amplitude as a perfect sinus shape. For the left column, the minimum imperfection at the top of this column can be determined using Eq. (4.8) and this is shown in figure 4.5.

$$\Delta_{c,j} = \sin\left(\pi \cdot \frac{L_{c,j}}{L_{cr;c,j}}\right) \cdot \eta_{init;c,j} \quad (4.8)$$

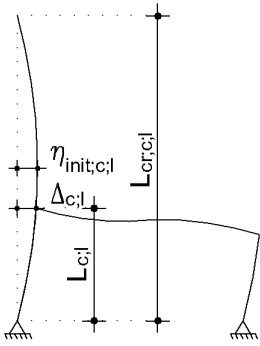


Figure 4.5: Imperfection $\Delta_{c;l}$ at the top of the left column

The minimum imperfection at the top of the right column can be determined using Eq. (4.9) and is shown in figure 4.6.

$$\Delta_{c;r} = \sin\left(\pi \cdot \frac{L_{c;r}}{L_{cr;c;r}}\right) \cdot \eta_{init;c;r} \quad (4.9)$$

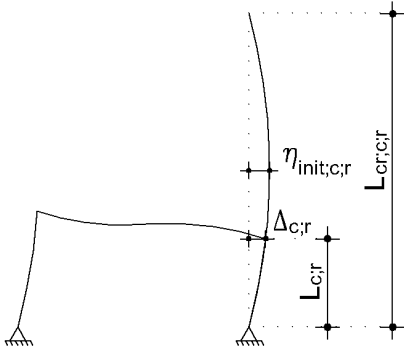


Figure 4.6: Imperfection $\Delta_{c;r}$ at the top of the right column

In cases where the beam is loaded in compression an imperfection for the beam should be determined also. The minimum imperfection at the top of the buckling mode of the beam $\Delta_{b;2}$, as given in figure 4.7, can be determined using:

$$\Delta_{b;2} = \eta_{init;b} - \Delta_{b;1} = \eta_{init;b} - \sin\left(\pi \cdot \frac{L_1}{L_{cr;b}}\right) \cdot \eta_{init;b} \quad (4.10)$$

Where:

$$L_1 = \frac{L_{cr;b} - L_2}{2}$$

$$L_2 = L_{cr;b} - 2 \cdot L_1 \quad (\text{see figure 4.7})$$

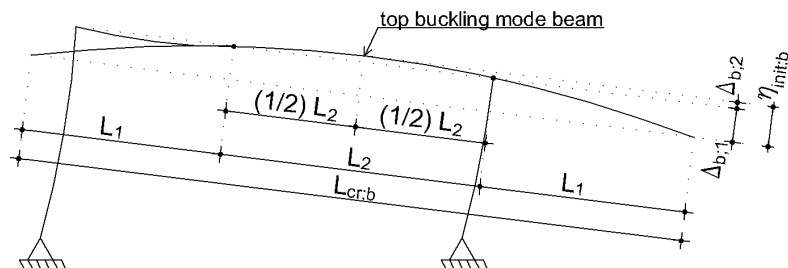


Figure 4.7: Imperfection $\Delta_{b;2}$ for the beam

To determine which displacement ($\Delta_{c,1}$, $\Delta_{c,r}$ or $\Delta_{b,2}$) gives the greatest scaling of the buckling mode the scale factor of all imperfection should be determined. The scale factor can be determined by analyzing the ratio between the displacements in the buckling mode. Buckling mode displacements using LBA in Ansys are expressed in values between 0 and 1. Zero displacement implies no displacement in buckling mode and one displacement implies maximum displacement in buckling mode. Using the command *UPGEOM* in Ansys the buckling mode can be scaled as imperfection. To obtain a specific displacement ($\Delta_{c,1}$, $\Delta_{c,r}$ or $\Delta_{b,2}$) the scale factor can be determined using:

$$s = \frac{1}{\Delta_{ANSYS;i}} \cdot \Delta_i \quad (4.11)$$

Where:

s is the scale factor
 $\Delta_{ANSYS;i}$ is the displacement ratio in Ansys varying from 0 to 1
 Δ_i displacements for unique sway and bow imperfections ($\Delta_{c,1}$, $\Delta_{c,r}$ or $\Delta_{b,2}$)

For each case in table 4.1, two GMNIA will be executed. A first GMNIA (GMNIA 1) will be performed using bow and sway imperfections according to Eq. (4.4) and (4.5). A second GMNIA (GMNIA 2) will be performed using the alternative method of Eurocode 3 by which the first buckling mode of the structure is applied as a unique sway and bow imperfection according to Eq. (4.6).

4.4 GMNIA 1 using initial sway and bow imperfections

The initial bow imperfections depend among others on the in-plane non-dimensional slenderness factor and thus on the critical buckling load of the frame. Bow imperfection will be considered separately from sway imperfections. Therefore critical buckling loads of the frames should be determined for cases where no sway displacements occur. NEN 6771 and Eurocode 3 have not described how to determine the critical buckling load for obtaining bow imperfections. There are several methods which can be imagined for determining critical buckling loads in sway frames. Three different methods will be discussed below.

As first method, vertical rollers can be modeled at the top of the column which prevent horizontal displacements at the top of the columns as shown in figure 4.7a. The critical buckling load of the beam will be determined by introducing an axial compression parallel to the beam as given in figure 4.7b. The connections between beam and column serve as rotational springs at the ends of the beam and prevent displacements perpendicular to the ends of the beam.

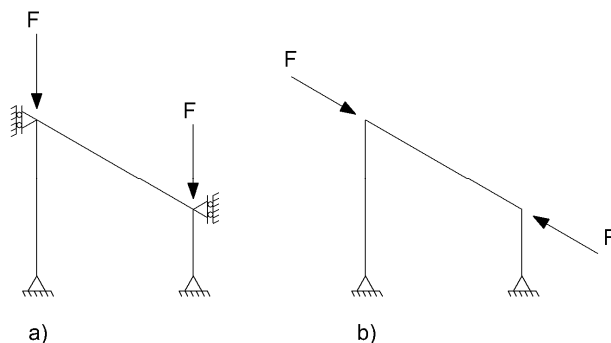


Figure 4.7: Method 1. a) Model to determine the critical buckling load in each column for initial bow imperfections of the columns. b) Model to determine the critical buckling load in the beam for the initial bow imperfection of the beam

As second method, the critical buckling load of each member can be analyzed separately as given in figure 4.8. A vertical roller will be modeled at the top of the column which will be analyzed. Also for this method, the critical buckling load of the beam will be determined using a compression force parallel to beam.

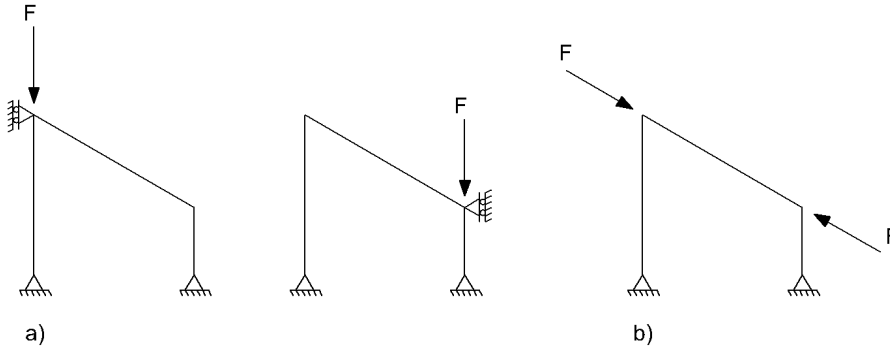


Figure 4.8: Method 2. a) Models to determine the critical buckling load in each column for initial bow imperfections of the columns. b) Model to determine the critical buckling load in the beam for the initial bow imperfection of the beam

As third method the critical buckling loads can be determined where the critical buckling length of the members are assumed as the design lengths of the members as given in figure 4.9.

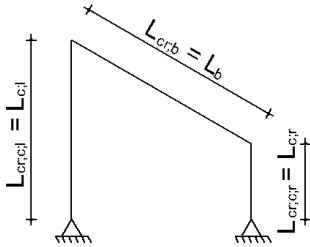


Figure 4.9: Method 3. Critical buckling lengths assumed as design length of the members for determining initial bow imperfections.

For determining design values for initial bow imperfections according to table 5.1 of Eurocode 3 (given in table 4.2) each member will be analyzed separately. Therefore, separate analyzes for each member is preferred for Eq. (4.5) to achieve somewhat equal ratios between member imperfections and member lengths. Method 1 in figure 4.7 will not be considered since two column imperfections will be determined in one analysis.

For all analyses, the second method will be considered where each member will be analyzed separately (figure 4.8). In this case the connection between beam and column will be considered and results in an exact solution of the critical buckling load. Therefore this method is preferred over the method in which the critical buckling lengths are assumed as design length of the members.

The critical buckling loads of all considered cases in table 4.1 using the method of figure 4.8 (method 2) for determining initial bow imperfections are given in table 4.3. These critical buckling loads are determined using LBA in Ansys as described in Appendix E.3.

Table 4.3: Critical buckling loads in kN for determining initial bow imperfections

Case	$F_{cr,c;l}$	$F_{cr,c;r}$	$F_{cr,b}$
1	2759,67	2759,67	3628,54
2	2758,91	3851,68	3609,44
3	2745,61	5933,11	3308,84
4	2718,89	11428,96	2707,86
5	2759,67	2759,67	3628,54
6	2758,91	3851,68	3609,44
7	2745,61	5933,11	3308,84
8	2718,89	11428,96	2707,86
9	19082,11	19082,11	3302,80
10	19106,55	38588,08	3153,41
11	19089,28	105927,68	2502,64
12	19082,11	19082,11	3302,80
13	19106,55	38588,08	3153,41
14	19089,28	105927,68	2502,64

Figure 4.10 gives, as example, the critical buckling modes for case 4.

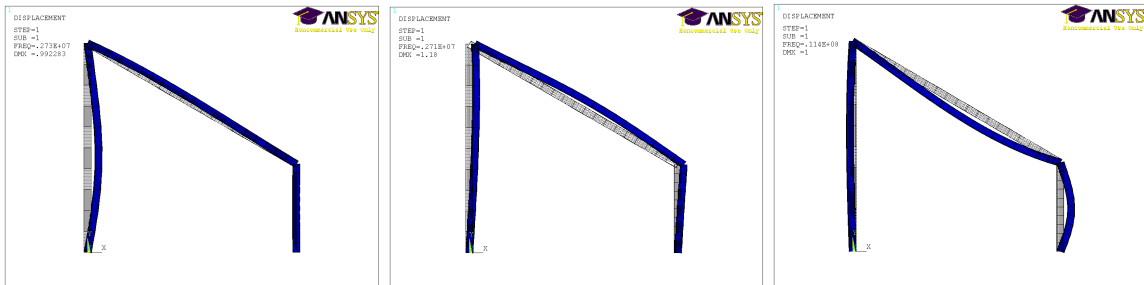


Figure 4.10: Buckling modes of case 4. Left: left column. Middle: beam. Right: right column

For case 4 this results in the following bow imperfections:

$$\delta_{c;l} = \alpha \cdot (\bar{\lambda} - 0,2) \cdot \frac{M_{c;Rd}}{N_{c;Rd}} = 0,34 \cdot \left(\sqrt{\frac{4332 \cdot 235}{2718890}} - 0,2 \right) \cdot \frac{73,04}{1018,02} \cdot 1000 = 10,1\text{mm} \quad (4.11)$$

$$\delta_{c;r} = \alpha \cdot (\bar{\lambda} - 0,2) \cdot \frac{M_{c;Rd}}{N_{c;Rd}} = 0,34 \cdot \left(\sqrt{\frac{4332 \cdot 235}{114280960}} - 0,2 \right) \cdot \frac{73,04}{1018,02} \cdot 1000 = 2,4\text{mm} \quad (4.12)$$

$$\delta_b = \alpha \cdot (\bar{\lambda} - 0,2) \cdot \frac{M_{c;Rd}}{N_{c;Rd}} = 0,34 \cdot \left(\sqrt{\frac{4332 \cdot 235}{2707860}} - 0,2 \right) \cdot \frac{73,04}{1018,02} \cdot 1000 = 10,1\text{mm} \quad (4.13)$$

Angle of rotations for determining sway imperfections at the top of the columns will be determined using Eq. (4.4). Eurocode 3 mentioned that α_h (given in Eq. 4.4) depends on the structure height. However, for trapezoidal frames a clear structure height can not be given. Seen from the geometry, each column can serve as structure height. Therefore the structure height for obtaining α_h will be assumed as column height. For case 4 this results in an angle of rotation for the left column of:

$$\varphi_{c,l} = \varphi_0 \cdot \alpha_h \cdot \alpha_m = \frac{1}{200} \cdot \frac{2}{\sqrt{5}} \cdot \sqrt{0,5 \cdot \left(1 + \frac{1}{2}\right)} = 3,873 \cdot 10^{-3} \text{ rad.} \quad (4.14)$$

And gives a sway imperfection at the top of the left column of:

$$\Delta_{c,l} = \tan(3,873 \cdot 10^{-3}) \cdot 5000 = 19,4 \text{ mm} \quad (4.15)$$

The angle of rotation for the right column is:

$$\varphi_{c,r} = \varphi_0 \cdot \alpha_h \cdot \alpha_m = \frac{1}{200} \cdot \frac{2}{\sqrt{2,113}} \cdot \sqrt{0,5 \cdot \left(1 + \frac{1}{2}\right)} = 4,331 \cdot 10^{-3} \text{ rad.} \quad (4.16)$$

Note: $\frac{2}{3} \leq \alpha_h \leq 1$

And gives a sway imperfection at the top of the right column of:

$$\Delta_{c,r} = \tan(4,331 \cdot 10^{-3}) \cdot 2113 = 9,2 \text{ mm} \quad (4.17)$$

All applied initial sway and bow imperfections which are used for GMNIA 1 are given in table 4.4.

Table 4.4: Initial sway and bow imperfection in mm for GMNIA 1

Case	$\Delta_{c,l}$	$\Delta_{c,r}$	$\delta_{c,l}$	$\delta_{c,r}$	δ_b
1	19,4	19,4	9,9	9,9	8,0
2	19,4	17,6	9,9	7,7	8,1
3	19,4	13,8	10,0	5,2	8,7
4	19,4	9,2	10,1	2,4	10,1
5	19,4	19,4	9,9	9,9	8,0
6	19,4	17,6	9,9	7,7	8,1
7	19,4	13,8	10,0	5,2	8,7
8	19,4	9,2	10,1	2,4	10,1
9	19,4	19,4	8,1	8,1	31,9
10	19,4	14,1	8,1	3,0	32,8
11	19,4	6,4	8,1	0,0	37,9
12	19,4	19,4	8,1	8,1	31,9
13	19,4	14,1	8,1	3,0	32,8
14	19,4	6,4	8,1	0,0	37,9

For the cases where the column lengths are not equal in the frame, different initial sway imperfections occur. Due to these different imperfections the beam will increase or decrease in stress-free design length depending on the sway direction. This is an unfavorable situation, however the GMNIA will be executed using these different sway distances since this are the requirements for imperfections of Eurocode 3.

Sway and bow imperfection should be considered in the most unfavorable direction and form. In table 4.5 an overview of different directions and forms is given with corresponding ultimate bearing capacity for case 4.

Table 4.5: Ultimate bearing capacities using different sway directions and bow forms

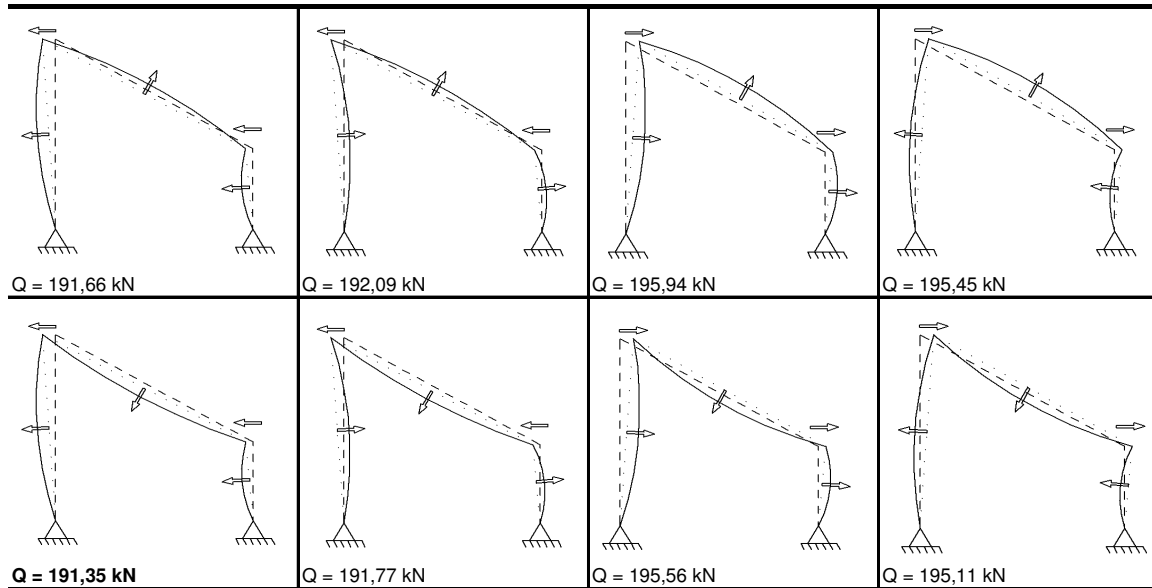


Table 4.4 shows that initial sway and bow imperfections to the left, results in the lowest ultimate bearing capacity ($Q = 191,35 \text{ kN}$) for case 4. These directions are the most unfavorable, which is partly due to the beam elongation in this case. The load-displacement diagram using the Newton-Raphson method and the arc-length method for case 4 is given in figure 4.11 and 4.12 respectively. The displacements are measured horizontally in the connection between left column and beam. In chapter E.4 sensitivity analyses are executed for GMNIA. The input of different parameters are based on these sensitivity analyses and gives therefore reliable results for all GMNIA.

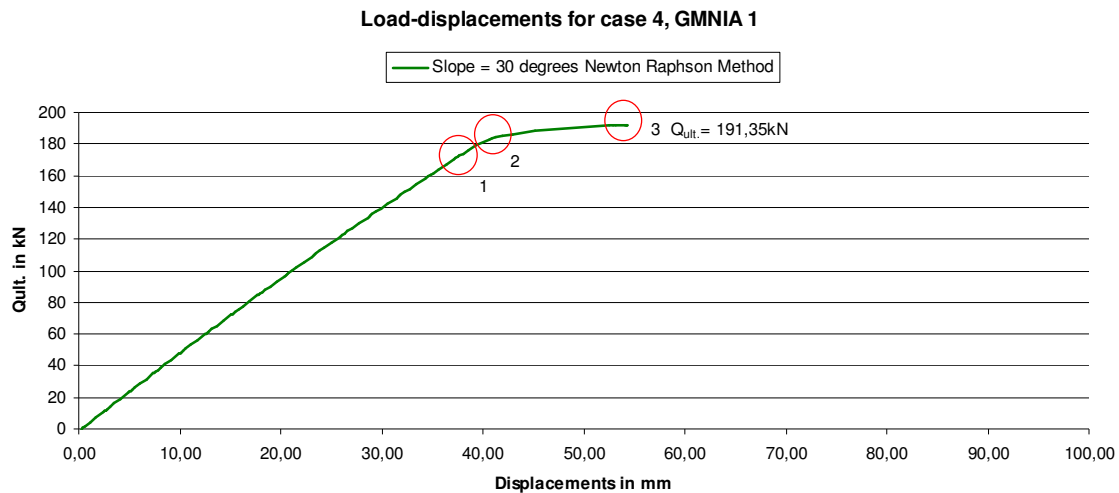


Figure 4.11: Load-displacements for case 4 obtained using the Newton-Raphson method.

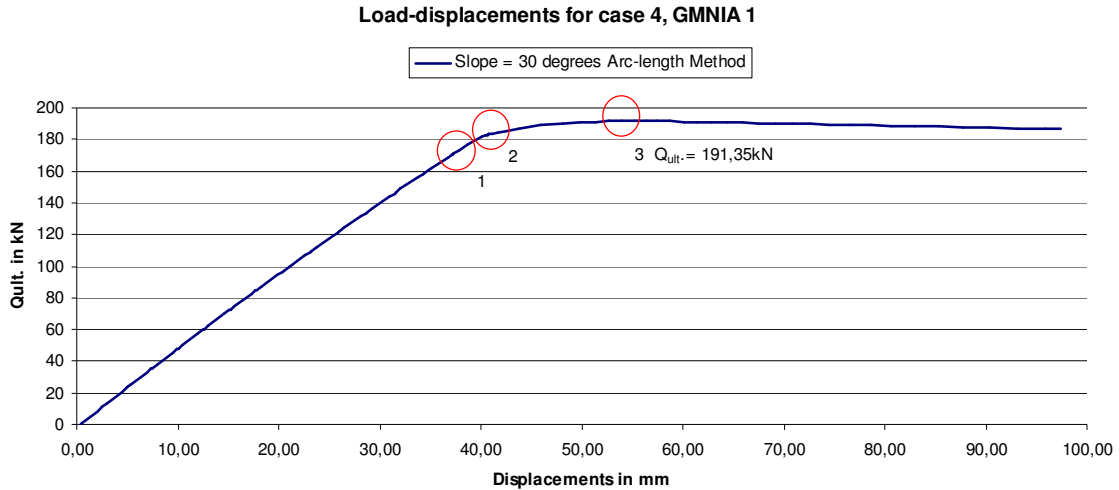


Figure 4.12: Load-displacements for case 4 obtained using the arc-length method.

Figure 4.11 and 4.12 show that both methods result in exactly the same ultimate bearing capacity (point 3), since the increase in load using the Newton-Raphson method will not be interrupted until reaching the ultimate bearing capacity of the frame. In both graphs, points are given at positions where initial yielding in the cross section occurs. Point 1 in the load displacement diagrams presents initial yielding at half beam length as given in figure 4.13. At point 2, initial yielding in the connection between left column and beam occurs as shown in figure 4.14. Point 3 gives the ultimate bearing capacity and the related stresses are given in figure 4.15 and 4.16.

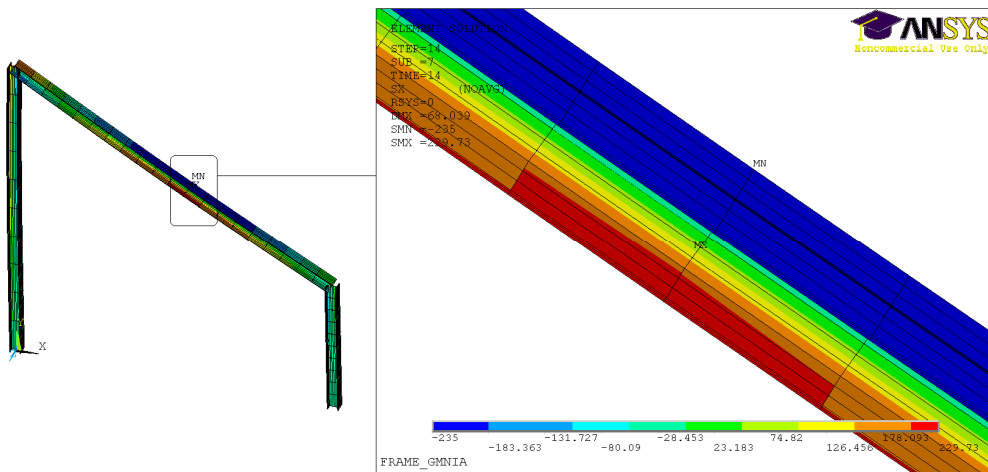


Figure 4.13: Initial yielding at half beam length (point 1 in figure 4.11 and 4.12)

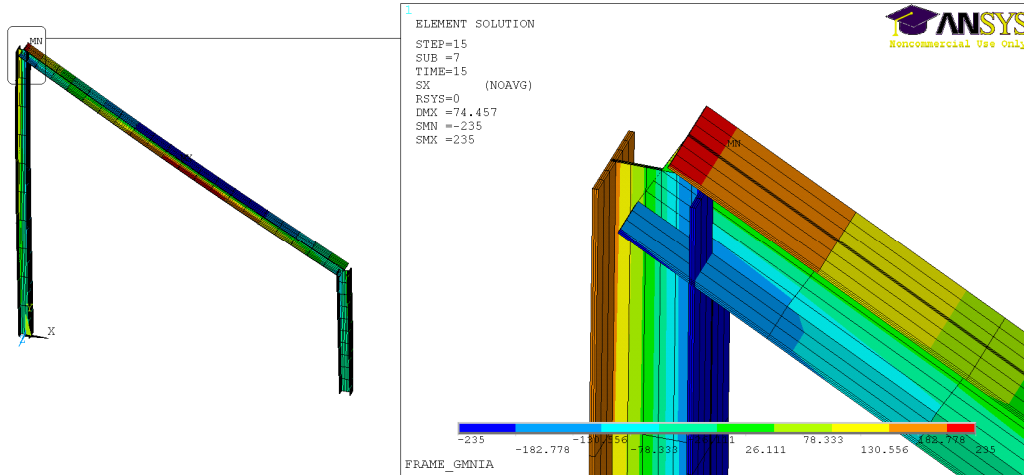


Figure 4.14: Initial yielding in the connection between left column and beam (point 2 in figure 4.11 and 4.12)

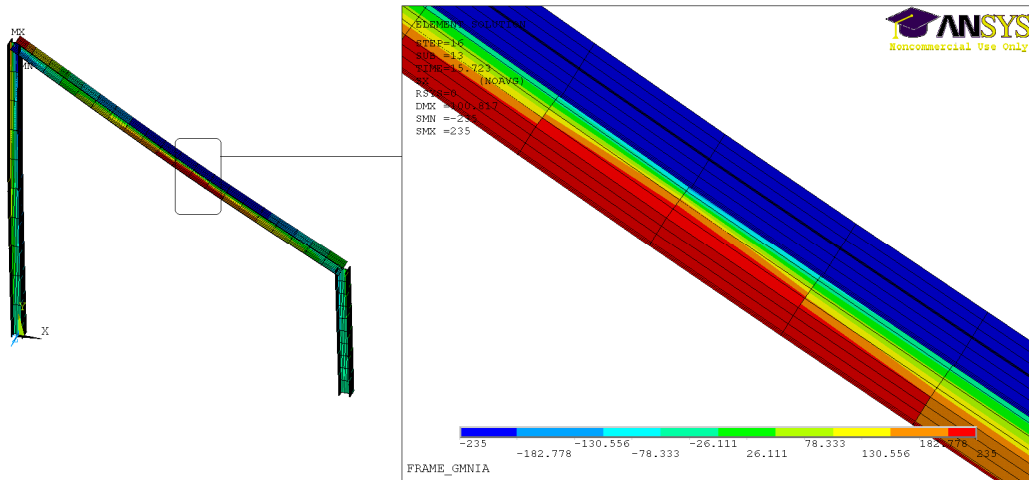


Figure 4.15: Stresses at half beam length when the ultimate bearing capacity is reached (point 3 in figure 4.11 and 4.12)

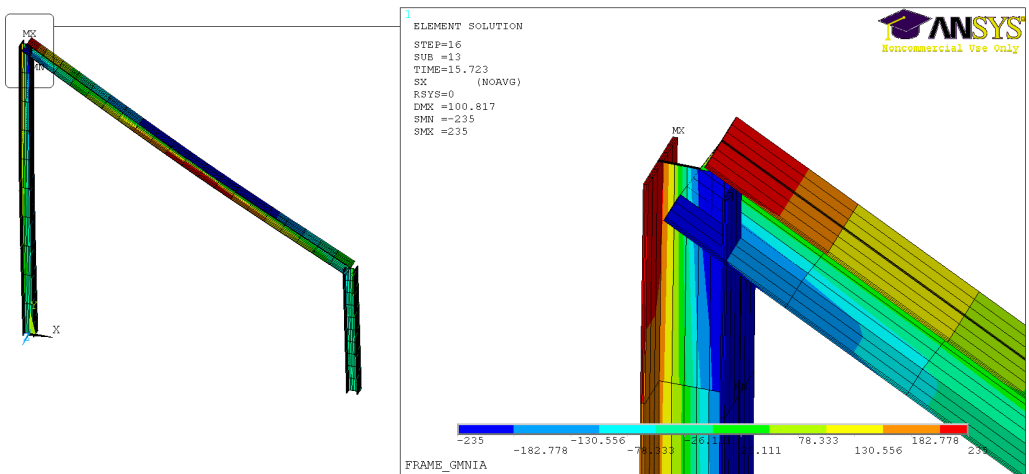


Figure 4.16: Stresses in the connection between left column and beam when the ultimate bearing capacity is reached (point 3 in figure 4.11 and 4.12)

The ultimate bearing capacities of all other GMNIA 1 cases are given in chapter 4.6.

4.5 GMNIA 2 using unique initial sway and bow imperfections

A second GMNIA (GMNIA 2) will be performed using the alternative method by which the shape of the elastic critical buckling mode of the structure is applied as a unique sway and bow imperfection using Eq. (4.6). To determine the amplitude η_{init} , the critical buckling loads of the frames should be determined without sway constraints at the top of the columns and using the properties and load combinations as given in table 4.1. The critical buckling loads are determined using LBA in Ansys as described in Appendix E.3.

An overview of the critical buckling loads and critical buckling lengths is given in table 4.6.

Table 4.6: Critical buckling loads and critical buckling lengths for determining imperfections for GMNIA 2

Case	$F_{cr;c,l}$ in kN	$L_{cr;c,l}$ in mm	$F_{cr;c,r}$ in kN	$L_{cr;c,r}$ in mm	$F_{cr;b}$ in kN	$L_{cr;b}$ in mm
1	362,60	11732	362,60	11732	35,23	37640
2	431,65	10753	431,65	10753	49,37	31796
3	555,06	9483	555,06	9483	71,22	26473
4	831,46	7748	831,46	7748	113,30	20989
5	506,44	9928	217,05	15165	35,15	37683
6	604,58	9086	281,43	13318	6,24	89436
7	781,33	7993	396,07	11226	not loaded in compr.	
8	1185,35	6489	660,22	8695	not loaded in compr.	
9	1604,82	16784	1604,82	16784	890,17	22539
10	1962,38	15178	1962,38	15178	1314,84	18543
11	2246,31	14187	2246,31	14187	1711,30	16254
12	1644,90	16578	1564,66	16998	890,17	22536
13	2021,18	14956	1939,46	15268	1292,04	18706
14	2359,70	13841	2284,49	14067	1681,99	16395

As an example the corresponding critical buckling mode for case 4 is given in figure 4.17.

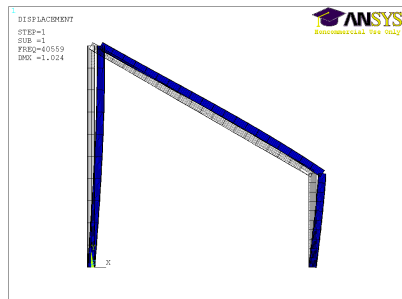


Figure 4.17: Buckling mode for case 4

For case 4 this results in the following amplitudes:

$$\eta_{init;c,l} = \alpha \cdot (\bar{\lambda} - 0,2) \cdot \frac{M_{c;Rd}}{N_{c;Rd}} = 0,34 \cdot \left(\sqrt{\frac{4332 \cdot 235}{831460}} - 0,2 \right) \cdot \frac{73,04}{1018,02} \cdot 1000 = 22,1\text{mm} \quad (4.18)$$

$$\eta_{\text{init};c;r} = \alpha \cdot (\bar{\lambda} - 0,2) \cdot \frac{M_{c;Rd}}{N_{c;Rd}} = 0,34 \cdot \left(\sqrt{\frac{4332 \cdot 235}{831460}} - 0,2 \right) \cdot \frac{73,04}{1018,02} \cdot 1000 = 22,1\text{mm} \quad (4.19)$$

$$\eta_{\text{init};b} = \alpha \cdot (\bar{\lambda} - 0,2) \cdot \frac{M_{c;Rd}}{N_{c;Rd}} = 0,34 \cdot \left(\sqrt{\frac{4332 \cdot 235}{113300}} - 0,2 \right) \cdot \frac{73,04}{1018,02} \cdot 1000 = 68,2\text{mm} \quad (4.20)$$

The minimum imperfections at the top of the columns (figure 4.5 and 4.6) should be:

$$\Delta_{c;l} = \sin \left(\pi \cdot \frac{L_{c;l}}{L_{cr;c;l}} \right) \cdot \eta_{\text{init};c;l} = \sin \left(\pi \cdot \frac{5000}{7748} \right) \cdot 22,1 = 19,8\text{mm} \quad (4.21)$$

$$\Delta_{c;r} = \sin \left(\pi \cdot \frac{L_{c;r}}{L_{cr;c;r}} \right) \cdot \eta_{\text{init};c;r} = \sin \left(\pi \cdot \frac{2213}{7748} \right) \cdot 22,1 = 16,7\text{mm} \quad (4.22)$$

The minimum imperfection for the beam (figure 4.7) should be:

$$\Delta_{b;2} = \eta_{\text{init};b} - \sin \left(\pi \cdot \frac{L_1}{L_{cr;b}} \right) \cdot \eta_{\text{init};b} = 68,2 - \sin \left(\pi \cdot \frac{(20989 - 4510)/2}{20989} \right) \cdot 68,2 = 3,9\text{mm} \quad (4.23)$$

where L_1 of Eq. (4.23) is determined by measuring L_2 in Ansys.

An overview of the minimum imperfection $\Delta_{c;l}$, $\Delta_{c;r}$ and $\Delta_{b;2}$ for all cases is given in table 4.7.

Table 4.7: Minimum imperfections for unique sway and bow imperfections

Case	$\Delta_{c;l}$ in mm	$\Delta_{c;r}$ in mm	$\Delta_{b;2}$ in mm
1	35,0	35,0	0,7
2	32,4	30,4	2,4
3	28,1	24,5	3,0
4	19,8	16,7	3,9
5	29,7	41,3	0,7
6	26,4	34,3	0,7
7	21,2	26,6	x
8	11,7	17,6	x
9	39,9	39,9	16,2
10	37,8	27,4	39,2
11	36,3	13,0	46,3
12	39,7	40,2	16,2
13	37,5	27,5	39,0
14	35,7	13,0	46,4

Table 4.8 gives the scale factors for scaling the first buckling mode. The scale factors are determined using Eq. (4.11) and the greatest scale factor should be used as scale factor for GMNIA 2.

Table 4.8: Scale factors for unique sway and bow imperfections

Case	n for $\Delta_{c,l}$	n for $\Delta_{c,r}$	n for $\Delta_{b,2}$
1	35,0	35,0	24,1
2	32,7	30,7	31,2
3	29,2	25,5	27,8
4	22,6	19,2	17,5
<hr/>			
5	29,7	41,3	20,4
6	26,7	34,7	10,9
7	22,1	27,7	x
8	13,4	20,2	x
<hr/>			
9	39,9	39,9	57,9
10	40,3	29,3	55,2
11	100,6	36,0	46,3
<hr/>			
12	39,7	40,2	57,8
13	40,0	29,3	55,3
14	97,8	35,6	46,4

4.6 GMNIA results

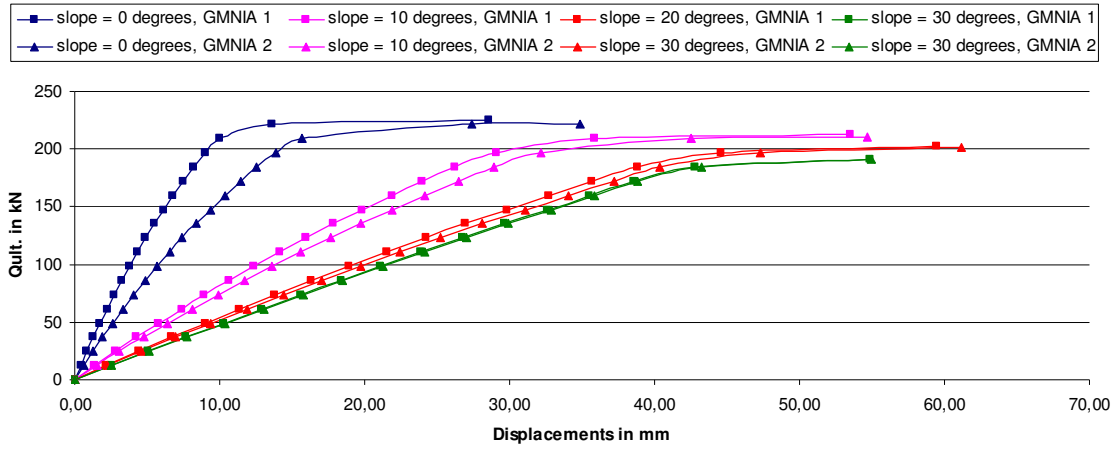
The results of the ultimate bearing capacities for the considered cases are shown in table 4.9. GMNIA 1 gives the ultimate bearing capacities using bow and sway imperfections. GMNIA 2 gives the ultimate bearing capacities using the shape of the first buckling mode as imperfection.

Table 4.9: Ultimate bearing capacity in kN

Case	$Q_{ult.}$ GMNIA 1	$Q_{ult.}$ GMNIA 2
1	225,32	222,13
2	213,22	210,97
3	202,42	201,97
4	191,35	190,93
<hr/>		
5	103,06	101,82
6	111,82	110,93
7	121,96	121,46
8	135,33	135,26
<hr/>		
9	282,55	280,79
10	255,26	253,80
11	228,18	225,60
<hr/>		
12	267,34	265,73
13	246,95	245,54
14	225,21	222,78

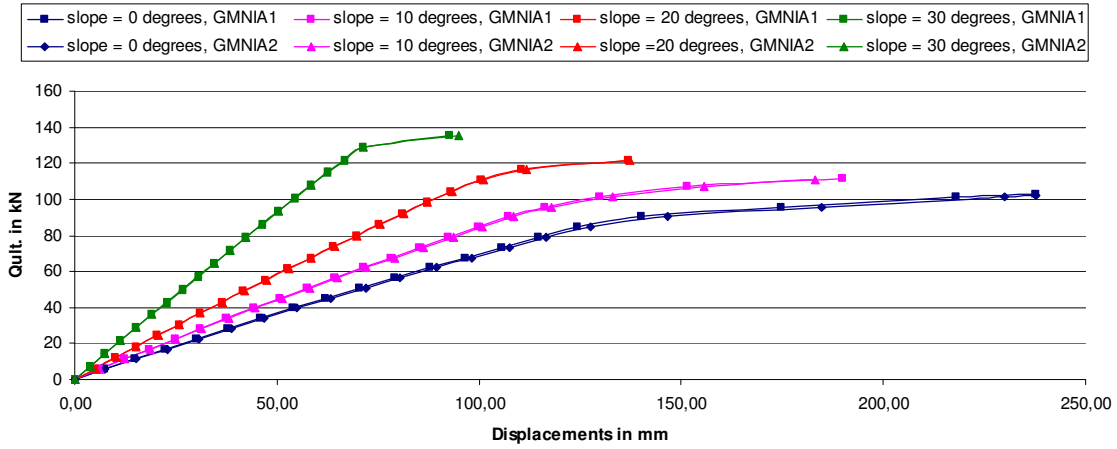
Graph 4.1 to 4.4 gives the load-displacements diagrams for each case and GMNIA. In these graphs the loadsteps are plotted with the corresponding displacements. The displacements are measured horizontally in the connection between left column and beam.

Load-displacements for case 1 to 4



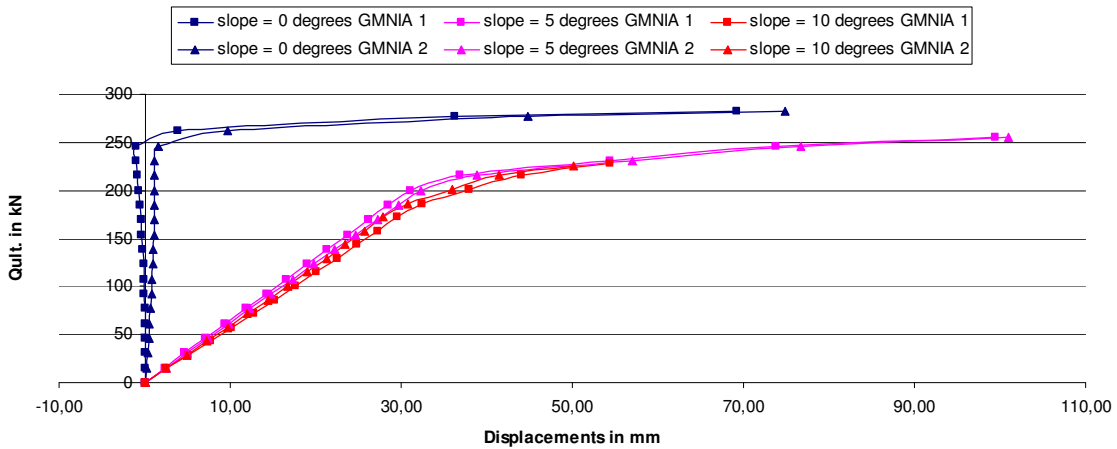
Graph 4.1: Load-displacements for case 1 to 4

Load-displacements for case 5 to 8

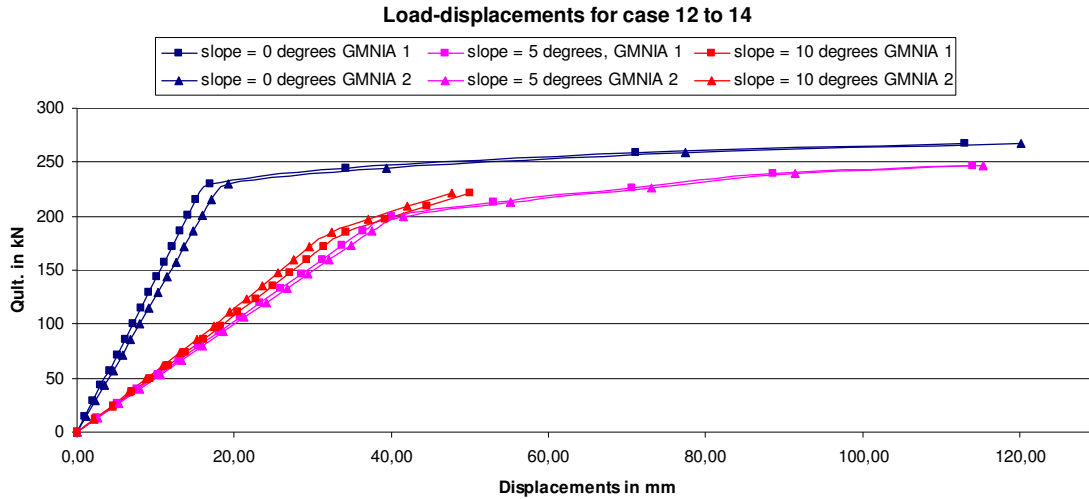


Graph 4.2: Load-displacements for case 5 to 8

Load-displacements for case 9 to 11



Graph 4.3: Load-displacements for case 9 to 11



Graph 4.4: Load-displacements for case 12 to 14

4.6 Discussion and conclusions

For GMNIA 1 different assumptions have been made for determining initial bow and sway imperfections, because Eurocode 3 does not describe this in detail. For the non-orthogonal cases which are investigated, different sway distances occur at the top of the columns. Due to these different sway imperfections the beam will stress-free increase or decrease in length. Given the different assumptions in GMNIA 1 and the beam elongation or shortening for the non-orthogonal cases, GMNIA 1 is not recommended for obtaining ultimate bearing capacities. Besides that, GMNIA 2 results for all cases in a lower ultimate bearing capacity, so GMNIA 1 can be considered as the most unfavorable analysis for verifying the stability checks of Eurocode 3. Therefore, in the remainder of this report, stability checks and cross-resistance checks will be performed where the ultimate bearing capacity is based on GMNIA 2.

In table 4.10 critical buckling loads (expressed as Q-load) determined using LBA in Ansys as described in Appendix E.3, ultimate bearing capacities using GMNIA 2 and ratios between these both loads are given.

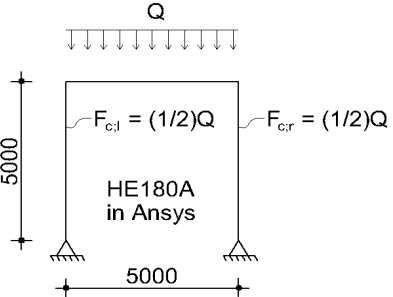
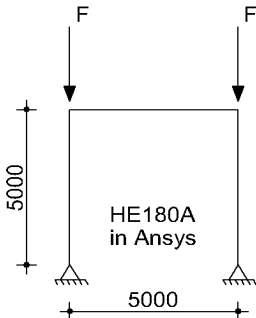
Table 4.10: Ratios between critical buckling loads and ultimate bearing capacities.

Case	Q_{cr} in kN	Q_{ult} in kN	Q_{ult} / Q_{cr}
1	725,20	222,13	0,31
2	863,30	210,97	0,24
3	1110,12	201,97	0,18
4	1662,92	190,93	0,11
5	723,49	101,82	0,14
6	886,01	110,93	0,13
7	1177,40	121,46	0,10
8	1845,57	135,26	0,07
9	3209,64	280,79	0,09
10	3924,76	253,80	0,06
11	4492,62	225,60	0,05
12	3209,56	265,73	0,08
13	3960,64	245,54	0,06
14	4644,19	222,78	0,05

Table 4.10 shows that an increase in slope will result in greater ratio between critical buckling load and ultimate bearing capacity. The critical buckling load will be higher by increasing the slope and the ultimate buckling load will be lower by increasing the slope due to greater bending moments in the structure. For case 5 to 8 and 12 to 14 the addition of lateral loads results also in a greater bending moment in the connection between left column and beam. Therefore the ultimate bearing capacity is lower for these cases in comparison with the cases in which no lateral loads are applied. For case 5 to 8 the decrease in ultimate bearing capacity is as such that the ratios between critical buckling loads and ultimate bearing capacities increase significantly.

By comparing an orthogonal frame loaded by a uniformly distributed load (case 1) with an orthogonal frame loaded by concentrated loads at the top of the columns, as given in table 4.11, a little difference in critical buckling load has been found due to a small compression force in the beam for case 1. A great difference has been found in ultimate bearing capacities which are determined using scaling the first buckling mode as a unique sway and bow imperfection. In contrast to case 1, only bending moments will occur due to second order effects in orthogonal frames loaded by concentrated loads at the top of the columns. The bending moments in case 1 are much greater due to the uniformly distributed load. Therefore plastic hinges arise earlier and gives a lower ultimate bearing capacity.

Table 4.11: Orthogonal frames with different loads

	
Case 1	Geometry of case 1 loaded by concentrated loads at the top of the columns
$F_{cr,c} = 362,60 \text{ kN}$	$F_{cr,c} = 362,84 \text{ kN}$
$F_{ult.} = 111,07 \text{ kN}$	$F_{ult.} = 289,20 \text{ kN}$

In figure 4.18 the load displacements of the both GMNIA are given as well as the critical buckling load (set on 363 kN).

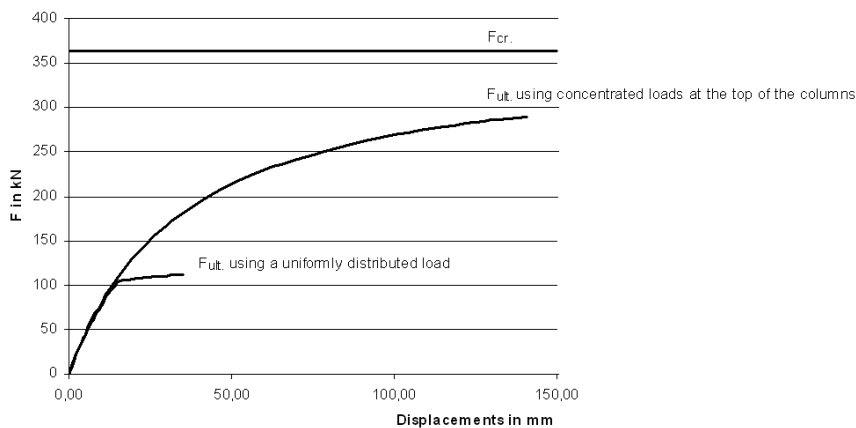


Figure 4.18: Load-displacements diagram for the considered frames in table 4.4

5. Stability checks according to Eurocode 3

5.1 Overview of checks

The ultimate bearing capacities determined using GMNIA 2 in chapter 4, serve as applied load for performing stability checks using the diagram given in figure 5.1. This diagram distinguishes stability checks for sway and non-sway frames. Repeated from Eq. (4.1), frames can be defined as non-sway if:

$$\alpha_{cr} = \frac{F_{cr}}{F_{Ed}} \geq 10 \quad (5.1)$$

Cases which do not fulfill Eq. (5.1) will be classified as sway frames.

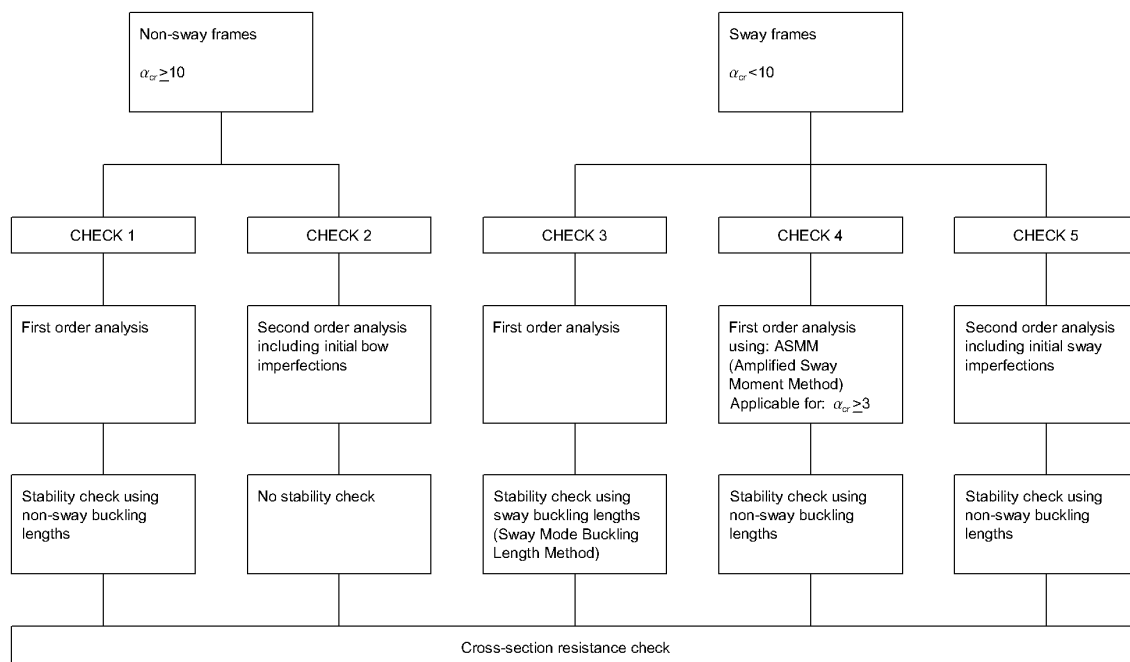


Figure 5.1: Stability checks for non-sway and sway frames

5.2 Stability checks for non-sway frames

5.2.1 Check 1: First order analysis and non-sway buckling lengths

For this check internal forces will be determined using first order elastic theory without sway imperfections or bow imperfections. The stability of the frames will be checked using section 6.3 of Eurocode 3, which describes the methods for individual stability checks of members using buckling lengths. The checks should be executed using non-sway buckling lengths.

5.2.2. Check 2: Second order analysis

Non-sway frames which will be checked using second order elastic analysis require no stability check using section 6.3 of Eurocode 3. For this second order elastic analysis, initial bow imperfections are required for second order elastic analysis.

5.3 Stability checks for sway frames

5.3.1 Check 3: First order analysis and sway buckling lengths

Check 3 using first order elastic analysis and sway buckling lengths is called the Sway Mode Buckling Length Method (SMBLM). First order elastic analyses should be executed without sway and bow imperfections. The stability of the frames will be checked using section 6.3 of Eurocode 3. The influences of bow imperfections are included in this analysis and the critical buckling length of the frame should be taken which takes the second order $F-\Delta$ effects into account.

5.3.2 Check 4: First order analysis with amplified sway moments and non-sway buckling lengths

In the Amplified Sway Moment Method (ASMM), a first order elastic analysis with amplification of horizontal loads and equivalent loads due to initial sway imperfections should be executed. In this first order analysis the horizontal loads and equivalent loads due to initial sway imperfections are amplified by the amplification factor:

$$C = \frac{1}{1 - \frac{1}{\alpha_{cr}}} \quad (5.2)$$

The equivalent horizontal loads due to initial sway imperfections can be determined by multiplication of the angle of rotation (given in Eq. (4.4)) by the design axial force in the element. This replacement is shown in figure 5.2.

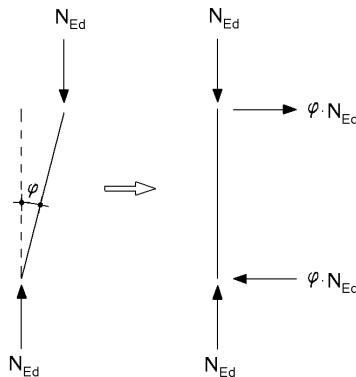


Figure 5.2: Replacement of initial sway imperfection by equivalent horizontal forces

Eurocode 3 describes that the ASMM can only be applied for cases in which $\alpha_{cr} \geq 3$, since the method is too inaccurate for ratios below 3.

After obtaining the internal forces, the members are checked using section 6.3 of Eurocode 3 where the buckling lengths may be based on buckling lengths equal to the system lengths of the members, because the second order $F-\Delta$ sway effects are included in the amplification factor.

5.3.2 Check 5: Second order analysis and non-sway buckling lengths

For this check internal forces will be determined using second order elastic theory in which initial sway imperfections are taken into account. Bow imperfections will be taken into account in the stability check given in Eurocode 3. Since the second order elastic analysis will be executed with sway imperfections, stability check may be based on non-sway buckling lengths. For this check frames with different column lengths results in stress-free beam elongation or shortening due to different sway distances at the top of the columns.

5.4 Stability checks according to section 6.3 of Eurocode 3

For check 1 and 3 to 5, stability checks according to section 6.3 of Eurocode 3 should be executed, to verify the buckling stability of the members. For uniform members loaded in combined bending and compression the members should satisfy:

$$\frac{N_{Ed}}{\chi_y \cdot N_{Rk}} + k_{yy} \cdot \frac{M_{y,Ed} + \Delta M_{y,Ed}}{\chi_{LT} \cdot \frac{M_{y,Rk}}{\gamma_{M1}}} + k_{yz} \cdot \frac{M_{z,Ed} + \Delta M_{z,Ed}}{\frac{M_{z,Rk}}{\gamma_{M1}}} \leq 1,0 \quad (5.3)$$

$$\frac{N_{Ed}}{\chi_z \cdot N_{Rk}} + k_{zy} \cdot \frac{M_{y,Ed} + \Delta M_{y,Ed}}{\chi_{LT} \cdot \frac{M_{y,Rk}}{\gamma_{M1}}} + k_{zz} \cdot \frac{M_{z,Ed} + \Delta M_{z,Ed}}{\frac{M_{z,Rk}}{\gamma_{M1}}} \leq 1,0 \quad (5.4)$$

Where:

N_{Ed} , $M_{y,Ed}$ and $M_{z,Ed}$	are the design values of the compression force and the maximum moments about the y-y and z-z axis along the member respectively
N_{Rk}	is the characteristic value of resistance to compression and can be obtained by: $f_y \cdot A_i$
$M_{y,Rk}$ and $M_{z,Rk}$	are the characteristic values of resistance to bending moments about y-y axis and z-z-axis respectively and can be obtained by: $f_y \cdot W_y$ and $f_y \cdot W_z$
$\Delta M_{y,Ed}$, $\Delta M_{z,Ed}$	are the moments due to the shift of the centroidal axis for class 4 sections
χ_y and χ_z	are the reduction factors due to flexural buckling
χ_{LT}	is the reduction factor due to lateral torsional buckling
γ_{M1}	is the partial factor for resistance of members to instability
k_{yy} , k_{yz} , k_{zy} , k_{zz}	are the interaction factors

Only in-plane stability and class 1 sections have been considered for the investigated frames. Moments about the z-z axis, moments due to shift of the centroidal axis and torsional deformations can not occur. Therefore the reduction factor due to torsional buckling would be 1,0 and Eq. (5.3) and (5.4) can be reduced to:

$$\frac{N_{Ed}}{\chi_y \cdot N_{Rk}} + k_{yy} \cdot \frac{M_{y,Ed}}{M_{y,Rk}} \leq 1,0 \quad (5.5)$$

$$\frac{N_{Ed}}{\chi_z \cdot N_{Rk}} + k_{zy} \cdot \frac{M_{y,Ed}}{M_{y,Rk}} \leq 1,0 \quad (5.6)$$

The reduction factors due to flexural buckling for the appropriate non-dimensional slenderness $\bar{\lambda}$ should be determined from the relevant buckling curve according to:

$$\chi = \frac{1}{\Phi + \sqrt{\Phi^2 - \bar{\lambda}^2}} \quad (5.7)$$

Where

$$\Phi = 0,5 \cdot (1 + \alpha \cdot (\bar{\lambda} - 0,2) + \bar{\lambda}^2) \quad (5.8)$$

$$\bar{\lambda} = \sqrt{\frac{A \cdot f_y}{F_{cr}}} \quad (5.9)$$

The imperfection factor α depends on the appropriate buckling curve. The selection of a buckling curve depends on the cross-section, the method of manufacture, the steel grade and the buckling axis of the section and can be determined using table 6.2 of Eurocode 3. The corresponding imperfection factors are given in table 6.1 of Eurocode 3 and shown in table 5.1.

Table 5.1: Imperfection factors for buckling curves

Buckling curve	a ₀	a	b	c	d
Imperfection factor α	0,13	0,21	0,34	0,49	0,76

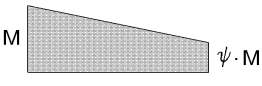
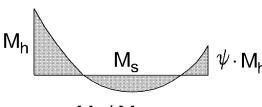
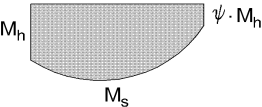
To determine the interaction factors k_{yy} and k_{zy} , Eurocode gives two methods in Annex A (Method 1) and Annex B (Method 2). According to the Dutch National Annex, method 2 must be used to determine these interaction values. Interaction factor k_{yy} and k_{zy} for class 1 section can be determined using:

$$k_{yy} = C_{my} \cdot \left(1 + (\bar{\lambda}_y - 0,2) \cdot \frac{N_{Ed}}{\chi_y \cdot N_{Rk} / \gamma_{M1}} \right) \leq C_{my} \cdot \left(1 + 0,8 \cdot \frac{N_{Ed}}{\chi_y \cdot N_{Rk} / \gamma_{M1}} \right) \quad (5.10)$$

$$k_{zy} = 0,6 \cdot k_{yy} \quad (5.11)$$

Equivalent uniform moment factor C_{my} of Eq (5.10) can be determined using table B.3 of Eurocode 3 and is also given in table 5.2 below.

Table 5.2: Equivalent uniform moment factors C_m

Moment diagram	range		C_{my} and C_{mz} and C_{mLT}	
			uniform loading	concentrated load
 $\psi \cdot M$	$-1 \leq \psi \leq 1$		$0,6 + 0,4\psi \geq 0,4$	
 $\psi \cdot M_h$ $\alpha_s = M_s / M_h$	$0 \leq \alpha_s \leq 1$	$-1 \leq \psi \leq 1$	$0,2 + 0,8\alpha_s \geq 0,4$	$0,2 + 0,8\alpha_s \geq 0,4$
	$-1 \leq \alpha_s \leq 0$	$0 \leq \psi \leq 1$	$0,1 - 0,8\alpha_s \geq 0,4$	$-0,8\alpha_s \geq 0,4$
$-1 \leq \psi < 0$		$0,1(1-\psi) - 0,8\alpha_s \geq 0,4$	$0,2(-\psi) - 0,8\alpha_s \geq 0,4$	
 $\psi \cdot M_h$ $\alpha_h = M_h / M_s$	$0 \leq \alpha_h \leq 1$	$-1 \leq \psi \leq 1$	$0,95 + 0,05\alpha_h$	$0,90 + 0,10\alpha_h$
	$-1 \leq \alpha_h \leq 0$	$0 \leq \psi \leq 1$	$0,95 + 0,05\alpha_h$	$0,90 + 0,10\alpha_h$
		$-1 \leq \psi < 0$	$0,95 + 0,05\alpha_h (1+2\psi)$	$0,90 + 0,10\alpha_h (1+2\psi)$

For members with sway buckling mode the equivalent uniform moment factor should be taken $C_{my} = 0,9$ or $C_{mz} = 0,9$ respectively

5.5 Cross section resistance check according to Eurocode 3

According to section 6.2.9.1, class 1 and class 2 cross-sections should satisfy:

$$\frac{M_{Ed}}{M_{N,Rd}} \leq 1 \quad (5.12)$$

Where $M_{N,Rd}$ is the design plastic moment resistance reduced due to axial force N_{Ed}

$$M_{N,Rd} = \frac{M_{pl,Rd} \cdot (1-n)}{(1-0,5 \cdot a)} \quad \text{but} \quad M_{N,Rd} \leq M_{pl,Rd} \quad (5.13)$$

where

$$n = \frac{N_{Ed}}{N_{pl,Rd}}$$

$$a = \frac{(A - 2 \cdot b \cdot t_f)}{A} \quad \text{but} \quad a \leq 0,5$$

If shear force V_{Ed} exceeds 50% of $V_{pl,Rd}$ the design resistance of the cross-section to combinations of moment and axial force should be calculated using a reduced yield strength for the shear area. The reduction of the yield strength should be determined using:

$$(1-\rho) \cdot f_y \quad (5.14)$$

Where

$$\rho = \left(\frac{2 \cdot V_{Ed}}{V_{pl,Rd}} - 1 \right)^2$$

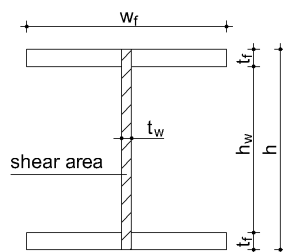


Figure 5.3: Shear area in the cross-section

If the shear force V_{Ed} does not exceeds 50% of $V_{pl,Rd}$, no reduction of the resistance defined for combined bending and axial force need to be made.

5.6 Classification of the considered trapezoidal frames

For determining which type of checks (ie checks related to sway or non-sway frames) should be performed on the considered frames in table 4.1, first order elastic analyses without sway or bow imperfections and using the calculated loads of GMNIA 2, have been executed to determine the design axial forces in each frame. Using the design axial forces and the critical buckling loads of the frames, each frame can be classified as sway or non-sway using Eq. (5.1). Table 5.3 and 5.4 give the axial forces, critical buckling loads and classification of each case for column and beam respectively.

Table 5.3: Axial forces and critical buckling loads in the column and classification of the case

Case	$N_{Ed;c,l}$	$F_{cr;c,l}$	α_{cr}	classification
1	111,07	362,60	3,26	sway
2	105,49	431,65	4,09	sway
3	100,99	555,06	5,50	sway
4	95,47	831,46	8,71	sway
5	71,27	506,44	7,11	sway
6	75,69	604,58	7,99	sway
7	80,60	781,33	9,69	sway
8	86,87	1185,35	13,64	non-sway
9	140,39	1604,82	11,43	non-sway
10	126,90	1962,38	15,46	non-sway
11	112,80	2246,31	19,91	non-sway
12	136,19	1644,90	12,08	non-sway
13	125,30	2021,18	16,13	non-sway
14	113,19	2359,70	20,85	non-sway

Table 5.4: Axial forces and critical buckling loads in the beam and classification of the case

Case	$N_{Ed;b}$	$F_{cr;b}$	α_{cr}	classification
1	10,79	35,23	3,26	sway
2	12,07	49,37	4,09	sway
3	12,96	71,22	5,50	sway
4	13,01	113,30	8,71	sway
5	4,95	35,15	7,11	sway
6	0,78	6,24	7,99	sway
7	not loaded in compression			
8	not loaded in compression			
9	77,87	890,17	11,43	non-sway
10	85,03	1314,84	15,46	non-sway
11	85,93	1711,30	19,91	non-sway
12	73,70	890,17	12,08	non-sway
13	80,10	1292,04	16,13	non-sway
14	80,68	1681,99	20,85	non-sway

The critical buckling loads and the axial forces in column and beam as given in table 5.3 and 5.4, are all determined using first order analysis without imperfections. Hence, the ratio α_{cr} is for both the beam and the columns equal in each case.

5.7 Overview results

Table 5.5 gives the results of the stability checks and the cross-section resistance checks for column and beam for the non-sway considered frames. Table 5.6 gives the results of the stability checks and the cross-section resistance checks for column and beam for the sway considered frames.

Stability checks which exceed the value 1 do not meet the stability requirements of Eurocode as given in Eq. (5.5) and (5.6). If cross-section resistance checks exceed the value 1, they do not meet the cross sectional requirements of Eurocode 3 as given in Eq. (5.12).

For all cases the maximum bearing capacity is applied on the frame so the structure should exceed at least one requirement (stability or cross-section resistance) given by Eurocode 3 to show that the rules in Eurocode 3 are on the safe side.

For check 4 and check 5, stability checks should be performed using non-sway buckling lengths because the second order $F-\Delta$ sway effects are included using amplified sway moments. For determining equivalent uniform moment factor C_{my} , Eurocode 3 has not described for these checks whether C_{my} belongs to the definition sway or non-sway buckling modes. Therefore C_{my} is determined twice, once using a non-sway buckling mode and once using a sway buckling mode ($C_{my} = 0,9$).

Appendix F gives more detailed information about the checks of table 5.5 and 5.6.

Table 5.5: Overview verification non-sway checks

Case	check	Check 1		Check 2	
		unity check		unity check	
		column	beam	column	beam
8	stability	0,71	-	-	-
	cross-section	0,97	0,96	0,98	0,98
9	stability	0,70	0,82	-	-
	cross-section	1,07	1,07	1,09	1,09
10	stability	0,76	0,78	-	-
	cross-section	1,17	1,17	1,21	1,21
11	stability	0,76	0,82	-	-
	cross-section	1,19	1,19	1,23	1,23
12	stability	0,72	0,79	-	-
	cross-section	1,11	1,11	1,13	1,13
13	stability	0,77	0,77	-	-
	cross-section	1,19	1,19	1,23	1,23
14	stability	0,77	0,82	-	-
	cross-section	1,20	1,20	1,23	1,23

Table 5.6: Overview verification sway frame checks

Case	check	Check 3		Check 4		Check 5	
		unity check		unity check		unity check	
		column	beam	column	beam	column	beam
1	stability	1,25	1,59	0,87 (C _{my} =0,9) 0,63 (C _{my} =n.s.)	1,04 (C _{my} =0,9) 1,06 (C _{my} =n.s.)	0,86 (C _{my} =0,9) 0,62 (C _{my} =n.s.)	1,03 (C _{my} =0,9) 1,05 (C _{my} =n.s.)
	cross-section	0,74	1,12	0,79	1,12	0,77	1,13
2	stability	1,20	1,40	0,90 (C _{my} =0,9) 0,65 (C _{my} =n.s.)	0,98 (C _{my} =0,9) 0,99 (C _{my} =n.s.)	0,93 (C _{my} =0,9) 0,65 (C _{my} =n.s.)	0,97 (C _{my} =0,9) 0,98 (C _{my} =n.s.)
	cross-section	0,79	1,04	0,82	1,04	0,85	1,06
3	stability	1,17	1,23	0,95 (C _{my} =0,9) 0,67 (C _{my} =n.s.)	0,93 (C _{my} =0,9) 0,94 (C _{my} =n.s.)	0,98 (C _{my} =0,9) 0,66 (C _{my} =n.s.)	0,94 (C _{my} =0,9) 0,95 (C _{my} =n.s.)
	cross-section	0,85	0,99	0,87	0,99	0,91	0,99
4	stability	1,09	1,09	0,96 (C _{my} =0,9) 0,68 (C _{my} =n.s.)	0,92 (C _{my} =0,9) 0,92 (C _{my} =n.s.)	0,99 (C _{my} =0,9) 0,69 (C _{my} =n.s.)	0,93 (C _{my} =0,9) 0,93 (C _{my} =n.s.)
	cross-section	0,89	0,97	0,90	0,98	0,92	1,02
5	stability	1,26	1,19	1,18 (C _{my} =0,9) 0,82 (C _{my} =n.s.)	1,08 (C _{my} =0,9) 0,76 (C _{my} =n.s.)	1,16 (C _{my} =0,9) 0,80 (C _{my} =n.s.)	1,04 (C _{my} =0,9) 0,73 (C _{my} =n.s.)
	cross-section	1,03	1,03	1,17	1,18	1,15	1,15
6	stability	1,23	1,15	1,16 (C _{my} =0,9) 0,80 (C _{my} =n.s.)	-	1,15 (C _{my} =0,9) 0,79 (C _{my} =n.s.)	-
	cross-section	1,03	1,04	1,14	1,04	1,13	1,04
7	stability	1,18	-	1,11 (C _{my} =0,9) 0,77 (C _{my} =n.s.)	-	1,10 (C _{my} =0,9) 0,77 (C _{my} =n.s.)	-
	cross-section	1,01	1,01	1,08	1,01	1,07	1,01

C_{my}=0,9 for sway buckling mode, C_{my}=n.s. for non-sway buckling mode (calculated C_{my})

5.8 Conclusions

In this chapter different frames have been checked according to the requirements of Eurocode 3 for stability and cross-section resistance. Two checks especially for non-sway frames and three checks especially for sway frames.

Non-sway frames are not sensitive for sway displacements and in both checks initial sway imperfection will not be modeled. From the verification results in table 5.5 for the non-sway cases, only case 8 gives unity checks below 1. This means that all members are stable and will not exceed the maximum cross-section resistance. This is an unsafe case, however it is not critical since the cross-section resistance check are close to 1. For all other non-sway cases the members will exceed the cross-section resistance which leads to safe results.

The Sway Mode Buckling Length Method (check 3) leads for all sway cases to safe but conservative stability checks. It is useful to note that by increasing the slope the critical buckling loads of the columns increase for all sway cases and the critical buckling load of the beam increases for case 1 to 4. Due to these increases in critical buckling load the unity checks for stability come closer to 1.

The Amplified Sway Moment Method (check 4) gives unsafe results for case 3 and 4. However also for these cases the cross-resistance checks are close to 1. Case 3 and 4 are unsafe because the lateral loads due to sway imperfections and the amplification of these lateral loads have less influence on the design forces in the structure. For the cases 5 to 7 besides lateral loads for sway imperfection, lateral loads due to wind will also amplified by factor C (given in Eq. (5.2)). This results in greater design forces in the structure and therefore a significantly higher unity check for the cross-section resistance.

The results of check 5 differ not significantly from the results of check 4. Both checks are based on the same analysis methodology: sway imperfection will be included in the design forces and stability checks are based on non-sway buckling lengths.

For the stability checks in check 4 and 5, it is recommended to use an equivalent uniform moment factor C_{my} of 0,9. This factor gives in general more safe and accurate results especially for the columns.

6. Conclusions and recommendations

6.1 Conclusions

6.1.1 Critical buckling loads

- Using the differential equation of equilibrium, the exchange between the left-hand column and the right-hand column cannot be described accurately using two separate column approaches.
- Using Betti's theorem and kinematic models critical buckling loads can be determined accurately. The more the buckling mode can be simulated by adding degrees of freedom, the more accurate the critical buckling load can be determined.
- The approaches which are developed for taking the compression force in the beam into account give accurate results especially for non-orthogonal trapezoidal frames.

6.1.2 Ultimate bearing capacity and stability checks

- For GMNIA using sway and bow imperfections, different assumptions should be made to determine these imperfections because Eurocode 3 does not describe this in detail.
- GMNIA using scaling the first buckling mode result for all cases in the lowest ultimate bearing capacity and these analyses are recommended to determine ultimate bearing capacities.
- Most non-sway frames exceed the cross-section resistance and therefore the rules in Eurocode 3 are on the safe side for these types of frames.
- The Sway Mode Buckling Length Method results in safe but conservative stability checks.
- Sway frame checks using non-sway buckling lengths leads to unsafe results when the slope of the beam increases. However the unity checks are close to 1.
- A factor of 0,9 for C_{my} should be used for all sway frame cases, since this factor gives in general more safe and accurate results especially for the columns.

6.2 Recommendations

6.2.1 Critical buckling loads

- For frame 1, critical buckling loads have been determined using the differential equation of equilibrium where each column has been analyzed separately. The lowest critical buckling gives an approximation of the overall critical buckling load of the columns. In the discussion, it is stressed that in some cases the approximation of the overall critical buckling load is inaccurate. This is due to the interaction between the left side of the frame and the right side of the frame. This interaction can not be accurately taken into account using the separate column approaches. Therefore more research is recommended for taking the interaction between the left side and the right side of the frame into account.
- Approaches have been developed in chapter 3.4, in which the decrease in critical buckling load as a result of compression forces in the beam can be approximated. These approaches are based on the table of Rieckmann for symmetrical non-orthogonal frames and were tested for determining its accuracy. Only non-orthogonal frames hinged connected at the base and rigid connections between the members are tested. It is recommended to test more frames with different

connections in order to get more insight if the approach gives reliable results for different connections. Also extension in flexural rigidity ratios (cases where the flexural rigidity of the beam is greater than the flexural rigidity of the columns) is recommended to get more insight in the accuracy of the approach.

6.2.2 Stability checks

- The frames which are investigated are all loaded by a uniformly distributed load. Therefore in many cases the cross-sectional resistance check of Eurocode 3 is decisive due to great bending moments in the structure. It is recommended to analyze frames which are only loaded by concentrated loads at the top of the columns. These kinds of loads give less or no (dependent on the analysis check) bending moments in the structure. Therefore the stability check becomes decisive and gives more insight in the accuracy of the different stability checks.

7. References

- [1] NEN 6770, May 1997
TGB 1990 – Steel structures – Basic requirements and basic rules for calculation of predominantly statically loaded structures, Delft: Nederlands Normalisatie-instituut (in Dutch)
- [2] NEN-EN 1993-1-1, January 2006
Eurocode 3: Design of steel structures- Part 1-1: General rules and rules for buildings (includes C1:2006), Delft: Nederlands Normalisatie-instituut (in Dutch)
- [3] C.M. Wang, C.Y. Wang, J.N. Reddy
EXACT SOLUTIONS FOR BUCKLING OF STRUCTURAL MEMBERS, 2005, CRC Press LLC, Florida
- [4] M.L. Gambhir
STABILITY ANALYSIS AND DESIGN OF STRUCTURES, 2004. Springer-Verlag Berlin Heidelberg, New York
- [5] H.P. Rieckmann
KNIKLINGENBEIWERTE FUR ZWEIFELKRAHMEN MET DRUCKKRAFTEN IM RIEGEL, 1982, Der Stahlbau, pag. 41 – 43 (in German)
- [6] Website: www.bouwenmetstaal.nl (in Dutch, visited on July 1, 2011)
- [7] M.T.A.M Sesink
IN-PLANE STABILITY OF PITCHED-ROOF FRAMES IN LINE WITH EUROCODE 3, in preparation, Eindhoven University of Technology
- [8] N. Silvestre, D. Camotim
ELASTIC BUCKLING AND SECOND-ORDER BEHAVIOUR OF PITCHED-ROOF STEEL FRAMES, 2006, Journal of Constructional Steel Research 63 (2007), pag. 804 – 818
- [9] N.S. Trahair, M.A. Bradford, D.A. Nethercot, L. Gradner
THE BEHAVIOUR AND DESIGN OF STEEL STRUCTURES TO EC3, 2008 fourth edition, Taylor and Francis, Abingdon
- [10] K. Girgin, G. Ozmen, E. Orakdogan
BUCKLING LENGTHS OF IRREGULAR FRAME COLUMNS, 2005, Journal of Constructional Steel Research 62 (2006), pag. 605 – 613
- [11] V. Galambos, E. Surovek
STRUCTURAL STABILITY OF STEEL, CONCEPTS AND APPLICATIONS FOR STRUCTURAL ENGINEERS, 2008, Wiley London
- [12] Bouwen met Staal
STABILITEIT VOOR DE STAALCONSTRUCTEUR, 2004 3^e druk, Zoetermeer (in Dutch)
- [13] NEN 6771, January 2000
TGB 1990 – Steel structures – Stability, Delft: Nederlands Normalisatie-instituut (in Dutch)
- [14] B.W. Klemann
COMPARISON OF GLOBAL ANALYSIS METHODS AND DESIGN RULES FOR STEEL FRAMES ACCORDING TO EUROCODE 3, 2009, Eindhoven University of Technology
- [15] A.A.Becker
UNDERSTANDING NON-LINEAR FINITE ELEMENT ANALYSIS THROUGH ILLUSTRATIVE BENCHMARKS, 2001, NAFEMS, Glasgow

- [16] H. Anton, R.C. Busby, L. Argabright
CONTEMPORARY LINEAR ALGEBRA, 2003, Wiley, New York

Appendix A – Derivation of the stability criterion for columns with rotational springs

Consider the column with rotational springs at both ends as given in figure A.1.

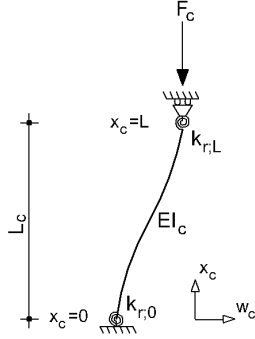


Figure A.1 Column with rotational spring constants at both ends

The four boundary conditions can be formulated as:

$$BC.1 \quad w_c(0) = 0 \quad (A.1)$$

$$BC.2 \quad \zeta_0 \cdot w_c'(0) - w_c''(0) = 0 \quad \text{where: } \zeta_0 = \frac{k_{r,0}}{EI_c} \quad (A.2)$$

$$BC.3 \quad \zeta_L \cdot w_c'(L) + w_c''(L) = 0 \quad \text{where: } \zeta_{L,j} = \frac{k_{r,L}}{EI_c} \quad (A.3)$$

$$BC.4 \quad w_c'''(L) + \alpha_c^2 \cdot w_c'(L) = 0 \quad \text{where: } \alpha_c^2 = \frac{F_c}{EI_c} \quad (A.4)$$

Where:

$w_c'(0)$ and $w_c''(0)$ are the first and second derivative of displacement $w_c(0)$ respectively.

$w_c'(L)$, $w_c''(L)$ and $w_c'''(L)$ are the first, second and third derivative of displacement $w_c(L)$ respectively.

The differential equation of equilibrium is:

$$\frac{d^4 w_c}{dx_c^4} + \alpha_c^2 \cdot \frac{d^2 w_c}{dx_c^2} = 0 \quad (A.5)$$

The general solution of this differential equation is:

$$w_c(x_c) = A_c \cdot \sin(\alpha_c \cdot x_c) + B_c \cdot \cos(\alpha_c \cdot x_c) + C_c \cdot \frac{x_c}{L_c} + D_c \quad (A.6)$$

The first, second and third derivative of the general solution are respectively:

$$w_c'(x_c) = A_c \cdot \cos(\alpha_c \cdot x_c) \cdot \alpha_c - B_c \cdot \sin(\alpha_c \cdot x_c) \cdot \alpha_c + \frac{C_c}{L_c} \quad (A.7)$$

$$w_c''(x_c) = -A_c \cdot \sin(\alpha_c \cdot x_c) \cdot \alpha_c^2 - B_c \cdot \cos(\alpha_c \cdot x_c) \cdot \alpha_c^2 \quad (A.8)$$

$$w_c'''(x_c) = -A_c \cdot \cos(\alpha_c \cdot x_c) \cdot \alpha_c^3 + B_c \cdot \sin(\alpha_c \cdot x_c) \cdot \alpha_c^3 \quad (A.9)$$

Substituting the general solution into the boundary conditions gives:

$$BC.1 \quad w_c(0) = B_c + D_c = 0 \quad (A.10)$$

$$BC.2 \quad \zeta_0 \cdot w_c'(0) - w_c''(0) = \zeta_0 \cdot \left(A_c \cdot \alpha_c + \frac{C_c}{L_c} \right) - (-B_c \cdot \alpha_c^2) = 0 \quad (A.11)$$

$$BC.3 \quad \zeta_L \cdot w_c'(L) - w_c''(L) = \zeta_L \cdot \left(A_c \cdot \cos(\alpha_c \cdot L_c) \cdot \alpha_c - B_c \cdot \sin(\alpha_c \cdot L_c) \cdot \alpha_c + \frac{C_c}{L_c} \right) + (-A_c \cdot \sin(\alpha_c \cdot L_c) \cdot \alpha_c^2 - B_c \cdot \cos(\alpha_c \cdot L_c) \cdot \alpha_c^2) = 0 \quad (A.12)$$

$$BC.4 \quad w_c'''(L) + \alpha_c^2 \cdot w_c'(L) = (-A_c \cdot \cos(\alpha_c \cdot L_c) \cdot \alpha_c^3 - B_c \cdot \sin(\alpha_c \cdot L_c) \cdot \alpha_c^3) + \alpha_c^2 \cdot \left(A_c \cdot \cos(\alpha_c \cdot L_c) \cdot \alpha_c - B_c \cdot \sin(\alpha_c \cdot L_c) \cdot \alpha_c + \frac{C_c}{L_c} \right) = 0 \quad (A.13)$$

Eq. (A.10) - (A.13) expressed in matrix form:

$$\begin{pmatrix} 0 & 1 & 0 & 1 \\ \zeta_0 \cdot \alpha_c & \alpha_c^2 & \frac{\zeta_0}{L_c} & 0 \\ \zeta_L \cdot \cos(\alpha_c \cdot L_c) \cdot \alpha_c - \sin(\alpha_c \cdot L_c) \cdot \alpha_c^2 & -\zeta_L \cdot \sin(\alpha_c \cdot L_c) \cdot \alpha_c - \cos(\alpha_c \cdot L_c) \cdot \alpha_c^2 & \frac{\zeta_L}{L_c} & 0 \\ 0 & 0 & \frac{\alpha_c^2}{L_c} & 0 \end{pmatrix} \cdot \begin{pmatrix} A_c \\ B_c \\ C_c \\ D_c \end{pmatrix} = 0 \quad (A.14)$$

To find a non-trivial solution the determinant of matrix (A.14) is:

$$\frac{-\alpha_c^6 \cdot \sin(\alpha_c \cdot L_c)}{L_c} + \frac{\alpha_c^5 \cdot \cos(\alpha_c \cdot L_c) \cdot \zeta_0}{L_c} + \frac{\alpha_c^5 \cdot \cos(\alpha_c \cdot L_c) \cdot \zeta_L}{L_c} + \frac{\alpha_c^4 \cdot \sin(\alpha_c \cdot L_c) \cdot \zeta_0 \cdot \zeta_L}{L_c} = 0 \quad (A.15)$$

Dividing Eq. (A.15) by $\frac{\alpha_c^6 \cdot \cos(\alpha_c \cdot L_c)}{L_c}$ gives:

$$-\tan(\alpha_c \cdot L_c) + \frac{\zeta_0}{\alpha_c} + \frac{\zeta_L}{\alpha_c} + \frac{\tan(\alpha_c \cdot L_c) \cdot \zeta_0 \cdot \zeta_L}{\alpha_c^2} = 0 \quad (A.16)$$

Eq. (A.16) is the stability criterion of the column, where α_c can be solved, which results in the following critical buckling load formula:

$$F_{cr,c} = \alpha_c^2 \cdot EI_c \quad (A.17)$$

Appendix B - Derivation of the rotational spring stiffness of symmetrical pitched-roof frames

The antisymmetrical buckling mode of a symmetric pitched-roof frame gives the following features of the beam:

- The displacements at the ends of the beam are the same
- There is no bending moment in the apex
- The maximum bending moment occurs in the eaves

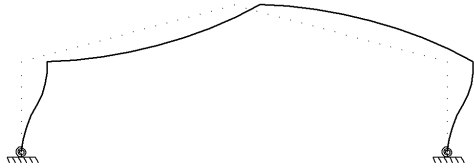


Figure B.1: Antisymmetrical buckling (ASB) mode

These features can be written as the following boundary conditions:

$$BC.1 \quad w_b(0) = 0 \quad (B.1)$$

$$BC.2 \quad w_b(L) = 0 \quad (B.2)$$

$$BC.3 \quad w_b''(0) \cdot EI_b = M_b \quad (B.3)$$

$$BC.4 \quad w_b''(L) = 0 \quad (B.4)$$

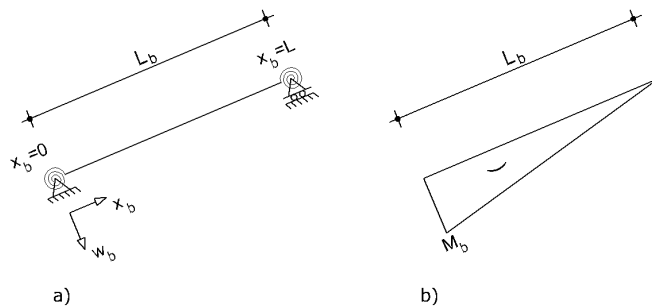


Figure B.2: a) Beam b) Moment distribution in the beam

The differential equation of equilibrium is:

$$\frac{d^4 w_b}{dx_b^4} + \alpha_b^2 \cdot \frac{d^2 w_b}{dx_b^2} = 0 \quad (B.5)$$

The general solution of this differential equation is:

$$w_b(x_b) = A_b \cdot \sin(\alpha_b \cdot x_b) + B_b \cdot \cos(\alpha_b \cdot x_b) + C_b \cdot \frac{x_b}{L_b} + D_b \quad (B.6)$$

The first and second derivative of the general solution are respectively:

$$w_b'(x_b) = A_b \cdot \cos(\alpha_b \cdot x_b) \cdot \alpha_b - B_b \cdot \sin(\alpha_b \cdot x_b) \cdot \alpha_b + \frac{C_b}{L_b} \quad (B.7)$$

$$w_b''(x_b) = -A_b \cdot \sin(\alpha_b \cdot x_b) \cdot \alpha_b^2 - B_b \cdot \cos(\alpha_b \cdot x_b) \cdot \alpha_b^2 \quad (B.8)$$

Substituting the general solution into the boundary conditions gives:

$$BC.1 \quad w_b(0) = B_b + D_b = 0 \quad (B.9)$$

$$BC.2 \quad w_b(L) = A_b \cdot \sin(\alpha_b \cdot L_b) + B_b \cdot \cos(\alpha_b \cdot L_b) + C_b + D_b = 0 \quad (B.10)$$

$$BC.3 \quad w_b''(0) \cdot E I_b = -\alpha_b^2 \cdot B_b \cdot E I_b = M \quad (B.11)$$

$$BC.4 \quad w_b''(L) = -A_b \cdot \sin(\alpha_b \cdot L_b) \cdot \alpha_b^2 - B_b \cdot \cos(\alpha_b \cdot L_b) \cdot \alpha_b^2 = 0 \quad (B.12)$$

Eq. (B.11) / BC.3 leads to:

$$\boxed{B_b = -\frac{M}{\alpha_b^2 \cdot E I_b}} \quad (B.13)$$

Eq. (B.12) / BC.4 leads to:

$$w_b''(L) = -A_b \cdot \sin(\alpha_b \cdot L_b) \cdot \alpha_b^2 + \frac{M}{\alpha_b^2 \cdot E I_b} \cdot \cos(\alpha_b \cdot L_b) \cdot \alpha_b^2 = 0 \quad (B.14)$$

$$\boxed{A_b = \frac{M \cdot \cos(\alpha_b \cdot L_b)}{\sin(\alpha_b \cdot L_b) \cdot \alpha_b^2 \cdot E I_b}} \quad (B.15)$$

Eq. (B.9) / BC.1 leads to:

$$w_b(0) = -\frac{M}{\alpha_b^2 \cdot E I_b} + D_b = 0 \quad (B.16)$$

$$\boxed{D_b = \frac{M}{\alpha_b^2 \cdot E I_b}} \quad (B.17)$$

Eq. (B.10) / BC.2 leads to:

$$w_b(L) = \frac{M \cdot \cos(\alpha_b \cdot L_b)}{\sin(\alpha_b \cdot L_b) \cdot \alpha_b^2 \cdot E I_b} \cdot \sin(\alpha_b \cdot L_b) - \frac{M}{\alpha_b^2 \cdot E I_b} \cdot \cos(\alpha_b \cdot L_b) + C_b + \frac{M}{\alpha_b^2 \cdot E I_b} = 0 \quad (B.18)$$

$$\boxed{C_b = -\frac{M}{\alpha_b^2 \cdot E I_b}} \quad (B.19)$$

The functions A_b to D_b substituted in Eq. (B.6) gives:

$$w_b(x_b) = \frac{M \cdot \cos(\alpha_b \cdot L_b)}{\sin(\alpha_b \cdot L_b) \cdot \alpha_b^2 \cdot E I_b} \cdot \sin(\alpha_b \cdot x_b) - \frac{M}{\alpha_b^2 \cdot E I_b} \cdot \cos(\alpha_b \cdot x_b) - \frac{M}{\alpha_b^2 \cdot E I_b} \cdot \frac{x_b}{L_b} + \frac{M}{\alpha_b^2 \cdot E I_b} \quad (B.20)$$

The deflection function given in Eq. (B.20) can be written in an angle of rotation by differentiating the function once. To obtain the rotational spring stiffness the general formula,

$$k_{r,L} = \frac{M}{\phi_b} = \frac{M}{-w'(0)} \quad (B.21)$$

should be solved and results in:

$$k_{r,L} = \frac{M}{\phi_b} = \frac{M}{-\left(\frac{M \cdot \cos(\alpha_b \cdot L_b)}{\sin(\alpha_b \cdot L_b) \cdot \alpha_b \cdot EI_b} - \frac{M}{\alpha_b^2 \cdot EI_b \cdot L_b} \right)} \quad (B.22)$$

The parameters δ and γ developed by Rieckmann should be integrated in the rotational spring stiffness to account for the effects on the stiffness due to the compression force in the beams. Parameter δ , as given in Eq. (2.9) can be integrated in EI_b and L_b which give the following equations:

$$EI_b = \frac{EI_c \cdot L_b}{\delta \cdot L_c} \quad (B.23)$$

$$L_b = \frac{\delta \cdot EI_b \cdot L_c}{EI_c} \quad (B.24)$$

Parameter γ as given in Eq. (2.10) can be written as:

$$\gamma = \sqrt{\frac{EI_c \cdot L_b}{EI_b \cdot L_c} \cdot \frac{N_b \cdot L_b}{N_c \cdot L_c}} = \frac{\alpha_b \cdot L_b}{\alpha_c \cdot L_c} \quad \text{where } \alpha_b = \sqrt{\frac{N_b}{EI_b}} \text{ and } \alpha_c = \sqrt{\frac{N_c}{EI_c}} \text{ (Derived from Eq. (A.4))} \quad (B.25)$$

and can be written as:

$$\alpha_b = \frac{\gamma \cdot \alpha_c \cdot L_c}{L_b}, \text{ and} \quad (B.26)$$

$$\alpha_b \cdot L_b = \gamma \cdot \alpha_c \cdot L_c \quad (B.27)$$

Eq. (B.23), (B.24), (B.26) and (B.27) substituted in Eq. (B.22) gives:

$$k_{r,L} = \frac{M}{\phi_b} = \frac{M}{-\left(\frac{M \cdot \cos(\gamma \cdot \alpha_c \cdot L_c) \cdot \delta}{\sin(\gamma \cdot \alpha_c \cdot L_c) \cdot \gamma \cdot \alpha_c \cdot EI_c} - \frac{M \cdot L_b}{(\gamma \cdot \alpha_c \cdot L_c)^2 \cdot EI_b} \right)} \quad (B.28)$$

Eq. (B.28) is the rotational spring stiffness for symmetrical pitched-roof frames and can be substituted in Eq. (A.3) to obtain the critical buckling load of the column.

Appendix C – Critical buckling loads according to Silvestre and Camotim

The critical buckling loads are yielded by:

$$\alpha_{cr} = \left[\left(\frac{N_c}{\rho_{c,0} \cdot N_{E,c}} \right)^D + \left(\frac{N_b}{\rho_{b,0} \cdot N_{E,b}} \right)^D \right]^{-1/D} \quad (C.1)$$

Where:

α_{cr} is the multiplier of the compressive force to obtain the critical buckling loads of the columns and the beams

$$D = \frac{1.2 + 1.6 \cdot K}{1 + K} \quad \text{where: } K = \frac{k_{r,0} \cdot L_c}{EI_c}$$

The factors $\rho_{c,0}$ and $\rho_{b,0}$ are the parameters of the buckling mode type. $\rho_{c,0}$ for antisymmetrical (ASB) and symmetrical buckling (SB) can be obtained by:

$$\rho_{c,0;ASB} = \frac{K \cdot (\delta + 3) + 3}{10 \cdot \delta + 12 + K \cdot (4 \cdot \delta + 3)} \quad (C.2)$$

$$\rho_{c,0;SB} = \frac{4.8 + 12 \cdot \delta \cdot (1 + R_H) + K \cdot (1 + 4.8 \cdot \delta + 4.2 \cdot \delta \cdot R_H)}{2.4 + 12 \cdot \delta \cdot (1 + R_H) + 7 \cdot \delta^2 \cdot R_H^2 + K \cdot (2.4 \cdot \delta + 2 \cdot \delta^2 \cdot R_H^2)} \quad (C.3)$$

Where:

$$\delta = \frac{EI_c \cdot L_b}{EI_b \cdot L_c} \quad (C.4)$$

$$R_H = \frac{L_b \cdot \sin(\theta)}{L_c} \quad (C.5)$$

$\rho_{b,0}$ for antisymmetrical and symmetrical buckling can be obtained by:

$$\rho_{b,0;ASB} = \frac{4 + \rho_0 \cdot (2 \cdot \delta + 4)}{4 + \rho_0 \cdot (\delta + 4)} \quad (C.6)$$

$$\rho_{b,0;SB} = \frac{12 \cdot \delta + 8.4 \cdot \delta \cdot R_H + \rho_0 \cdot (4 \cdot \delta + 4.2 \cdot \delta \cdot R_H + \delta^2 \cdot R_H^2)}{12 \cdot \delta + 4 + \rho_0 \cdot (4 \cdot \delta + 2)} \quad (C.7)$$

Appendix D – Calculation of a kinematic model with four degrees of freedom

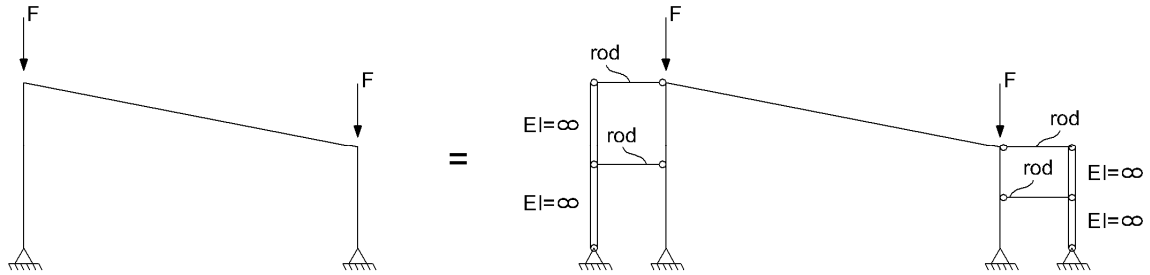


Figure D.1: Coupling of columns with pendulum columns results in a kinematical model with two degrees of freedom for each column.

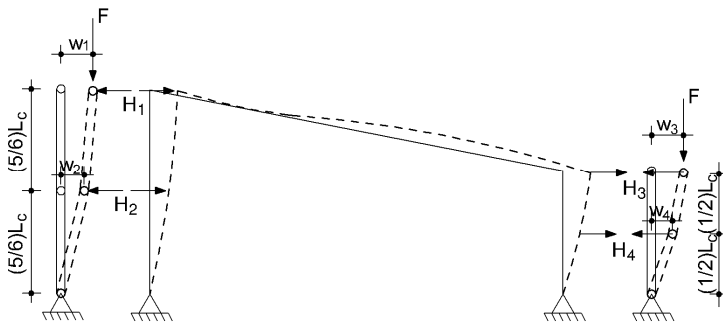


Figure D.2: Pendulum columns of the frame

From the equilibrium follows:

$$F \cdot w_1 - F \cdot w_2 = H_1 \cdot (5/6) \cdot L_c \quad \rightarrow \quad H_1 = \frac{1.2 \cdot F \cdot (w_1 - w_2)}{L_c} \quad (D.1)$$

$$F \cdot w_1 = H_1 \cdot (5/3) \cdot L_c + H_2 \cdot (5/6) \cdot L_c \quad \rightarrow \quad H_2 = \frac{1.2 \cdot F \cdot (-w_1 + 2 \cdot w_2)}{L_c} \quad (D.2)$$

$$F \cdot w_3 - F \cdot w_4 = H_3 \cdot (1/2) \cdot L_c \quad \rightarrow \quad H_3 = \frac{2 \cdot F \cdot (w_3 - w_4)}{L_c} \quad (D.3)$$

$$F \cdot w_3 = H_3 \cdot L_c + H_4 \cdot (1/2) \cdot L_c \quad \rightarrow \quad H_4 = \frac{2 \cdot F \cdot (-w_3 + 2 \cdot w_4)}{L_c} \quad (D.4)$$

The displacements can be written as:

$$w_1 = \frac{0.7446 \cdot H_1 \cdot L_c^3}{EI_c} + \frac{0.4593 \cdot H_2 \cdot L_c^3}{EI_c} + \frac{0.7446 \cdot H_3 \cdot L_c^3}{EI_c} + \frac{0.4162 \cdot H_4 \cdot L_c^3}{EI_c} \quad (D.5)$$

$$w_2 = \frac{0.4593 \cdot H_1 \cdot L_c^3}{EI_c} + \frac{0.3591 \cdot H_2 \cdot L_c^3}{EI_c} + \frac{0.4593 \cdot H_3 \cdot L_c^3}{EI_c} + \frac{0.2535 \cdot H_4 \cdot L_c^3}{EI_c} \quad (D.6)$$

$$w_3 = \frac{0.7446 \cdot H_1 \cdot L_c^3}{EI_c} + \frac{0.4593 \cdot H_2 \cdot L_c^3}{EI_c} + \frac{0.7446 \cdot H_3 \cdot L_c^3}{EI_c} + \frac{0.4162 \cdot H_4 \cdot L_c^3}{EI_c} \quad (D.7)$$

$$w_4 = \frac{0.4162 \cdot H_1 \cdot L_c^3}{EI_c} + \frac{0.2535 \cdot H_2 \cdot L_c^3}{EI_c} + \frac{0.4162 \cdot H_3 \cdot L_c^3}{EI_c} + \frac{0.2504 \cdot H_4 \cdot L_c^3}{EI_c} \quad (D.8)$$

Eq. (D.1) to (D.4) substituted in Eq. (D.5) to (D.8) gives:

$$w_1 = \frac{0.8935 \cdot F \cdot (w_1 - w_2) \cdot L_c^2}{EI_c} + \frac{0.5512 \cdot F \cdot (-w_1 + 2 \cdot w_2) \cdot L_c^2}{EI_c} + \frac{1.4892 \cdot F \cdot (w_3 - w_4) \cdot L_c^3}{EI_c} + \frac{0.8324 \cdot F \cdot (-w_3 + 2 \cdot w_4) \cdot L_c^2}{EI_c} \quad (D.9)$$

$$w_2 = \frac{0.5512 \cdot F \cdot (w_1 - w_2) \cdot L_c^2}{EI_c} + \frac{0.4309 \cdot F \cdot (-w_1 + 2 \cdot w_2) \cdot L_c^2}{EI_c} + \frac{0.9186 \cdot F \cdot (w_3 - w_4) \cdot L_c^3}{EI_c} + \frac{0.507 \cdot F \cdot (-w_3 + 2 \cdot w_4) \cdot L_c^2}{EI_c} \quad (D.10)$$

$$w_3 = \frac{0.8935 \cdot F \cdot (w_1 - w_2) \cdot L_c^2}{EI_c} + \frac{0.5512 \cdot F \cdot (-w_1 + 2 \cdot w_2) \cdot L_c^2}{EI_c} + \frac{1.4892 \cdot F \cdot (w_3 - w_4) \cdot L_c^3}{EI_c} + \frac{0.8324 \cdot F \cdot (-w_3 + 2 \cdot w_4) \cdot L_c^2}{EI_c} \quad (D.11)$$

$$w_4 = \frac{0.4994 \cdot F \cdot (w_1 - w_2) \cdot L_c^2}{EI_c} + \frac{0.3042 \cdot F \cdot (-w_1 + 2 \cdot w_2) \cdot L_c^2}{EI_c} + \frac{0.8324 \cdot F \cdot (w_3 - w_4) \cdot L_c^3}{EI_c} + \frac{0.5008 \cdot F \cdot (-w_3 + 2 \cdot w_4) \cdot L_c^2}{EI_c} \quad (D.12)$$

Eq. (D.9) can be written as:

$$\left(1 - 0.3423 \cdot \frac{F \cdot L_c^2}{EI_c}\right) \cdot w_1 + \left(-0.2089 \cdot \frac{F \cdot L_c^2}{EI_c}\right) \cdot w_2 + \left(-0.6568 \cdot \frac{F \cdot L_c^2}{EI_c}\right) \cdot w_3 + \left(-0.1756 \cdot \frac{F \cdot L_c^2}{EI_c}\right) \cdot w_4 = 0 \quad (D.13)$$

Eq. (D.10) can be written as:

$$\left(-0.1203 \cdot \frac{F \cdot L_c^2}{EI_c}\right) \cdot w_1 + \left(1 - 0.3106 \cdot \frac{F \cdot L_c^2}{EI_c}\right) \cdot w_2 + \left(-0.4116 \cdot \frac{F \cdot L_c^2}{EI_c}\right) \cdot w_3 + \left(-0.0954 \cdot \frac{F \cdot L_c^2}{EI_c}\right) \cdot w_4 = 0 \quad (D.14)$$

Eq. (D.11) can be written as:

$$\begin{aligned} &\left(-0.3423 \cdot \frac{F \cdot L_c^2}{EI_c}\right) \cdot w_1 + \left(-0.2089 \cdot \frac{F \cdot L_c^2}{EI_c}\right) \cdot w_2 + \left(1 - 0.6568 \cdot \frac{F \cdot L_c^2}{EI_c}\right) \cdot w_3 + \\ &\left(-0.1756 \cdot \frac{F \cdot L_c^2}{EI_c}\right) \cdot w_4 = 0 \end{aligned} \quad (D.15)$$

Eq. (D.12) can be written as:

$$\begin{aligned} &\left(-0.1952 \cdot \frac{F \cdot L_c^2}{EI_c}\right) \cdot w_1 + \left(-0.109 \cdot \frac{F \cdot L_c^2}{EI_c}\right) \cdot w_2 + \left(-0.3316 \cdot \frac{F \cdot L_c^2}{EI_c}\right) \cdot w_3 + \\ &\left(1 - 0.1692 \cdot \frac{F \cdot L_c^2}{EI_c}\right) \cdot w_4 = 0 \end{aligned} \quad (D.16)$$

Eq. (D.13) to (D.16) expressed in matrix form:

$$\begin{pmatrix} 1 - 0.3423 \cdot \frac{F \cdot L_c^2}{EI_c} & -0.2089 \cdot \frac{F \cdot L_c^2}{EI_c} & -0.6568 \cdot \frac{F \cdot L_c^2}{EI_c} & 0.1756 \cdot \frac{F \cdot L_c^2}{EI_c} \\ -0.1203 \cdot \frac{F \cdot L_c^2}{EI_c} & 1 - 0.3106 \cdot \frac{F \cdot L_c^2}{EI_c} & -0.4116 \cdot \frac{F \cdot L_c^2}{EI_c} & -0.0954 \cdot \frac{F \cdot L_c^2}{EI_c} \\ -0.3423 \cdot \frac{F \cdot L_c^2}{EI_c} & -0.2089 \cdot \frac{F \cdot L_c^2}{EI_c} & 1 - 0.6568 \cdot \frac{F \cdot L_c^2}{EI_c} & -0.1756 \cdot \frac{F \cdot L_c^2}{EI_c} \\ -0.1952 \cdot \frac{F \cdot L_c^2}{EI_c} & -0.109 \cdot \frac{F \cdot L_c^2}{EI_c} & -0.3316 \cdot \frac{F \cdot L_c^2}{EI_c} & 1 - 0.1692 \cdot \frac{F \cdot L_c^2}{EI_c} \end{pmatrix} \cdot \begin{pmatrix} w_1 \\ w_2 \\ w_3 \\ w_4 \end{pmatrix} = 0 \quad (D.17)$$

To find a non-trivial solution the determinant of matrix (D.17) is:

$$1 - \frac{1.4789 \cdot F \cdot L_c^2}{EI_c} + \frac{0.3179 \cdot F^2 \cdot L_c^4}{EI_c^2} - \frac{0.01526 \cdot F^3 \cdot L_c^6}{EI_c^3} + \frac{1.8909 \cdot 10^{-9} \cdot F^4 \cdot L_c^8}{EI_c^4} = 0 \quad (D.18)$$

Eq. (D.18) with an EI_c of $6.97095 \cdot 10^{11}$ and a column length of 3000mm results in a critical buckling load of 62938N and is an overestimation of 1.6% in comparison with the exact critical buckling load given by Ansys.

Appendix E - Finite element modeling

E.1 Element type

The choice for a certain element type depends on a number of properties which are required for the analyses. In the case of geometric non-linear behaviour, the elements should be able to describe (large) rotations and (large) strains accurately to obtain reliable results.

An element type which is widely used for modeling beams and columns in Ansys are beam189 elements. These elements are suitable for analyzing slender to moderately slender beam structures and are based on Timoshenko beam theory which takes first order shear deformations into account.

Beam189 consists of a quadratic three-node beam element in 3-D with six degrees of freedom at each node. Translations in the x, y and z direction and rotations about the x, y and z directions can occur at each node. Due to these features, the elements are well-suited for linear, large rotation and large strain nonlinear applications.

Klemann [14] incorporated in his thesis four benchmarks to investigate whether beam189 elements are accurate enough for applying first and second order analyses. These four benchmarks are prepared for:

- Plastic bending moments on a single beam (first order plastic analysis)
- Bending moments combined with axial forces on a single beam (first order plastic analysis)
- Shear forces in a cantilever beam (first order elastic and first order plastic analysis)
- Ultimate load of a single column (second order elastic-plastic analysis).

Klemann concluded that the full plastic design resistance for bending can be reached for all degrees of mesh density over the cross-section (see figure E.1). However the cross section will not be fully plastic. The greater the degree of mesh density, the more plastically the cross-section will be, but it will not influence the bending moment capacity of the element.

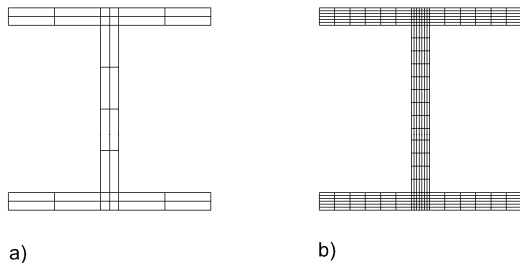


Figure E.1: a) low level of mesh density b) high level of mesh density

In the case where a beam is loaded in combined bending and compression the relation between these forces can be described accurately enough and is independent of the mesh density. Klemann has showed this by plotting the interaction between the bending moment and axial force according to Eurocode 3 and Ansys.

The benchmark which gives information about the degree of accuracy to describe the influence of shear forces, consists of a very short cantilever beam with a high concentrated load at the end of the beam. This model therefore gives large deformations due to shear forces in comparison with the deformations due to bending moments. In the benchmark the deformation due to bending moments is 0,02% of the deformations due to shear forces. For both plastic and elastic analyses beam189 elements give deformations that are between 4.2% and 2.8% underestimated compared to the analytical determined deformation. When the mesh density increases, the underestimation decreases. Beam189 elements are based on Timoshenko beam theory which is a first order shear deformation theory where the shear stress is assumed constant over the cross section. Cross sections remain plane and undistorted after deformation. Therefore the elements cannot become plastic as a result of shear stresses and has in this way no influence on plastic analyses. Shear force deformations are thus the same for elastic and plastic analyses.

The last benchmark which is investigated by Klemann is a single column hinged at both ends and loaded under compression. For this column a second order elastic-plastic analysis with an initial bow imperfection according to the Dutch code is executed to determine the ultimate load of the column. Six analyses are executed with different mesh densities. The results show that the ultimate loads found by Ansys are quite similar to the theoretical ultimate loads determined using Eurocode 3. The degree of mesh densities gives a difference between the results of 0.01% and the effects of mesh density are therefore negligible.

E.2 Cross sections

Wide flanges steel profiles are widely used for orthogonal and non-orthogonal steel frames. In this report profiles are composed derived from traditional hot rolled HE100A, HE180A and HE320A profiles. Using beam189 elements a so-called I-shape section can be modeled where only the width, height, thickness of the flanges and the thickness of the web can be defined. In the geometry of a traditional hot rolled HEA section, radii are present in the connections between flange and web. These radii can not be modeled using beam189 elements and give therefore a decrease in the characteristics especially in the plastic design shear resistance. Table E.1 to E.3 give the dimensions and other characteristics of the composed cross sections in Ansys. For determining N_{Rd} , $V_{el;z;Rd}$, $V_{pl;z;Rd}$, $M_{el;y;Rd}$ and $M_{pl;y;Rd}$ a yield stress of 235 N/mm² is assumed.

Table E.1: Characteristics of the composed HE100A cross-section

Cross section	HE100A in Ansys	HE100A traditional	Decrease in %	cross-section in Ansys
A in mm ²	2000	2124	5,8	
I_y in mm ⁴	$3319,5 \cdot 10^3$	$3492 \cdot 10^3$	4,9	
$W_{el;y}$ in mm ³	69156	72760	5	
$W_{pl;y}$ in mm ³	78400	83010	5,6	
N_{Rd} in kN	470	498,2	5,7	
$V_{el;z;Rd}$ in kN	54,3	54,5	0,4	
$V_{pl;z;Rd}$ in kN	65,1	103	36,8	
$M_{el;y;Rd}$ in kNm	16,3	17,1	5	
$M_{pl;y;Rd}$ in kNm	18,4	19,5	5,6	

Table E.2: Characteristics of the composed HE180A cross-section

Cross section	HE180A in Ansys	HE180A traditional	Decrease in %	cross-section in Ansys
A in mm ²	4332	4525	4,3	
I_y in mm ⁴	$2408 \cdot 10^4$	$2510 \cdot 10^4$	4,1	
$W_{el;y}$ in mm ³	$281,7 \cdot 10^3$	$293,6 \cdot 10^3$	4,1	
$W_{pl;y}$ in mm ³	310821	324900	4,3	
N_{Rd} in kN	1018	1063,4	4,3	
$V_{el;z;Rd}$ in kN	123,7	124	0,2	
$V_{pl;z;Rd}$ in kN	139,2	196	29	
$M_{el;y;Rd}$ in kNm	66,2	69	4,1	
$M_{pl;y;Rd}$ in kNm	73	76,4	4,3	

Table E.3: Characteristics of the composed HE320A cross-section

Cross section	HE320A in Ansys	HE320A traditional	Decrease in %	cross-section in Ansys
A in mm ²	11811	12440	5,1	
I _y in mm ⁴	21812 · 10 ⁴	22929 · 10 ⁴	4,9	
W _{el,y} in mm ³	1407,2 · 10 ³	1479 · 10 ³	4,9	
W _{pl,y} in mm ³	1544,6 · 10 ³	1628 · 10 ³	5,1	
N _{Rd} in kN	2775,6	2923,4	5,1	
V _{el,z;Rd} in kN	340,7	342	0,4	
V _{pl,z;Rd} in kN	378,5	558	32,2	
M _{el,y;Rd} in kNm	330,7	347,6	4,9	
M _{pl,y;Rd} in kNm	363	382,6	5,1	

E.3 Linear Buckling Analysis

E.3.1 Analysis method of FEM software

In order to determine the critical buckling load of a frame using linear buckling analysis (LBA) in finite element programs, as first step a first order elastic analysis will be executed where the system $\{F\} = [K] \cdot \{w\}$ will be solved. $[K]$ is the linear stiffness matrix and using this first order elastic analysis the axial forces in the structure can be determined.

Using this first order analysis, second order effects can be included in the analysis where the system $\{F\} = ([K] + [K_{\sigma}]) \cdot \{w\}$ will be solved. $[K_{\sigma}]$ is the stress-stiffness matrix and describes the second order effects.

In LBA using finite element modeling, multiplication of load F by eigenvalue α will cause that the axial forces in the structure also will be multiplied by α and so the stress-stiffness matrix will be multiplied by α_{cr} [15, 16]. A structure loaded by $\alpha_{cr}\{F\}$ where second order effects are included gives then the following equation:

$$\alpha_{cr} \cdot \{F\} = ([K] + \alpha_{cr} \cdot [K_{\sigma}]) \cdot \{w\} \quad (E.1)$$

where $\alpha_{cr}[K_{\sigma}]$ is the stress-stiffness matrix related to the load $\alpha_{cr}\{F\}$. If $\alpha_{cr}\{F\}$ equals the critical buckling load, Eq. (4.1) can be written as:

$$\{F_{cr}\} = ([K] + \alpha_{cr} \cdot [K_{\sigma}]) \cdot \{w\} \quad (E.2)$$

In case of buckling, a structure in deformed state has the same load capacity as in undeformed state. Therefore Eq. (E.2) can be written as:

$$\{F_{cr}\} = ([K] + \alpha_{cr} \cdot [K_{\sigma}]) \cdot \{w + \Delta w\} \quad (E.3)$$

where Δw is the difference between node displacement in the deformed shape and the undeformed shape. Eq. (E.2) minus Eq. (E.3) results in:

$$\{0\} = ([K] + \alpha_{cr} \cdot [K_{\sigma}]) \cdot \{\Delta w\} \quad (E.4)$$

The trivial solution of Eq. (E.4) is for cases where $\{\Delta w\} = 0$. However in buckling displacements occur, so a non-trivial solution should be determined. This non-trivial solution can be obtained by determining the determinant of $([K] + \alpha_{cr} \cdot [K_{\sigma}]) = 0$. In this way $([K] + \alpha_{cr} \cdot [K_{\sigma}])$ is singular and the eigenvalue α_{cr} can be determined and gives the critical buckling load: $\{F_{cr}\} = \alpha_{cr}\{F\}$.

E.3.2 Number of elements and mesh density

The number of elements and mesh densities influence the deformation behaviour of the structure and the analysis time of the software. The more elements will be used and the higher the level of mesh density the more solution time will be used by the finite element software. In order to guarantee reliable results a study has been executed that investigated to what extent the number of elements and mesh density influence the results in linear buckling analysis. The orthogonal frame given in figure E.2 has been investigated and consists of HE180A Ansys profiles (see table E.2).

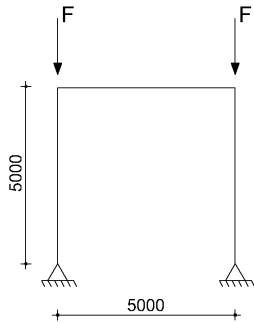


Figure E.2: Investigated orthogonal frame

The connection between column and beam is rigid and relatively easy to model in Ansys since the beam189 structure will be theoretically modeled as a continuous beam. Therefore no specific constraints should be used to model a rigid connection. The connection between column and beam as given by Ansys is given in figure E.3.

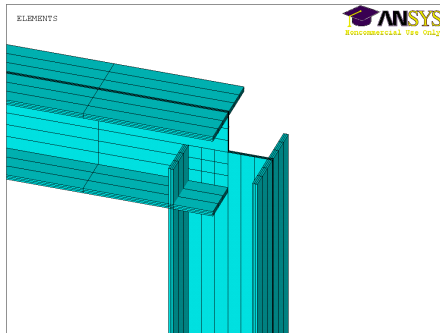


Figure E.3: Rigid connection between column and beam given by Ansys

For this frame, critical buckling loads for different mesh densities and number of elements have been determined. There has been varied in mesh densities between 0 and 5. The degree of mesh density over the cross-section is given in figure E.4. Table E.4 gives the results of this study.

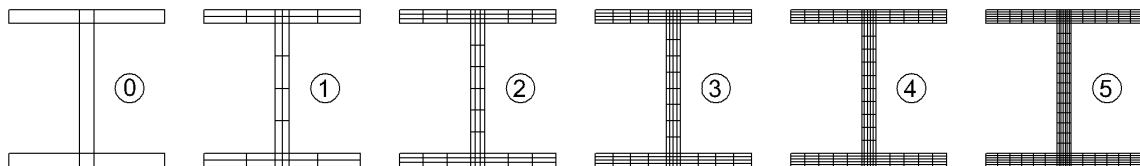


Figure E.4: Mesh densities between 0 and 5

Table E.4: Critical buckling loads in kN for the frame given in figure E.2 by varying in number of elements and mesh densities.

	Number of elements						
	Column	1	2	3	4	5	10
	Beam	2	4	6	8	10	20
Mesh density	0	365,42	363,05	362,91	362,89	362,88	362,88
	1	365,40	363,03	362,89	362,87	362,88	362,86
	2	365,38	363,01	362,87	362,85	362,86	362,84
	3	365,37	363,00	362,86	362,84	362,83	362,83
	4	365,37	362,99	362,86	362,83	362,83	362,82
	5	365,36	362,99	362,85	362,83	362,82	362,82

According to Eq. (2.8) the critical buckling load of the frame using the differential equation of equilibrium is:

$$F_{cr,c} = \frac{\pi^2 \cdot EI_c}{(2,328 \cdot L_c)^2} = \frac{\pi^2 \cdot 2,1 \cdot 10^5 \cdot 2408,2 \cdot 10^4}{(2,328 \cdot 5000)^2} = 368,39 \text{ kN} \quad (\text{E.5})$$

All results in table E.4 give a lower critical buckling load as obtained using the differential equation of equilibrium. The difference can be explained by the fact that shear deformations are taken into account when a LBA is performed using beam189 elements. Using the differential equation of equilibrium, shear deformations have not been taken into account. Beam3 elements in Ansys are elements which are comparable with beam189 for LBA, however shear deformations will not be taken into account. When executing a LBA of the frame given in figure E.2 modeled with 10 column elements and 20 beam elements consisting of type beam3, a critical buckling load of 367,89kN has been found as shown in figure E.5. This critical buckling load is close to the critical buckling load which is determined using the differential equation of equilibrium.

The results in table E.4 show that the influence of mesh density is for all number of elements equal. A mesh density of 5 gives a decrease in critical buckling load of 60N in comparison with a mesh density of 0. By varying in number of elements, it can be seen that 4 column elements or more and 8 beam elements or more, gives almost the same results. Therefore 4 column elements and 8 beam elements are sufficient to find reliable results for LBA.

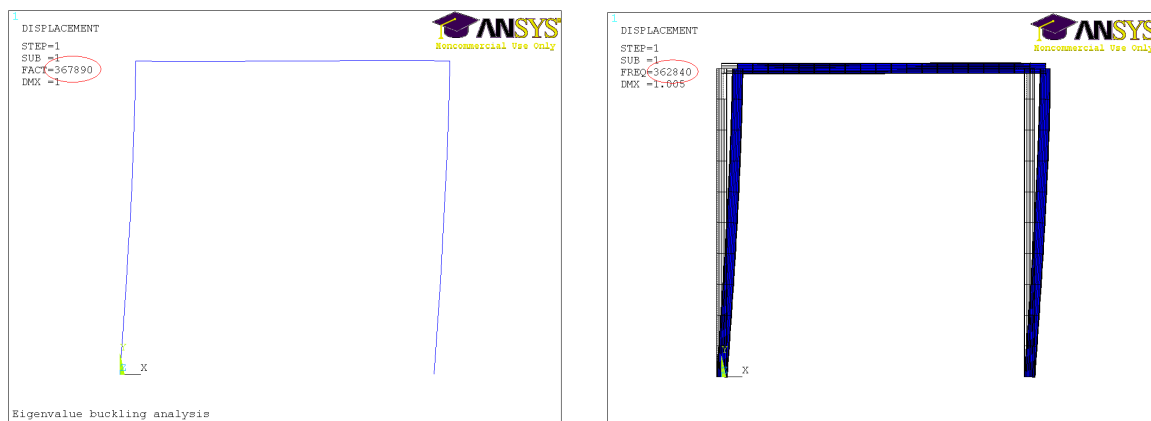


Figure E.5: Buckling mode and critical buckling loads. Left using beam3 elements, right using beam189 elements.

E.4 Geometric and Material Non-Linear Analysis

E.4.1 Number of elements and mesh density

A parameter study is executed to investigate to what extent the number of elements and mesh density influence the results for GMNIA. The frame of figure E.2, which is used for LBA, is analyzed using GMNIA. In the analyses are sway imperfections and bow imperfections considered. The angle of rotation for the sway imperfections are determined using Eq. (E.6) and gives:

$$\varphi = \varphi_0 \cdot \alpha_h \cdot \alpha_m = \frac{1}{200} \cdot \frac{2}{\sqrt{5}} \cdot \sqrt{0,5 \cdot \left(1 + \frac{1}{2}\right)} = 3,873 \cdot 10^{-3} \text{ rad.} \quad (\text{E.6})$$

This angle of rotation results in a sway displacement at the top of the columns of:

$$\Delta_{c,i} = \tan(3,873 \cdot 10^{-3}) \cdot 5000 = 19,4 \text{ mm} \quad (\text{E.7})$$

The initial bow imperfections are:

$$\delta_{c,i} = \alpha \cdot (\bar{\lambda} - 0,2) \cdot \frac{M_{c,Rd}}{N_{c,Rd}} = 0,34 \cdot \left(\sqrt{\frac{4332 \cdot 235}{2517623}} - 0,2 \right) \cdot \frac{73,04}{1018,02} \cdot 1000 = 10,6 \text{ mm} \quad (\text{E.8})$$

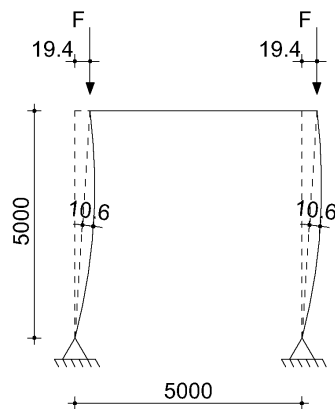


Figure E.6: Frame of figure E.2 using sway and bow imperfections

For the frame in figure E.6, different analyses are executed with various numbers of elements and mesh densities. The results of this parameter study are given in table E.5.

Table E.5: Ultimate bearing capacities in kN for the frame given in figure E.6 by varying in number of elements and mesh densities.

	Number of elements						
	Column	1	2	3	4	5	10
	Beam	2	4	6	8	10	20
Mesh density	0	285,65	284,19	284,03	283,67	283,67	283,64
	1	285,44	284,06	284,00	283,62	283,61	283,62
	2	285,45	284,01	283,97	283,62	283,59	283,62
	3	285,45	284,01	283,95	283,61	283,59	283,61
	4	285,44	284,01	283,95	283,61	283,59	283,61
	5	285,44	284,00	283,92	283,61	283,59	283,61

Table E.5 shows that between 4 and 10 column elements and 8 and 20 beam elements the results are practically equal. Therefore, 4 column elements and 8 beam elements are enough to find reliable

results for GMNIA. In the remainder of this report 10 column elements and 20 beam elements will be used with a mesh density of 2 to reduce the risk of inaccuracy in cases where different geometries and load combinations are analyzed.

E.4.2 Other preprocessing parameters

In the analyses of table E.5, the ultimate bearing capacities are load-controlled determined using the Newton-Raphson Iterative method [15]. The total load is divided into 20 loadsteps. The applied load is 300kN which means that the load of 300kN will be built up in 20 steps to the 300kN. Besides loadsteps, the number of substeps can be given in non-linear finite element modeling which give the number of steps between the loadsteps. This value is set on 20 for the analyses of table E.5.

The number of loadsteps and substeps influences accuracy of the results and the solution time of the analyses. To find a reliable number of substeps related to 20 loadsteps a study has been conducted for which number of substeps the results will converge. The results of this parameter study are given in table E.6.

Table E.6: Ultimate bearing capacity in kN by varying in number of substeps

	Number of substeps					
	8	12	16	20	24	28
F_{ult}	283,61	283,61	283,61	283,62	283,62	283,62

The number of substeps given in table E.6 does not have a significant influence on the ultimate bearing capacity of the frame. In all non-linear analyses 20 substeps will be applied.

To investigate the influence of convergence tolerances, a number of analyses have been executed on the frame with different convergence tolerances. The convergence tolerances varying from 0,05 to 0,0001. The corresponding ultimate bearing capacity is given in table E.7.

Table E.7: Ultimate bearing capacity in kN by varying in convergence tolerance

	Convergence tolerance					
	0,05	0,025	0,005	0,001	0,0005	0,0001
F_{ult}	284,28	284,01	283,70	283,62	283,62	283,62

From the results in table E.7 it can be concluded that a convergence tolerance of 0.001 can be used since a smaller tolerance results in exactly the same capacity.

E.5 Input files Ansys

E.5.1 LBA of frame 1

```
FINISH
/CLEAR

*ASK,COLUMNLEFT,Height of the left column,5000
*ASK,COLUMNRIGHT,Height of the right column,3000
*ASK,APEX,Height of the apex,7500
*ASK,APEXLEFT,Distance of the apex considered from the left column,8000
*ASK,SPAN,Total span,20000
*ASK,E,Number of elements,10
*ASK,MESH,Mesh refinement,2

!Geometry
/PREP7
N,1,0,0,0
N,2*E+1,0,COLUMNLEFT,0
FILL
N,6*E+1,APEXLEFT,APEX,0
FILL
N,12*E+1,SPAN,COLUMNRIGHT,0
FILL
N,14*E+1,SPAN,0,0
FILL
N,14*E+2,SPAN*1.2,0,0

ET,1,BEAM189
KEYOPT,1,4,1
KEYOPT,1,8,3
KEYOPT,1,9,3

!COLUMN LEFT
SECTYPE,1,BEAM,I,Isection1,MESH
SECDATA,180,180,171,9.5,9.5,6
SECPLOT,1

!BEAM LEFT
SECTYPE,2,BEAM,I,Isection1,MESH
SECDATA,180,180,171,9.5,9.5,6
SECPLOT,2

!BEAM RIGHT
SECTYPE,3,BEAM,I,Isection1,MESH
SECDATA,180,180,171,9.5,9.5,6
SECPLOT,3

!COLUMN RIGHT
SECTYPE,4,BEAM,I,Isection1,MESH
SECDATA,180,180,171,9.5,9.5,6
SECPLOT,4

SECNUM,1
*DO,C,1,2*E,2
EN,(C+1)/2,C,C+2,C+1,14*E+2
*ENDDO

SECNUM,2
*DO,C,1,4*E,2
```

```
EN,(C+1)/2+E,C+2*E,C+2+2*E,C+1+2*E,14*E+2
*ENDDO
```

```
SECNUM,3
*DO,C,1,6*E,2
EN,(C+1)/2+3*E,C+6*E,C+2+6*E,C+1+6*E,14*E+2
*ENDDO
```

```
SECNUM,4
*DO,C,1,2*E,2
EN,7*E+1-(C+1)/2,14*E+2-C,14*E-C,14*E+1-C,14*E+2
*ENDDO
```

```
!Material properties
```

```
MP,EX,1,2.1E5
MP,PRXY,1,0.3
```

```
!Boundary conditions
```

```
D,1,UX,,,,,UY
D,14*E+1,UX,,,,,UY
D,ALL,UZ
D,ALL,ROTX
D,ALL,ROTY
```

```
!Load configuration
```

```
!Uniformly distributed load
F,2*E+1,FY,-1,,6*E+1
F,6*E+1,FY,-1,,12*E+1
```

```
!Concentrated load at the top of the column
```

```
!F,2*E+1,FY,-1
!F,12*E+1,FY,-1
```

```
FINISH
```

```
!First-order analysis
```

```
/SOLU
ANTYPE,STATIC
PSTRES,ON
SOLVE
FINISH
```

```
/POST1
ETABLE,NFORCE1,SMISC,1
ETABLE,MOMENTY1,SMISC,2
ETABLE,shearZ1,SMISC,5
ETABLE,NFORCE2,SMISC,14
ETABLE,MOMENTY2,SMISC,15
ETABLE,shearz2,SMISC,18
FINISH
```

```
!Eigenvalue Buckling Analysis
```

```
/SOLU
ANTYPE,BUCKLE
BUCOPT,LANB,2
MXPAND,2,,,YES
SOLVE
FINISH
```

```
/ESHAPE,1
/POST1
SET,FIRST
```

```
PLDISP,1
```

```
FINISH
```

E.5.2 LBA of frame 2

```
FINISH
/CLEAR

*ASK,COLUMNLEFT,Heigth of the left column,5000
*ASK,COLUMNRIGHT,Heigth of the right colomn,2113
*ASK,SPAN,span,5000
*ASK,E,Number of elements,10
*ASK,MESH,Mesh refinement,2

!Geometry
/PREP7
N,1,0,0,0
N,2*E+1,0,COLUMNLEFT,0
FILL
N,6*E+1,SPAN,COLUMNRIGHT,0
FILL
N,8*E+1,SPAN,0,0
FILL
N,8*E+2,SPAN*1.2,0,0

ET,1,BEAM189
KEYOPT,1,4,1
KEYOPT,1,8,3
KEYOPT,1,9,3

!COLUMN LEFT
SECTYPE,1,BEAM,I,Isection1,MESH
SECDATA,180,180,171,9.5,9.5,6
SECPLOT,1

!COLUMN RIGHT
SECTYPE,2,BEAM,I,Isection1,MESH
SECDATA,180,180,171,9.5,9.5,6
SECPLOT,2

!BEAM
SECTYPE,3,BEAM,I,Isection1,MESH
SECDATA,180,180,171,9.5,9.5,6
SECPLOT,3

SECNUM,1
*DO,C,1,2*E,2
EN,(C+1)/2,C,C+2,C+1,8*E+2
*ENDDO

SECNUM,2
*DO,C,1,2*E,2
EN,4*E+1-(C+1)/2,8*E+2-C,8*E-C,8*E+1-C,8*E+2
*ENDDO

SECNUM,3
*DO,C,1,4*E,2
EN,(C+1)/2+E,C+2*E,C+2+2*E,C+1+2*E,8*E+2
*ENDDO

!Material properties
MP,EX,1,2.1E5
MP,PRXY,1,0.3
```

!Boundary conditions

D,1,UX,,,,,UY
D,8*E+1,UX,,,,,UY
D,ALL,UZ
D,ALL,ROTX
D,ALL,ROTY

!Load configuration

!Uniformly distributed load
F,2*E+1,FY,-1,,6*E+1
FINISH

!Concentrated load at the top of the column

!F,2*E+1,FY,-1
!F,6*E+1,FY,-1

!First-order analysis

/SOLU
ANTYPE,STATIC
PSTRES,ON
SOLVE
FINISH

/POST1

ETABLE,NFORCE1,SMISC,1
ETABLE,MOMENTY1,SMISC,2
ETABLE,shearZ1,SMISC,5
ETABLE,NFORCE2,SMISC,14
ETABLE,MOMENTY2,SMISC,15
ETABLE,shearZ2,SMISC,18
FINISH

!Eigenvalue Buckling Analysis

/SOLU
ANTYPE,BUCKLE
BUCOPT,LANB,2
MXPAND,2,,,YES
SOLVE
FINISH

/ESHAPE,1

/POST1
SET,FIRST

PLDISP,1

FINISH

E.5.3 Ultimate bearing capacity using sway and bow imperfections

FINISH
/CLEAR

!Basic input

*ASK,COLUMNLEFT,Height of the left column,5
*ASK,COLUMNRIGHT,Height of the right column,2.113
*ASK,SPAN,Total span,5
*ASK,LBEAM,Length of the beam,5.774
*ASK,MESH,Mesh refinement,2
*ASK,SWAYLEFT,Initial left sway imperfection,-0.0194
*ASK,SWAYRIGHT,Initial right sway imperfection,-0.0092
*ASK,BOWLEFT,Initial left column bow imperfection,-0.0101
*ASK,BOWRIGHT,Initial right column bow imperfection,-0.0024
*ASK,BOWBEAM,Initial beam bow imperfection,0.0101

/PREP7
/ESHAPE,1
ET,1,BEAM189
SECTYPE,1,BEAM,I,Isection1,MESH
SECDATA,180,180,171,9.5,9.5,6

!Material properties

MP,EX,1,2.1E5
MP,PRXY,1,0.3

K,1,0,0,0
K,2,SWAYLEFT,COLUMNLEFT,0
K,3,SPAN+SWAYRIGHT,COLUMNRIGHT,0
K,4,SPAN,0,0

LARC,1,2,3,-(((COLUMNLEFT/2)*(COLUMNLEFT/2))+(BOWLEFT*BOWLEFT))/(2*BOWLEFT)
LARC,2,3,1,-(((LBEAM/2)*(LBEAM/2))+(BOWBEAM*BOWBEAM))/(2*BOWBEAM)
LARC,3,4,2,-(((COLUMNRIGHT/2)*(COLUMNRIGHT/2))+(BOWRIGHT*BOWRIGHT))/(2*BOWRIGHT)

LSSCALE,ALL,,,1000,1000,1000,,1,1

LSEL,,,1
LATT,,,,,3
LSEL,,,2
LATT,,,,,1
LSEL,,,3
LATT,,,,,1

ALLSEL

LESIZE,1,,,10
LESIZE,2,,,20
LESIZE,3,,,10

LMESH,ALL,ALL

!Boundary conditions

D,1,UX,0
D,1,UY,0
D,92,UX,0
D,92,UY,0
D,ALL,UZ,0
D,ALL,ROTX,0
D,ALL,ROTY,0

```
TB,BKIN,1,1
TBDATA,1,235,0
```

```
FINISH
```

```
/SOLU
ANTYPE,STATIC
PSTRES,ON
NLGEOM,ON
NSUBST,20
OUTRES,ALL,ALL
SSTIFF,ON
NEQIT,50
```

```
CNVTOL,F,,0.001,,1
CNVTOL,U,,0.001,,1
```

```
nls=20
force=-6000
```

```
*DO,var,1,nls
F,2,FY,(force/nls)*var
F,32,FY,(force/nls)*var
F,33,FY,(force/nls)*var,,71
!F,2,FX,(41/10)*(force/nls)*var      !(lateral load due to wind)
!F,32,FX,(41/10)*(force/nls)*var     !(lateral load due to wind)
```

```
SOLVE
*ENDDO
```

```
FINISH
```

```
/POST1
*DIM,tabout_2a,TABLE,nls,2,1
*DO,var,1,nls
SET,var,LAST
*GET,Displacement_2,NODE,2,U,Y
*GET,Frequ,ACTIVE,,SET,FREQ
*VFILL,tabout_2a(var,1),DATA,Displacement_2
*VFILL,tabout_2a(var,2),DATA,Frequ
*ENDDO
*CFOPEN,FRAME2,OUTPUT
```

```
*VWRITE,
('FRAME2')
*VWRITE,
('Displ. node 2 [mm]',          ',Time/Freq [Loadsteps]')
*VWRITE,tabout_2a(1,1),tabout_2a(1,2)
(E18.10,'          ',E18.10,)
*CFCLOS
```

```
/POST26
RFORCE,2,1,F,Y
RFORCE,3,92,F,Y
ADD,4,2,3
NSOL,5,2,U,Y
XVAR,5
PLVAR,4
```

```
/AXLAB,Y,FORCE
/AXLAB,X,DEFLECTION
```

/REPLOT
FINISH

E.5.3 Ultimate bearing capacity using the buckling shape as a unique sway and bow imperfections

```
FINISH
/CLEAR

/FILENAME,LBA
/TITLE,LBA

!Basic input
*ASK,COLUMNLEFT,Height of the left column,5000
*ASK,COLUMNRIGHT,Height of the right column,2113
*ASK,SPAN,Total span,5000
*ASK,MESH,Mesh refinement,2

/PREP7
/ESHAPE,1
ET,1,BEAM189
SECTYPE,1,BEAM,I,Isection1,MESH
SECDATA,180,180,171,9.5,9.5,6

!Material properties
MP,EX,1,2.1E5
MP,PRXY,1,0.3

K,1,0,0,0
K,2,0,COLUMNLEFT,0
K,3,SPAN,COLUMNRIGHT,0
K,4,SPAN,0,0

L,1,2
L,2,3
L,3,4

LSEL,,,1
LATT,,,,,3
LSEL,,,2
LATT,,,,,1
LSEL,,,3
LATT,,,,,1

ALLSEL

LESIZE,1,,,10
LESIZE,2,,,20
LESIZE,3,,,10

LMESH,ALL,ALL

!Boundary conditions
D,1,UX,0
D,1,UY,0
D,92,UX,0
D,92,UY,0
D,ALL,UZ,0
D,ALL,ROTX,0
D,ALL,ROTY,0

/SOLU
ANTYPE,STATIC
```



```

PSTRES,ON

F,2,FY,-1
F,32,FY,-1
F,33,FY,-1,,71
!F,2,FX,-(41/40)                !(lateral load due to wind)
!F,32,FX,-(41/40)              !(lateral load due to wind)

SOLVE
FINISH

/SOLU
ANTYPE,BUCKLE
BUCOPT,LANB,1
MXPAND,1

SOLVE
FINISH

/FILENAME,FRAME_GMNIA
/TITLE,FRAME_GMNIA

/PREP7
/ESHAPE,1

UPGEOM,-22.6,,,LBA

TB,BKIN,1,1
TBDATA,1,235,0

FINISH

/SOLU
ANTYPE,STATIC
NLGEOM,ON
NSUBST,20
OUTRES,ALL,ALL
SSTIFF,ON
NEQIT,50

CNVTOL,F,,0.001,,1
CNVTOL,U,,0.001,,1

nls=20
force=-6000

*DO,var,1,nls
F,2,FY,(force/nls)*var
F,32,FY,(force/nls)*var
F,33,FY,(force/nls)*var,,71
!F,2,FX,(41/40)*(force/nls)*var                !(lateral load due to wind)
!F,32,FX,(41/40)*(force/nls)*var              !(lateral load due to wind)

SOLVE
*ENDDO

FINISH

/POST1
SET,LAST
ETABLE,NFORCE1,SMISC,1
ETABLE,MOMENTY1,SMISC,2

```

```

ETABLE,shearZ1,SMISC,5
ETABLE,NFORCE2,SMISC,14
ETABLE,MOMENTY2,SMISC,15
ETABLE,shearz2,SMISC,18
FINISH

/POST1
*DIM,tabout_2a,TABLE,nls,2,1
*DO,var,1,nls
SET,var,LAST
*GET,Displacement_2,NODE,2,U,X
*GET,Frequ,ACTIVE,,SET,FREQ
*VFILL,tabout_2a(var,1),DATA,Displacement_2
*VFILL,tabout_2a(var,2),DATA,Frequ
*ENDDO
*CFOPEN,FRAME2,OUTPUT

*VWRITE,
('FRAME2')
*VWRITE,
('Displ. node 2 [mm]',          ',Time/Freq [Loadsteps]')
*VWRITE,tabout_2a(1,1),tabout_2a(1,2)
(E18.10,'          ',E18.10,)
*CFCLOS

/POST26
RFORCE,2,1,F,Y
RFORCE,3,92,F,Y
ADD,4,2,3
NSOL,5,2,U,X
XVAR,5
PLVAR,4

/AXLAB,Y,FORCE
/AXLAB,X,DEFLECTION
/REPLOT
FINISH

```

E.5.5 Second order analysis including initial bow imperfections

```
FINISH
/CLEAR

!Basic input
*ASK,COLUMNLEFT,Height of the left column,5
*ASK,COLUMNRIGHT,Height of the right column,2.113
*ASK,SPAN,Total span,5
*ASK,LBEAM,Length of the beam,5.774
*ASK,MESH,Mesh refinement,2
*ASK,BOWLEFT,Initial left column bow imperfection,-0.0103
*ASK,BOWRIGHT,Initial right column bow imperfection,-0.0089
*ASK,BOWBEAM,Initial beam bow imperfection,0.0101
*ASK,Q,Ultimate bearing load,190930

/PREP7
ET,1,BEAM189
SECTYPE,1,BEAM,I,Isection1,MESH
SECDATA,180,180,171,9.5,9.5,6

!Material properties
MP,EX,1,2.1E5
MP,PRXY,1,0.3

K,1,0,0,0
K,2,0,COLUMNLEFT,0
K,3,SPAN,COLUMNRIGHT,0

K,4,SPAN,0,0

LARC,1,2,3,-(((COLUMNLEFT/2)*(COLUMNLEFT/2))+ (BOWLEFT*BOWLEFT))/(2*BOWLEFT)
LARC,2,3,1,-(((LBEAM/2)*(LBEAM/2))+ (BOWBEAM*BOWBEAM))/(2*BOWBEAM)
LARC,3,4,2,-(((COLUMNRIGHT/2)*(COLUMNRIGHT/2))+ (BOWRIGHT*BOWRIGHT))/(2*BOWRIGHT)

LSSCALE,ALL,,1000,1000,1000,,1,1

LSEL,,,1
LATT,,,,,3
LSEL,,,2
LATT,,,,,1
LSEL,,,3
LATT,,,,,1

ALLSEL

LESIZE,1,,,10
LESIZE,2,,,20
LESIZE,3,,,10

LMESH,ALL,ALL

!Boundary conditions
D,1,UX,0
D,1,UY,0
D,92,UX,0
D,92,UY,0
D,ALL,UZ,0
D,ALL,ROTX,0
D,ALL,ROTY,0
```

```

FINISH

/SOLU
ANTYPE,STATIC
NLGEOM,ON
NSUBST,20
OUTRES,ALL,ALL
SSTIFF,ON
NEQIT,50

CNVTOL,F,,0.001,,1
CNVTOL,U,,0.001,,1

nls=20
force=-(Q/41)

*DO,var,1,nls
F,2,FY,(force/nls)*var
F,32,FY,(force/nls)*var
F,33,FY,(force/nls)*var,,71
!F,2,FX,(41/10)*(force/nls)*var      !(lateral load due to wind)
!F,32,FX,(41/10)*(force/nls)*var    !(lateral load due to wind)

SOLVE
*ENDDO

FINISH

/POST1
SET,LAST
ETABLE,NFORCE1,SMISC,1
ETABLE,MOMENTY1,SMISC,2
ETABLE,shearZ1,SMISC,5
ETABLE,NFORCE2,SMISC,14
ETABLE,MOMENTY2,SMISC,15
ETABLE,shearz2,SMISC,18
FINISH

```

E.5.6 Second order analysis including initial sway imperfections

```
FINISH
/CLEAR

!Basic input
*ASK,COLUMNLEFT,Height of the left column,5
*ASK,COLUMNRIGHT,Height of the right column,2.113
*ASK,SPAN,Total span,5
*ASK,SWAYLEFT,Initial left sway imperfection,-0.0194
*ASK,SWAYRIGHT,Initial right sway imperfection,-0.0092
*ASK,Q,Ultimate bearing load,190930

/PREP7
ET,1,BEAM189
SECTYPE,1,BEAM,I,Isection1,2
SECDATA,180,180,171,9.5,9.5,6

!Material properties
MP,EX,1,2.1E5
MP,PRXY,1,0.3

K,1,0,0,0
K,2,SWAYLEFT,COLUMNLEFT,0
K,3,SPAN+SWAYRIGHT,COLUMNRIGHT,0
K,4,SPAN,0,0

L,1,2
L,2,3
L,3,4

LSSCALE,ALL,,1000,1000,1000,,1,1

LSEL,,,1
LATT,,,,,3
LSEL,,,2
LATT,,,,,1
LSEL,,,3
LATT,,,,,1

ALLSEL

LESIZE,1,,10
LESIZE,2,,20
LESIZE,3,,10

LMESH,ALL,ALL

!Boundary conditions
D,1,UX,0
D,1,UY,0
D,92,UX,0
D,92,UY,0
D,ALL,UZ,0
D,ALL,ROTX,0
D,ALL,ROTY,0

FINISH

/SOLU
ANTYPE,STATIC
```

```
NLGEOM,ON
NSUBST,20
OUTRES,ALL,ALL
SSTIFF,ON
NEQIT,50
```

```
CNVTOL,F,,0.001,,1
CNVTOL,U,,0.001,,1
```

```
nls=20
force=-(Q/41)
```

```
*DO,var,1,nls
F,2,FY,(force/nls)*var
F,32,FY,(force/nls)*var
F,33,FY,(force/nls)*var,,71
!F,2,FX,(41/10)*(force/nls)*var
!F,32,FX,(41/10)*(force/nls)*var
```

```
SOLVE
*ENDDO
```

```
FINISH
```

```
/POST1
SET, LAST
ETABLE, NFORCE1, SMISC, 1
ETABLE, MOMENTY1, SMISC, 2
ETABLE, shearZ1, SMISC, 5
ETABLE, NFORCE2, SMISC, 14
ETABLE, MOMENTY2, SMISC, 15
ETABLE, shearz2, SMISC, 18
FINISH
```


Appendix F – Eurocode 3 checks

Check 1: Non-sway frames using first order analysis and stability checks using non-sway buckling lengths

Stability check for columns:

Case	8	9	10	11	12	13	14
N_{Ed} in N	86870	140390	126900	112800	136190	125300	113190
$M_{y;Ed}$ in Nm	70730	389360	424720	432670	401700	431870	435490
χ_y	0,831	0,933	0,933	0,933	0,933	0,933	0,933
Φ	0,757	0,604	0,603	0,604	0,604	0,603	0,604
λ	0,612	0,381	0,381	0,381	0,381	0,381	0,381
α	0,34	0,34	0,34	0,34	0,34	0,34	0,34
A in mm ²	4332	11811	11811	11811	11811	11811	11811
$W_{pl,y}$ in mm ³	310821	1544600	1544600	1544600	1544600	1544600	1544600
f_y in N/mm ²	235	235	235	235	235	235	235
F_{cr} in N	2718890	19082110	19106550	19089280	19082110	19106550	19089280
C_{my}	0,6	0,6	0,6	0,6	0,6	0,6	0,6
$k_{yy,1}$	0,625	0,606	0,605	0,605	0,606	0,605	0,605
$k_{yy,2}$	0,649	0,626	0,624	0,621	0,625	0,623	0,621
Check	0,71	0,70	0,76	0,76	0,72	0,77	0,77

Cross-section resistance check for columns:

Case	8	9	10	11	12	13	14
N_{Ed} in N	86870	140390	126900	112800	136190	125300	113190
M_{Ed} in Nm	70730	389360	424720	432670	401700	431870	435490
V_{Ed} in N	14070	77870	84940	86530	80340	86370	87100
$N_{pl,Rd}$ in N	1018020	2775590	2775590	2775590	2775590	2775590	2775590
$M_{pl,Rd}$ in Nm	73040	362980	362980	362980	362980	362980	362980
$V_{pl,Rd}$ in N	139200	378540	378540	378540	378540	378540	378540
reduction f_y	0,10 (no)	0,21 (no)	0,22 (no)	0,23 (no)	0,21 (no)	0,23 (no)	0,23 (no)
n	0,0853	0,0506	0,0457	0,0406	0,0491	0,0451	0,0408
a	0,2105	0,2126	0,2126	0,2126	0,2126	0,2126	0,2126
$M_{N,Rd}$ in Nm	74667	385610	387584	389648	386225	387819	389591
Check	0,97	1,07	1,17	1,19	1,11	1,19	1,20

Stability check for beam:

Case	8	9	10	11	12	13	14
N_{Ed} in N		77870	85030	85930	73700	80100	80680
$M_{y,Ed}$ in Nm		389360	424720	432670	401700	431870	435490
χ_y	not loaded in compression	0,650	0,637	0,564	0,650	0,637	0,564
Φ		1,042	1,066	1,200	1,042	1,066	1,200
λ		0,917	0,938	1,053	0,917	0,938	1,053
α		0,34	0,34	0,34	0,34	0,34	0,34
A in mm ²		11811,0	11811,0	11811,0	11811,0	11811,0	11811,0
$W_{pl,y}$ in mm ³		1544600	1544600	1544600	1544600	1544600	1544600
f_y in N/mm ²		235	235	235	235	235	235
F_{cr} in N		3302800	3153410	2502640	3302800	3153410	2502640
C_{my}		0,702	0,602	0,614	0,654	0,586	0,611
k_{yy} 1		0,724	0,623	0,642	0,673	0,606	0,638
k_{yy} 2	0,727	0,625	0,641	0,675	0,608	0,636	
Check		0,82	0,78	0,82	0,79	0,77	0,82

Cross-section resistance check for beam:

Case	8	9	10	11	12	13	14
N_{Ed} in N	41730	77870	73960	66350	73700	69400	61390
M_{Ed} in Nm	70370	389360	424720	432670	401700	431870	435490
V_{Ed} in N	73360	135260	129200	122050	131330	127340	121620
$N_{pl,Rd}$ in N	1018020	2775590	2775590	2775590	2775590	2775590	2775590
$M_{pl,Rd}$ in Nm	73040	362980	362980	362980	362980	362980	362980
$V_{pl,Rd}$ in N	139200	378540	378540	378540	378540	378540	378540
reduction f_y	0,53 (yes)	0,36 (no)	0,34 (no)	0,32 (no)	0,35 (no)	0,34 (no)	0,32 (no)
ρ	0,0029						
$f_{y,red}$ in N/mm ²	234,31						
n	0,0410	0,0281	0,0266	0,0239	0,0266	0,0250	0,0221
a	0,2105	0,2126	0,2126	0,2126	0,2126	0,2126	0,2126
$M_{N,Rd}$ in Nm	78259	394759	395331	396445	395369	395998	397171
$N_{pl,Rd;red}$ in N	1017316						
$M_{pl,Rd;red}$ in Nm	73016						
Check	0,96	1,07	1,17	1,19	1,11	1,19	1,20

Check 2: Cross-section resistance checks for non-sway frames using second order analysis including initial sway imperfections.

For columns:

Case	8	9	10	11	12	13	14
N_{Ed} in N	89520	142110	128880	114930	137940	127250	115310
M_{Ed} in Nm	71510	396110	437610	444740	410410	444730	446620
V_{Ed} in N	11380	76250	84650	86360	79130	86080	86720
$N_{pl,Rd}$ in N	1018020	2775590	2775590	2775590	2775590	2775590	2775590
$M_{pl,Rd}$ in Nm	73040	362980	362980	362980	362980	362980	362980
$V_{pl,Rd}$ in N	139200	378540	378540	378540	378540	378540	378540
reduction f_y	0,08 (no)	0,20 (no)	0,22 (no)	0,23 (no)	0,21 (no)	0,23 (no)	0,23 (no)
n	0,0879	0,0512	0,0464	0,0414	0,0497	0,0458	0,0415
a	0,2105	0,2126	0,2126	0,2126	0,2126	0,2126	0,2126
$M_{N,Rd}$ in Nm	74455	385359	387295	389336	385969	387533	389280
Check	0,98	1,09	1,21	1,23	1,13	1,23	1,23

For beam:

Case	8	9	10	11	12	13	14
N_{Ed} in N	45160	76280	73460	65650	72490	68890	60460
M_{Ed} in Nm	71510	396110	437610	444740	410410	444730	446620
V_{Ed} in N	74100	137040	131210	124240	133020	129240	123670
$N_{pl,Rd}$ in N	1018020	2775590	2775590	2775590	2775590	2775590	2775590
$M_{pl,Rd}$ in Nm	73040	362980	362980	362980	362980	362980	362980
$V_{pl,Rd}$ in N	139200	378540	378540	378540	378540	378540	378540
reduction f_y	0,53 (yes)	0,36 (no)	0,35 (no)	0,33 (no)	0,35 (no)	0,34 (no)	0,33 (no)
ρ	0,0042						
$f_{y,red}$ in N/mm ²	234,02						
n	0,0444	0,0275	0,0265	0,0237	0,0261	0,0248	0,0218
a	0,2105	0,2126	0,2126	0,2126	0,2126	0,2126	0,2126
$M_{N,Rd}$ in Nm	77971	394992	395404	396547	395546	396073	397307
$N_{pl,Rd;red}$ in N	1017012						
$M_{pl,Rd;red}$ in Nm	73005						
Check	0,98	1,09	1,21	1,23	1,13	1,23	1,23

Check 3: Sway frames using first order analysis and stability checks using sway buckling lengths (Sway Mode Buckling Length Method)

Stability check for columns:

Case	1	2	3	4	5	6	7
N_{Ed} in N	111070	105490	100990	95470	71270	75690	80600
$M_{y,Ed}$ in Nm	53960	57690	62220	65030	75570	75480	73750
χ_y	0,285	0,329	0,402	0,531	0,374	0,428	0,511
Φ	2,155	1,906	1,613	1,266	1,712	1,529	1,312
λ	1,676	1,536	1,354	1,107	1,418	1,298	1,141
α	0,34	0,34	0,34	0,34	0,34	0,34	0,34
A in mm ²	4332	4332	4332	4332	4332	4332	4332
W_{ply} in mm ³	310821	310821	310821	310821	310821	310821	310821
f_y in N/mm ²	235	235	235	235	235	235	235
F_{cr} in N	362600	431650	555060	831460	506440	604580	781330
C_{my}	0,9	0,9	0,9	0,9	0,9	0,9	0,9
k_{yy} 1	1,408	1,278	1,157	1,044	1,105	1,072	1,031
k_{yy} 2	1,176	1,126	1,078	1,027	1,035	1,025	1,012
Check	1,25	1,20	1,17	1,09	1,26	1,23	1,18

Cross-section resistance check for columns:

Case	1	2	3	4	5	6	7
N_{Ed} in N	111070	105490	100990	95470	71270	75690	80600
M_{Ed} in Nm	53960	57690	62220	65030	75570	75480	73750
V_{Ed} in N	10790	11570	12440	13010	15130	15100	14750
$N_{pl,Rd}$ in N	1018020	1018020	1018020	1018020	1018020	1018020	1018020
$M_{pl,Rd}$ in Nm	73040	73040	73040	73040	73040	73040	73040
$V_{pl,Rd}$ in N	139200	139200	139200	139200	139200	139200	139200
reduction f_y	0,08 (no)	0,08 (no)	0,09 (no)	0,09 (no)	0,11 (no)	0,11 (no)	0,11 (no)
n	0,1091	0,1036	0,0992	0,0938	0,0700	0,0744	0,0792
a	0,2105	0,2105	0,2105	0,2105	0,2105	0,2105	0,2105
$M_{N,Rd}$ in Nm	72726	73174	73535	73977	75918	75564	75170
Check	0,74	0,79	0,85	0,89	1,03	1,03	1,01

Stability check for beam:

Case	1	2	3	4	5	6	7
N_{Ed} in N	10790	12070	12960	13010	4950	780	
$M_{y,Ed}$ in Nm	81650	76050	72410	71020	75570	75480	
χ_y	0,033	0,045	0,064	0,100	0,032	0,006	
Φ	15,828	11,548	8,256	5,468	15,862	84,209	
λ	5,376	4,541	3,781	2,998	5,382	12,773	
α	0,34	0,34	0,34	0,34	0,34	0,34	
A in mm ²	4332,0	4332,0	4332,0	4332,0	4332,0	4332,0	
$W_{pl,y}$ in mm ³	310821	310821	310821	310821	310821	310821	
f_y in N/mm ²	235	235	235	235	235	235	
F_{cr} in N	35230	49370	71220	113300	35150	6240	
C_{my}	0,9	0,9	0,9	0,9	0,9	0,9	
$k_{yy,1}$	2,416	1,927	1,540	1,223	1,598	2,352	
$k_{yy,2}$	1,134	1,089	1,043	0,992	1,008	0,992	
Check	1,59	1,40	1,23	1,09	1,19	1,15	

not loaded in compression

Cross-section resistance check for beam:

Case	1	2	3	4	5	6	7
N_{Ed} in N	10790	11620	12120	15330	4950	8860	24360
M_{Ed} in Nm	81650	76050	72410	71020	75570	75480	73750
V_{Ed} in N	0	0	0	0	69410	73240	74540
$N_{pl,Rd}$ in N	1018020	1018020	1018020	1018020	1018020	1018020	1018020
$M_{pl,Rd}$ in Nm	73040	73040	73040	73040	73040	73040	73040
$V_{pl,Rd}$ in N	139200	139200	139200	139200	139200	139200	139200
reduction f_y	0 (no)	0 (no)	0 (no)	0 (no)	0,499 (no)	0,53 (yes)	0,54 (yes)
ρ						0,003	0,005
$f_{y,red}$ in N/mm ²						234,36	233,82
n	0,0106	0,0114	0,0119	0,0151	0,0049	0,0087	0,0240
a	0,2105	0,2105	0,2105	0,2105	0,2105	0,2105	0,2105
$M_{N,Rd}$ in Nm	80768	80701	80661	80404	81236	80922	79677
$N_{pl,Rd:red}$ in N						1017361	1016805
$M_{pl,Rd:red}$ in Nm						72843	72675
Check	1,12	1,04	0,99	0,97	1,03	1,04	1,01

Check 4: Sway frames using first order analysis with amplified sway moments and stability checks using non-sway buckling lengths (Amplified Sway Moment Method).

Stability check for columns, $C_{my} = \text{calculated (0.6)}$:

Case	1	2	3	4	5	6	7
N_{Ed} in N	112310	106520	101840	96160	75260	79230	83510
$M_{y;Ed}$ in Nm	57060	60160	63830	65980	85610	83360	79100
χ_y	0,833	0,833	0,833	0,831	0,833	0,833	0,833
Φ	0,754	0,754	0,755	0,757	0,754	0,754	0,755
λ	0,607	0,607	0,609	0,612	0,607	0,607	0,609
α	0,34	0,34	0,34	0,34	0,34	0,34	0,34
A in mm ²	4332	4332	4332	4332	4332	4332	4332
W_{ply} in mm ³	310821	310821	310821	310821	310821	310821	310821
f_y in N/mm ²	235	235	235	235	235	235	235
F_{cr} in N	2759670	2758910	2745610	2718890	2759670	2758910	2745610
C_{my}	0,6	0,6	0,6	0,6	0,6	0,6	0,6
k_{yy} 1	0,632	0,631	0,629	0,628	0,622	0,623	0,624
k_{yy} 2	0,664	0,660	0,658	0,655	0,643	0,645	0,647
Check	0,63	0,65	0,67	0,68	0,82	0,80	0,77

Stability check for columns, $C_{my} = 0.9$:

Case	1	2	3	4	5	6	7
N_{Ed} in N	112310	106520	101840	96160	75260	79230	83510
$M_{y;Ed}$ in Nm	57060	60160	63830	65980	85610	83360	79100
χ_y	0,833	0,833	0,833	0,831	0,833	0,833	0,833
Φ	0,754	0,754	0,755	0,757	0,754	0,754	0,755
λ	0,607	0,607	0,609	0,612	0,607	0,607	0,609
α	0,34	0,34	0,34	0,34	0,34	0,34	0,34
A in mm ²	4332	4332	4332	4332	4332	4332	4332
W_{ply} in mm ³	310821	310821	310821	310821	310821	310821	310821
f_y in N/mm ²	235	235	235	235	235	235	235
F_{cr} in N	2759670	2758910	2745610	2718890	2759670	2758910	2745610
C_{my}	0,9	0,9	0,9	0,9	0,9	0,9	0,9
k_{yy} 1	0,949	0,946	0,944	0,942	0,933	0,934	0,936
k_{yy} 2	0,995	0,990	0,987	0,982	0,964	0,967	0,971
Check	0,87	0,90	0,95	0,96	1,18	1,16	1,11

Cross-section resistance check for columns:

Case	1	2	3	4	5	6	7
N_{Ed} in N	112300	106520	101840	96160	75260	79230	83510
M_{Ed} in Nm	57060	60160	63830	65980	85610	83360	79100
V_{Ed} in N	11410	12030	12770	13200	17120	16670	15820
$N_{pl,Rd}$ in N	1018020	1018020	1018020	1018020	1018020	1018020	1018020
$M_{pl,Rd}$ in Nm	73040	73040	73040	73040	73040	73040	73040
$V_{pl,Rd}$ in N	139200	139200	139200	139200	139200	139200	139200
reduction f_y	0,08 (no)	0,09 (no)	0,09 (no)	0,09 (no)	0,12 (no)	0,12 (no)	0,11 (no)
n	0,1103	0,1046	0,1000	0,0945	0,0739	0,0778	0,0820
a	0,2105	0,2105	0,2105	0,2105	0,2105	0,2105	0,2105
$M_{N,Rd}$ in Nm	72628	73091	73467	73922	75598	75280	74936
Check	0,79	0,82	0,87	0,90	1,17	1,14	1,08

Stability check for beam, C_{my} = calculated:

Case	1	2	3	4	5	6	7
N_{Ed} in N	10790	11810	12520	12470	4950	not loaded in compression	not loaded in compression
$M_{y,Ed}$ in Nm	83300	77870	73990	72760	86870		
χ_y	0,871	0,870	0,859	0,830	0,871		
Φ	0,696	0,697	0,714	0,758	0,696		
λ	0,530	0,531	0,555	0,613	0,530		
α	0,34	0,34	0,34	0,34	0,34		
A in mm ²	4332	4332	4332	4332	4332		
W_{ply} in mm ³	310821	310821	310821	310821	310821		
f_y in N/mm ²	235	235	235	235	235		
F_{cr} in N	3628540	3609440	3308840	2707860	3628540		
C_{my}	0,915	0,911	0,906	0,904	0,631		
k_{yy} 1	0,919	0,915	0,911	0,910	0,632		
k_{yy} 2	0,924	0,921	0,916	0,915	0,634		
Check	1,06	0,99	0,94	0,92	0,76		

Stability check for beam, $C_{my} = 0.9$:

Case	1	2	3	4	5	6	7
N_{Ed} in N	10790	11810	12520	12470	4950	not loaded in compression	not loaded in compression
$M_{y,Ed}$ in Nm	83300	77870	73990	72760	86870		
χ_y	0,871	0,870	0,859	0,830	0,871		
Φ	0,696	0,697	0,714	0,758	0,696		
λ	0,530	0,531	0,555	0,613	0,530		
α	0,34	0,34	0,34	0,34	0,34		
A in mm ²	4332	4332	4332	4332	4332		
$W_{pl,y}$ in mm ³	310821	310821	310821	310821	310821		
f_y in N/mm ²	235	235	235	235	235		
F_{cr} in N	3628540	3609440	3308840	2707860	3628540		
C_{my}	0,9	0,9	0,9	0,9	0,9		
k_{yy} 1	0,904	0,904	0,905	0,905	0,902		
k_{yy} 2	0,909	0,910	0,910	0,911	0,904		
Check	1,04	0,98	0,93	0,92	1,08		

Cross-section resistance check for beam:

Case	1	2	3	4	5	6	7
N_{Ed} in N	10790	10910	11680	12910	4950	8860	24360
M_{Ed} in Nm	81650	76290	72900	71610	85610	75480	73750
V_{Ed} in N	0	0	0	0	73400	73240	74540
$N_{pl,Rd}$ in N	1018020	1018020	1018020	1018020	1018020	1018020	1018020
$M_{pl,Rd}$ in Nm	73040	73040	73040	73040	73040	73040	73040
$V_{pl,Rd}$ in N	139200	139200	139200	139200	139200	139200	139200
reduction f_y	0,00 (no)	0,00 (no)	0,00 (no)	0,00 (no)	0,53 (yes)	0,53 (yes)	0,54 (yes)
ρ					0,003	0,003	0,005
$f_{y,red}$ in N/mm ²					234,30	234,36	233,82
n	0,0106	0,0107	0,0115	0,0127	0,0049	0,0087	0,0240
a	0,2105	0,2105	0,2105	0,2105	0,2105	0,2105	0,2105
$M_{N,Rd}$ in Nm	80768	80758	80696	80598	81236	80922	79677
$N_{pl,Rd;red}$ in N					1017301	1017361	1016805
$M_{pl,Rd;red}$ in Nm					72825	72843	72675
Check	1,12	1,04	0,99	0,98	1,18	1,04	1,01

Check 5: Sway frames using second order analysis including initial sway imperfections and stability checks using non-sway buckling lengths

Stability check for columns, C_{my} = calculated (0.6):

Case	1	2	3	4	5	6	7
N_{Ed} in N	112270	107620	103610	98090	74330	78760	83510
$M_{y;Ed}$ in Nm	56260	61810	66220	67530	84020	82300	78470
χ_y	0,833	0,833	0,833	0,831	0,833	0,833	0,833
Φ	0,754	0,754	0,755	0,757	0,754	0,754	0,755
λ	0,607	0,607	0,609	0,612	0,607	0,607	0,609
α	0,34	0,34	0,34	0,34	0,34	0,34	0,34
A in mm ²	4332	4332	4332	4332	4332	4332	4332
W_{ply} in mm ³	310821	310821	310821	310821	310821	310821	310821
f_y in N/mm ²	235	235	235	235	235	235	235
F_{cr} in N	2759670	2758910	2745610	2718890	2759670	2758910	2745610
C_{my}	0,6	0,6	0,6	0,6	0,6	0,6	0,6
k_{yy} 1	0,632	0,631	0,630	0,629	0,621	0,623	0,624
k_{yy} 2	0,664	0,661	0,659	0,656	0,642	0,645	0,647
Check	0,62	0,66	0,69	0,70	0,80	0,79	0,77

Stability check for columns, C_{my} = 0.9:

Case	1	2	3	4	5	6	7
N_{Ed} in N	112270	107620	103610	98090	74330	78760	83510
$M_{y;Ed}$ in Nm	56260	61810	66220	67530	84020	82300	78470
χ_y	0,833	0,833	0,833	0,831	0,833	0,833	0,833
Φ	0,754	0,754	0,755	0,757	0,754	0,754	0,755
λ	0,607	0,607	0,609	0,612	0,607	0,607	0,609
α	0,34	0,34	0,34	0,34	0,34	0,34	0,34
A in mm ²	4332	4332	4332	4332	4332	4332	4332
W_{ply} in mm ³	310821	310821	310821	310821	310821	310821	310821
f_y in N/mm ²	235	235	235	235	235	235	235
F_{cr} in N	2759670	2758910	2745610	2718890	2759670	2758910	2745610
C_{my}	0,9	0,9	0,9	0,9	0,9	0,9	0,9
k_{yy} 1	0,949	0,947	0,945	0,943	0,932	0,934	0,936
k_{yy} 2	0,995	0,991	0,988	0,983	0,963	0,967	0,971
Check	0,86	0,93	0,98	0,99	1,16	1,15	1,10

Cross-section resistance check for columns:

Case	1	2	3	4	5	6	7
N_{Ed} in N	112420	107800	103820	98320	74550	79090	83810
M_{Ed} in Nm	56260	61810	66220	67530	84020	82300	78470
V_{Ed} in N	9690	10090	10900	11280	14690	14260	76980
$N_{pl,Rd}$ in N	1018020	1018020	1018020	1018020	1018020	1018020	1018020
$M_{pl,Rd}$ in Nm	73040	73040	73040	73040	73040	73040	73040
$V_{pl,Rd}$ in N	139200	139200	139200	139200	139200	139200	139200
reduction f_y	0,07 (no)	0,07 (no)	0,08 (no)	0,08 (no)	0,11 (no)	0,10 (no)	0,10 (no)
n	0,1104	0,1059	0,1020	0,0966	0,0732	0,0777	0,0823
a	0,2105	0,2105	0,2105	0,2105	0,2105	0,2105	0,2105
$M_{N,Rd}$ in Nm	72618	72989	73308	73749	75655	75291	74912
Check	0,77	0,85	0,91	0,92	1,15	1,13	1,07

Stability check for beam, C_{my} = calculated:

Case	1	2	3	4	5	6	7
N_{Ed} in N	9640	8360	9910	7800	4010	not loaded in compression	not loaded in compression
$M_{y,Ed}$ in Nm	82810	77530	75080	74200	84020		
χ_y	0,871	0,870	0,859	0,830	0,871		
Φ	0,696	0,697	0,714	0,758	0,696		
λ	0,530	0,531	0,555	0,613	0,530		
α	0,34	0,34	0,34	0,34	0,34		
A in mm ²	4332	4332	4332	4332	4332		
W_{ply} in mm ³	310821	310821	310821	310821	310821		
f_y in N/mm ²	235	235	235	235	235		
F_{cr} in N	3628540	3609440	3308840	2707860	3628540		
C_{my}	0,916	0,911	0,906	0,904	0,631		
k_{yy} 1	0,919	0,914	0,910	0,907	0,632		
k_{yy} 2	0,924	0,918	0,914	0,911	0,633		
Check	1,05	0,98	0,95	0,93	0,73		

Stability check for beam, $C_{my} = 0.9$:

Case	1	2	3	4	5	6	7
N_{Ed} in N	9640	8360	9910	7800	4010	not loaded in compression	not loaded in compression
$M_{y,Ed}$ in Nm	82810	77530	75080	74200	84020		
χ_y	0,87	0,870	0,859	0,830	0,87		
Φ	0,70	0,697	0,714	0,758	0,70		
λ	0,53	0,531	0,555	0,613	0,53		
α	0,34	0,34	0,34	0,34	0,34		
A in mm ²	4332	4332	4332	4332	4332		
W_{ply} in mm ³	310821	310821	310821	310821	310821		
f_y in N/mm ²	235	235	235	235	235		
F_{cr} in N	3628540	3609440	3308840	2707860	3628540		
C_{my}	0,9	0,9	0,9	0,9	0,9		
k_{yy} 1	0,903	0,903	0,904	0,903	0,901		
k_{yy} 2	0,908	0,907	0,908	0,907	0,903		
Check	1,03	0,97	0,94	0,93	1,04		

Cross-section resistance check for beam:

Case	1	2	3	4	5	6	7
N_{Ed} in N	10650	11650	12060	13070	4190	8860	24360
M_{Ed} in Nm	82810	77530	75080	74200	84020	75480	73750
V_{Ed} in N	0	0	0	0	72890	73240	74540
$N_{pl,Rd}$ in N	1018020	1018020	1018020	1018020	1018020	1018020	1018020
$M_{pl,Rd}$ in Nm	73040	73040	73040	73040	73040	73040	73040
$V_{pl,Rd}$ in N	139200	139200	139200	139200	139200	139200	139200
reduction f_y	0,00 (no)	0,00 (no)	0,00 (no)	0,00 (no)	0,52 (yes)	0,53 (yes)	0,54 (yes)
ρ					0,002	0,003	0,005
$f_{y,red}$ in N/mm ²					234,47	234,36	233,82
n	0,0105	0,0114	0,0118	0,0128	0,0041	0,0087	0,0240
a	0,2105	0,2105	0,2105	0,2105	0,2105	0,2105	0,2105
$M_{N,Rd}$ in Nm	80779	80699	80666	80585	81297	80922	79677
$N_{pl,Rd;red}$ in N					1017481	1017361	1016805
$M_{pl,Rd;red}$ in Nm					72880	72843	72675
Check	1,13	1,06	1,03	1,02	1,15	1,04	1,01

The checks for case 4 (sway frame) and case 8 (non-sway frame) have been described in detail.

Check 1: First order analysis and non-sway buckling lengths applied to case 8

In figure F.1 the axial force distribution, shear force distribution and bending moment distribution is given using a first order elastic analyses for case 8.

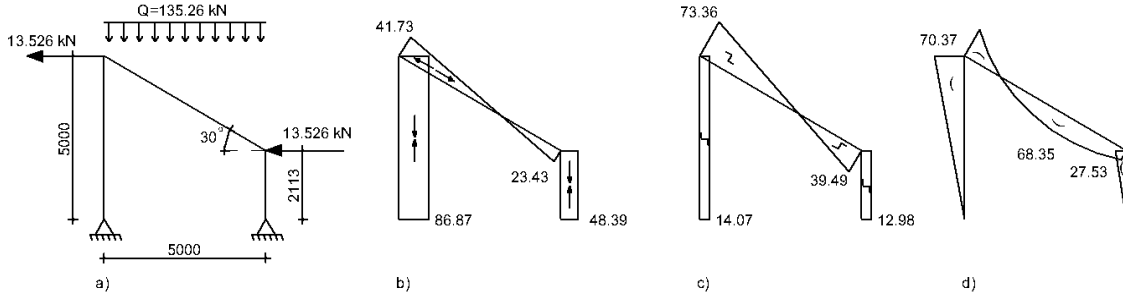


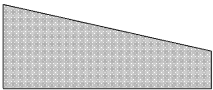
Figure F.1: a) Case 8 b) Axial force distribution in kN c) Shear force distribution in kN d) Bending moment distribution in kNm

Stability check for the columns according to section 6.3 of Eurocode 3:

$$\chi = \frac{1}{\Phi + \sqrt{\Phi^2 - \bar{\lambda}^2}} = \frac{1}{0,757 + \sqrt{0,757^2 - 0,612^2}} = 0,831$$

Where: $\Phi = 0,5 \cdot (1 + \alpha \cdot (\bar{\lambda} - 0,2) + \bar{\lambda}^2) = 0,5 \cdot (1 + 0,34 \cdot (0,612 - 0,2) + 0,612^2) = 0,757$

$$\bar{\lambda} = \sqrt{\frac{A \cdot f_y}{F_{cr}}} = \sqrt{\frac{4332 \cdot 235}{2718890}} = 0,612$$

M  $\psi \cdot M \quad C_{my} = 0,6 + 0,4 \cdot \psi = 0,6 + 0,4 \cdot 0 = 0,6$

$$k_{yy} = C_{my} \cdot \left(1 + (\bar{\lambda}_y - 0,2) \cdot \frac{N_{Ed}}{\chi_y \cdot N_{Rk} / \gamma_{M1}} \right) \leq C_{my} \cdot \left(1 + 0,8 \cdot \frac{N_{Ed}}{\chi_y \cdot N_{Rk} / \gamma_{M1}} \right) =$$

$$0,6 \cdot \left(1 + (0,612 - 0,2) \cdot \frac{86870}{0,831 \cdot (235 \cdot 4332) / 1} \right) \leq 0,6 \cdot \left(1 + 0,8 \cdot \frac{86870}{0,831 \cdot (235 \cdot 4332) / 1} \right) = 0,625$$

Stability check:

$$\frac{N_{Ed}}{\chi_y \cdot N_{Rk}} + k_{yy} \cdot \frac{M_{y,Ed}}{M_{y,Rk}} = \frac{86870}{0,831 \cdot (235 \cdot 4332)} + 0,625 \cdot \frac{70730}{(235 \cdot 310821)} = 0,71 \leq 1,0$$

Cross section resistance check for the columns

$$\frac{V_{Ed}}{V_{pl,Rd}} = \frac{14070}{139200} = 0,10 < 0,5 \quad \text{No reduction of the resistance for bending and axial force}$$

$$n = \frac{N_{Ed}}{N_{pl,Rd}} = \frac{86870}{1018020} = 0,0853$$

$$a = \frac{(A - 2 \cdot b \cdot t_f)}{A} = \frac{(4332 - 2 \cdot 180 \cdot 9,5)}{4332} = 0,2105$$

$$M_{N,Rd} = \frac{M_{pl,Rd} \cdot (1-n)}{(1-0,5 \cdot a)} = \frac{73040 \cdot (1-0,0853)}{(1-0,5 \cdot 0,2105)} = 74667 \text{ Nm} \rightarrow \text{requirement: } M_{N,Rd} \leq M_{pl,Rd}$$

$$\frac{M_{Ed}}{M_{pl,Rd}} = \frac{70730}{73040} = 0,97 \leq 1,0$$

Cross section resistance check for the beam

$$\frac{V_{Ed}}{V_{pl,Rd}} = \frac{73360}{139200} = 0,53 > 0,5 \quad \text{Reduction of the resistance for bending and axial force}$$

$$\rho = \left(\frac{2 \cdot V_{Ed}}{V_{pl,Rd}} - 1 \right)^2 = \left(\frac{2 \cdot 73360}{139200} - 1 \right)^2 = 0,0029$$

The reduced yield strength for the shear area is:

$$(1-\rho) \cdot f_y = (1-0,0029) \cdot 235 = 234,31 \text{ N/mm}^2$$

$$N_{pl,Rd} = (1-\rho) \cdot f_y \cdot h \cdot t_w + f_y \cdot (A - (h \cdot t_w)) = 234,3 \cdot 171 \cdot 6 + 235 \cdot (4332 - (171 \cdot 6)) = 1017316 \text{ N}$$

$$M_{pl,Rd} = W_{pl,v} \cdot (1-\rho) \cdot f_y + W_{pl,n} \cdot f_y = 39123 \cdot 234,31 + 271698 \cdot 235 = 73016 \text{ Nm}$$

$$W_{pl,n} = (b - t_w) \cdot t_f \cdot (h - t_f) + (t_w \cdot 0,5 \cdot t_f) \cdot (h - 0,5 \cdot t_f) =$$

$$(180 - 6) \cdot 9,5 \cdot (171 - 9,5) + (6 \cdot 0,5 \cdot 9,5) \cdot (171 - 0,5 \cdot 9,5) = 271698 \text{ mm}^3$$

$$W_{pl,v} = W_{pl} - W_{pl,n} = 310821 - 271698 = 39123 \text{ mm}^3$$

$$n = \frac{N_{Ed}}{N_{pl,Rd}} = \frac{41730}{1017316} = 0,0410$$

$$a = \frac{(A - 2 \cdot b \cdot t_f)}{A} = \frac{(4332 - 2 \cdot 180 \cdot 9,5)}{4332} = 0,2105$$

$$M_{N,Rd} = \frac{M_{pl,Rd:red} \cdot (1-n)}{(1-0,5 \cdot a)} = \frac{73016 \cdot (1-0,0410)}{(1-0,5 \cdot 0,2105)} = 78259 \text{ Nm} \rightarrow \text{requirement: } M_{N,Rd} \leq M_{pl,Rd}$$

$$\frac{M_{Ed}}{M_{pl,Rd:red}} = \frac{70370}{73016} = 0,96 \leq 1,0$$

Check 2: Second order analysis applied to case 8

In figure F.2 the axial force distribution, shear force distribution and bending moment distribution is given using a second order elastic analyses including bow imperfections for case 8. The bow imperfections for the cases are given in table 4.4.

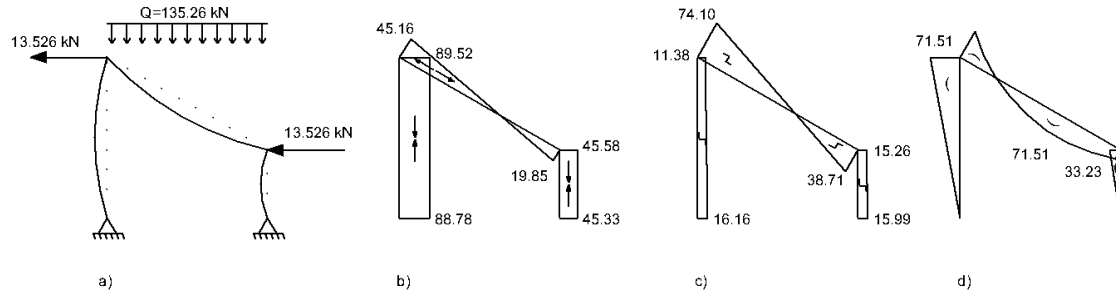


Figure F.2: a) Case 8 b) Axial force distribution in kN c) Shear force distribution in kN d) Bending moment distribution in kNm

Cross section resistance check for the columns

$$\frac{V_{Ed}}{V_{pl,Rd}} = \frac{11380}{139200} = 0,08 < 0,5 \quad \text{No reduction of the resistance for bending and axial force}$$

$$n = \frac{N_{Ed}}{N_{pl,Rd}} = \frac{89520}{1018020} = 0,0879$$

$$a = \frac{(A - 2 \cdot b \cdot t_f)}{A} = \frac{(4332 - 2 \cdot 180 \cdot 9,5)}{4332} = 0,2105$$

$$M_{N,Rd} = \frac{M_{pl,Rd} \cdot (1 - n)}{(1 - 0,5 \cdot a)} = \frac{73040 \cdot (1 - 0,0879)}{(1 - 0,5 \cdot 0,2105)} = 74455 \text{ Nm} \rightarrow \text{requirement: } M_{N,Rd} \leq M_{pl,Rd}$$

$$\frac{M_{Ed}}{M_{pl,Rd}} = \frac{71510}{73040} = 0,98 \leq 1,0$$

Cross section resistance check for the beam

$$\frac{V_{Ed}}{V_{pl,Rd}} = \frac{74100}{139200} = 0,53 > 0,5 \quad \text{Reduction of the resistance for bending and axial force}$$

$$\rho = \left(\frac{2 \cdot V_{Ed}}{V_{pl,Rd}} - 1 \right)^2 = \left(\frac{2 \cdot 74100}{139200} - 1 \right)^2 = 0,0042$$

The reduced yield strength for the shear area is:

$$(1 - \rho) \cdot f_y = (1 - 0,0042) \cdot 235 = 234,02 \text{ N/mm}^2$$

$$N_{pl,Rd} = (1 - \rho) \cdot f_y \cdot h \cdot t_w + f_y \cdot (A - (h \cdot t_w)) = 234,02 \cdot 171 \cdot 6 + 235 \cdot (4332 - (171 \cdot 6)) = 1017012 \text{ N}$$

$$M_{pl,Rd} = W_{pl,v} \cdot (1-\rho) \cdot f_y + W_{pl,n} \cdot f_y = 39123 \cdot 234,02 + 271698 \cdot 235 = 73005 \text{ Nm}$$

$$W_{pl,n} = (b - t_w) \cdot t_f \cdot (h - t_f) + (t_w \cdot 0,5 \cdot t_f) \cdot (h - 0,5 \cdot t_f) = \\ (180 - 6) \cdot 9,5 \cdot (171 - 9,5) + (6 \cdot 0,5 \cdot 9,5) \cdot (171 - 0,5 \cdot 9,5) = 271698 \text{ mm}^3$$

$$W_{pl,v} = W_{pl} - W_{pl,n} = 310821 - 271698 = 39123 \text{ mm}^3$$

$$n = \frac{N_{Ed}}{N_{pl,Rd,red}} = \frac{45160}{1017012} = 0,0444$$

$$a = \frac{(A - 2 \cdot b \cdot t_f)}{A} = \frac{(4332 - 2 \cdot 180 \cdot 9,5)}{4332} = 0,2105$$

$$M_{N,Rd} = \frac{M_{pl,Rd} \cdot (1-n)}{(1-0,5 \cdot a)} = \frac{73005 \cdot (1-0,0444)}{(1-0,5 \cdot 0,2105)} = 77971 \text{ Nm} \rightarrow \text{requirement: } M_{N,Rd} \leq M_{pl,Rd}$$

$$\frac{M_{Ed}}{M_{pl,Rd}} = \frac{71510}{73005} = 0,98 \leq 1,0$$

Check 3: First order analysis and sway buckling lengths applied to case 4

In figure F.3 the axial force distribution, shear force distribution and bending moment distribution is given using a first order elastic analysis for case 4.

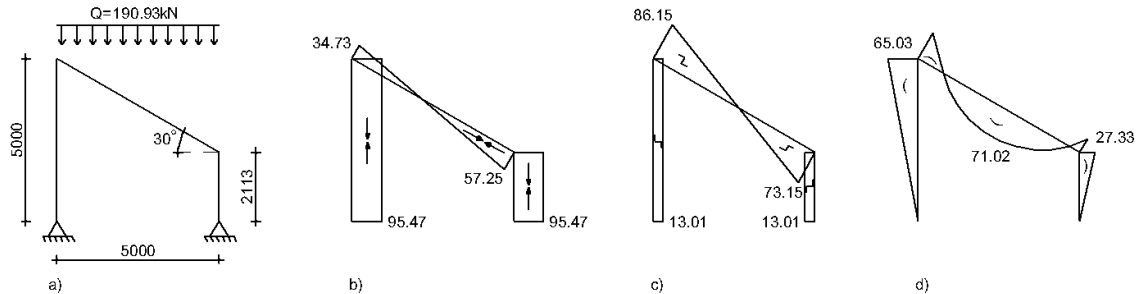


Figure F.3: a) Case 4 b) Axial force distribution in kN c) Shear force distribution in kN d) Bending moment distribution in kNm

Stability check for the columns according to section 6.3 of Eurocode 3:

$$\chi = \frac{1}{\Phi + \sqrt{\Phi^2 - \bar{\lambda}^2}} = \frac{1}{1,266 + \sqrt{1,266^2 - 1,107^2}} = 0,531$$

Where: $\Phi = 0,5 \cdot (1 + \alpha \cdot (\bar{\lambda} - 0,2) + \bar{\lambda}^2) = 0,5 \cdot (1 + 0,34 \cdot (1,107 - 0,2) + 1,107^2) = 1,266$

$$\bar{\lambda} = \sqrt{\frac{A \cdot f_y}{F_{cr}}} = \sqrt{\frac{4332 \cdot 235}{831460}} = 1,107$$

$$k_{yy} = C_{my} \cdot \left(1 + (\bar{\lambda}_y - 0,2) \cdot \frac{N_{Ed}}{\chi_y \cdot N_{Rk} / \gamma_{M1}} \right) \leq C_{my} \cdot \left(1 + 0,8 \cdot \frac{N_{Ed}}{\chi_y \cdot N_{Rk} / \gamma_{M1}} \right) =$$

$$0,9 \cdot \left(1 + (1,107 - 0,2) \cdot \frac{95470}{0,531 \cdot (235 \cdot 4332) / 1} \right) \leq 0,9 \cdot \left(1 + 0,8 \cdot \frac{95470}{0,531 \cdot (235 \cdot 4332) / 1} \right) = 1,027$$

Stability check:

$$\frac{N_{Ed}}{\chi_y \cdot N_{Rk}} + k_{yy} \cdot \frac{M_{y,Ed}}{M_{y,Rk}} = \frac{95470}{0,531 \cdot (235 \cdot 4332)} + 1,027 \cdot \frac{65030}{(235 \cdot 310821)} = 1,09 \geq 1,0$$

Cross section resistance check for the columns

$$\frac{V_{Ed}}{V_{pl,Rd}} = \frac{13010}{139200} = 0,09 < 0,5 \quad \text{No reduction of the resistance for bending and axial force}$$

$$n = \frac{N_{Ed}}{N_{pl,Rd}} = \frac{95470}{1018020} = 0,0938$$

$$a = \frac{(A - 2 \cdot b \cdot t_f)}{A} = \frac{(4332 - 2 \cdot 180 \cdot 9,5)}{4332} = 0,2105$$

$$M_{N,Rd} = \frac{M_{pl,Rd} \cdot (1 - n)}{(1 - 0,5 \cdot a)} = \frac{73040 \cdot (1 - 0,0938)}{(1 - 0,5 \cdot 0,2105)} = 73977 \text{ Nm} \rightarrow \text{requirement: } M_{N,Rd} \leq M_{pl,Rd}$$

$$\frac{M_{Ed}}{M_{pl,Rd}} = \frac{65030}{73040} = 0,89 \leq 1,0$$

Stability check for the beam according to section 6.3 of Eurocode 3:

$$\chi = \frac{1}{\Phi + \sqrt{\Phi^2 - \bar{\lambda}^2}} = \frac{1}{5,468 + \sqrt{5,468^2 - 2,998^2}} = 0,100$$

$$\text{Where: } \Phi = 0,5 \cdot (1 + \alpha \cdot (\bar{\lambda} - 0,2) + \bar{\lambda}^2) = 0,5 \cdot (1 + 0,34 \cdot (2,998 - 0,2) + 2,998^2) = 5,468$$

$$\bar{\lambda} = \sqrt{\frac{A \cdot f_y}{F_{cr}}} = \sqrt{\frac{4332 \cdot 235}{113300}} = 2,998$$

$$k_{yy} = C_{my} \cdot \left(1 + (\bar{\lambda}_y - 0,2) \cdot \frac{N_{Ed}}{\chi_y \cdot N_{Rk} / \gamma_{M1}} \right) \leq C_{my} \cdot \left(1 + 0,8 \cdot \frac{N_{Ed}}{\chi_y \cdot N_{Rk} / \gamma_{M1}} \right) =$$

$$0,9 \cdot \left(1 + (2,997 - 0,2) \cdot \frac{13010}{0,100 \cdot (235 \cdot 4332) / 1} \right) \leq 0,9 \cdot \left(1 + 0,8 \cdot \frac{13010}{0,100 \cdot (235 \cdot 4332) / 1} \right) = 0,992$$

Stability check:

$$\frac{N_{Ed}}{\chi_y \cdot N_{Rk}} + k_{yy} \cdot \frac{M_{y,Ed}}{M_{y,Rk}} = \frac{13010}{0,100 \cdot (235 \cdot 4332)} + 0,992 \cdot \frac{71020}{(235 \cdot 310821)} = 1,09 \geq 1,0$$

Cross section resistance check for the beam

$$\frac{V_{Ed}}{V_{pl,Rd}} = \frac{0}{139200} = 0,0 < 0,5 \quad \text{No reduction of the resistance for bending and axial force}$$

$$n = \frac{N_{Ed}}{N_{pl,Rd}} = \frac{15330}{1018020} = 0,0151$$

$$a = \frac{(A - 2 \cdot b \cdot t_f)}{A} = \frac{(4332 - 2 \cdot 180 \cdot 9,5)}{4332} = 0,2105$$

$$M_{N,Rd} = \frac{M_{pl,Rd} \cdot (1 - n)}{(1 - 0,5 \cdot a)} = \frac{73040 \cdot (1 - 0,0151)}{(1 - 0,5 \cdot 0,2105)} = 80404 \text{ Nm} \rightarrow \text{requirement: } M_{N,Rd} \leq M_{pl,Rd}$$

$$\frac{M_{Ed}}{M_{pl,Rd}} = \frac{71020}{73040} = 0,97 \leq 1,0$$

Check 4: First order analysis and with amplified sway moments and non-sway buckling lengths applied to case 4

The equivalent lateral loads due to initial sway imperfections are should be amplified with factor:

$$C = \frac{1}{1 - \frac{1}{\alpha_{cr}}} = \frac{1}{1 - \frac{1}{8,71}} = 1,130$$

This gives equivalent lateral loads of:

$$\varphi_{c,l} \cdot N_{Ed} \cdot C = 3,873 \cdot 10^{-3} \cdot 95470 \cdot 1,130 = 418 \text{ N}$$

$$\varphi_{c,l} \cdot N_{Ed} \cdot C = 4,331 \cdot 10^{-3} \cdot 95470 \cdot 1,130 = 467 \text{ N}$$

Figure F.4 gives the axial force distribution, shear force distribution and bending moment distribution using a first order elastic analysis with equivalent lateral loads due to initial sway imperfections.

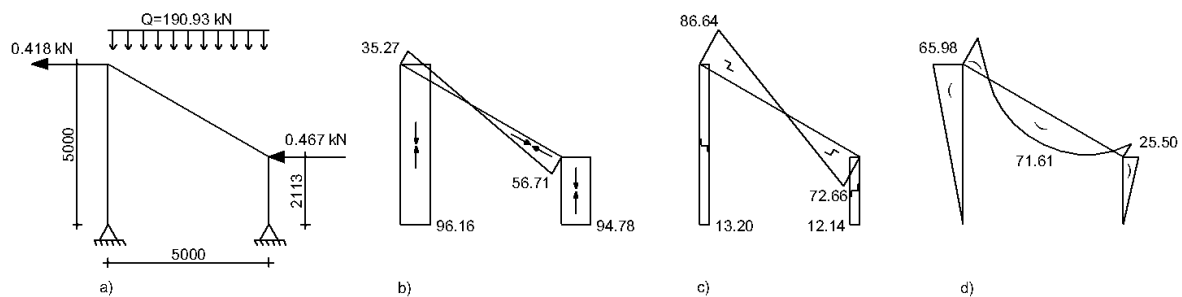



Figure F.4: a) Case 4 b) Axial force distribution in kN c) Shear force distribution in kN d) Bending moment distribution in kNm

Stability check for the columns according to section 6.3 of Eurocode 3:

$$\chi = \frac{1}{\Phi + \sqrt{\Phi^2 - \bar{\lambda}^2}} = \frac{1}{0,757 + \sqrt{0,757^2 - 0,612^2}} = 0,831$$

Where: $\Phi = 0,5 \cdot (1 + \alpha \cdot (\bar{\lambda} - 0,2) + \bar{\lambda}^2) = 0,5 \cdot (1 + 0,34 \cdot (0,612 - 0,2) + 0,612^2) = 0,757$

$$\bar{\lambda} = \sqrt{\frac{A \cdot f_y}{F_{cr}}} = \sqrt{\frac{4332 \cdot 235}{2718890}} = 0,612$$

M  $\psi \cdot M \quad C_{my} = 0,6 + 0,4 \cdot \psi = 0,6 + 0,4 \cdot 0 = 0,6$

Stability check using $C_{my} = 0,6$:

$$k_{yy} = C_{my} \cdot \left(1 + (\bar{\lambda}_y - 0,2) \cdot \frac{N_{Ed}}{\chi_y \cdot N_{Rk} / \gamma_{M1}} \right) \leq C_{my} \cdot \left(1 + 0,8 \cdot \frac{N_{Ed}}{\chi_y \cdot N_{Rk} / \gamma_{M1}} \right) =$$

$$0,6 \cdot \left(1 + (0,612 - 0,2) \cdot \frac{96160}{0,831 \cdot (235 \cdot 4332) / 1} \right) \leq 0,6 \cdot \left(1 + 0,8 \cdot \frac{96160}{0,831 \cdot (235 \cdot 4332) / 1} \right) = 0,628$$

$$\frac{N_{Ed}}{\chi_y \cdot N_{Rk}} + k_{yy} \cdot \frac{M_{y,Ed}}{M_{y,Rk}} = \frac{96160}{0,831 \cdot (235 \cdot 4332)} + 0,628 \cdot \frac{65980}{(235 \cdot 310821)} = 0,68 \leq 1,0$$

Stability check using $C_{my} = 0,9$:

$$k_{yy} = C_{my} \cdot \left(1 + (\bar{\lambda}_y - 0,2) \cdot \frac{N_{Ed}}{\chi_y \cdot N_{Rk} / \gamma_{M1}} \right) \leq C_{my} \cdot \left(1 + 0,8 \cdot \frac{N_{Ed}}{\chi_y \cdot N_{Rk} / \gamma_{M1}} \right) =$$

$$0,9 \cdot \left(1 + (0,612 - 0,2) \cdot \frac{96160}{0,831 \cdot (235 \cdot 4332) / 1} \right) \leq 0,9 \cdot \left(1 + 0,8 \cdot \frac{96160}{0,831 \cdot (235 \cdot 4332) / 1} \right) = 0,942$$

$$\frac{N_{Ed}}{\chi_y \cdot N_{Rk}} + k_{yy} \cdot \frac{M_{y,Ed}}{M_{y,Rk}} = \frac{96160}{0,831 \cdot (235 \cdot 4332)} + 0,942 \cdot \frac{65980}{(235 \cdot 310821)} = 0,96 \leq 1,0$$

Cross section resistance check for the columns

$$\frac{V_{Ed}}{V_{pl,Rd}} = \frac{13200}{139200} = 0,09 < 0,5 \quad \text{No reduction of the resistance for bending and axial force}$$

$$n = \frac{N_{Ed}}{N_{pl,Rd}} = \frac{96160}{1018020} = 0,0945$$

$$a = \frac{(A - 2 \cdot b \cdot t_f)}{A} = \frac{(4332 - 2 \cdot 180 \cdot 9,5)}{4332} = 0,2105$$

$$M_{N,Rd} = \frac{M_{pl,Rd} \cdot (1-n)}{(1-0,5 \cdot a)} = \frac{73040 \cdot (1-0,0945)}{(1-0,5 \cdot 0,2105)} = 73922 \text{ Nm} \rightarrow \text{requirement: } M_{N,Rd} \leq M_{pl,Rd}$$

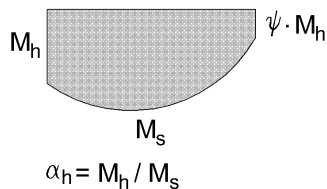
$$\frac{M_{Ed}}{M_{pl,Rd}} = \frac{65980}{73040} = 0,90 \leq 1,0$$

Stability check for the beam according to section 6.3 of Eurocode 3:

$$\chi = \frac{1}{\Phi + \sqrt{\Phi^2 - \bar{\lambda}^2}} = \frac{1}{0,758 + \sqrt{0,758^2 - 0,613^2}} = 0,830$$

Where: $\Phi = 0,5 \cdot (1 + \alpha \cdot (\bar{\lambda} - 0,2) + \bar{\lambda}^2) = 0,5 \cdot (1 + 0,34 \cdot (0,613 - 0,2) + 0,613^2) = 0,758$

$$\bar{\lambda} = \sqrt{\frac{A \cdot f_y}{F_{cr}}} = \sqrt{\frac{4332 \cdot 235}{2707860}} = 0,613$$



$$C_{my} = 0,95 + 0,05 \cdot \alpha_h = 0,95 + 0,05 \cdot \frac{-65840}{72763} = 0,905 \text{ (see table 5.2)}$$

Stability check using $C_{my} = 0,905$:

$$k_{yy} = C_{my} \cdot \left(1 + (\bar{\lambda}_y - 0,2) \cdot \frac{N_{Ed}}{\chi_y \cdot N_{Rk} / \gamma_{M1}} \right) \leq C_{my} \cdot \left(1 + 0,8 \cdot \frac{N_{Ed}}{\chi_y \cdot N_{Rk} / \gamma_{M1}} \right) =$$

$$0,905 \cdot \left(1 + (0,613 - 0,2) \cdot \frac{12470}{0,830 \cdot (235 \cdot 4332) / 1} \right) \leq 0,905 \cdot \left(1 + 0,8 \cdot \frac{12470}{0,830 \cdot (235 \cdot 4332) / 1} \right) = 0,911$$

$$\frac{N_{Ed}}{\chi_y \cdot N_{Rk}} + k_{yy} \cdot \frac{M_{y,Ed}}{M_{y,Rk}} = \frac{12470}{0,830 \cdot (235 \cdot 4332)} + 0,911 \cdot \frac{72760}{(235 \cdot 310821)} = 0,92 \leq 1,0$$

Stability check using $C_{my} = 0,9$:

$$k_{yy} = C_{my} \cdot \left(1 + (\bar{\lambda}_y - 0,2) \cdot \frac{N_{Ed}}{\chi_y \cdot N_{Rk} / \gamma_{M1}} \right) \leq C_{my} \cdot \left(1 + 0,8 \cdot \frac{N_{Ed}}{\chi_y \cdot N_{Rk} / \gamma_{M1}} \right) =$$

$$0,9 \cdot \left(1 + (0,613 - 0,2) \cdot \frac{12470}{0,830 \cdot (235 \cdot 4332) / 1} \right) \leq 0,9 \cdot \left(1 + 0,8 \cdot \frac{12470}{0,830 \cdot (235 \cdot 4332) / 1} \right) = 0,905$$

$$\frac{N_{Ed}}{\chi_y \cdot N_{Rk}} + k_{yy} \cdot \frac{M_{y,Ed}}{M_{y,Rk}} = \frac{12470}{0,830 \cdot (235 \cdot 4332)} + 0,905 \cdot \frac{72760}{(235 \cdot 310821)} = 0,92 \leq 1,0$$

Cross section resistance check for the beam

$$\frac{V_{Ed}}{V_{pl,Rd}} = \frac{0}{139200} = 0,0 < 0,5 \quad \text{No reduction of the resistance for bending and axial force}$$

$$n = \frac{N_{Ed}}{N_{pl,Rd}} = \frac{12910}{1018020} = 0,0127$$

$$a = \frac{(A - 2 \cdot b \cdot t_f)}{A} = \frac{(4332 - 2 \cdot 180 \cdot 9,5)}{4332} = 0,2105$$

$$M_{N,Rd} = \frac{M_{pl,Rd} \cdot (1-n)}{(1-0,5 \cdot a)} = \frac{66,79 \cdot (1-0,0127)}{(1-0,5 \cdot 0,2105)} = 80598 \text{Nm} \rightarrow \text{requirement: } M_{N,Rd} \leq M_{pl,Rd}$$

$$\frac{M_{Ed}}{M_{pl,Rd}} = \frac{71610}{73040} = 0,98 \leq 1$$

Check 5: Second order analysis and non-sway buckling lengths

As determined in table 4.4 a sway imperfection of 19,4mm should be applied at the top of the left column and a sway imperfection of 9,2mm should be applied at the top of the right column for case 4. Using a second order elastic analysis, the axial force distribution, shear force distribution and bending moment distribution as given in figure F.5 has been found.

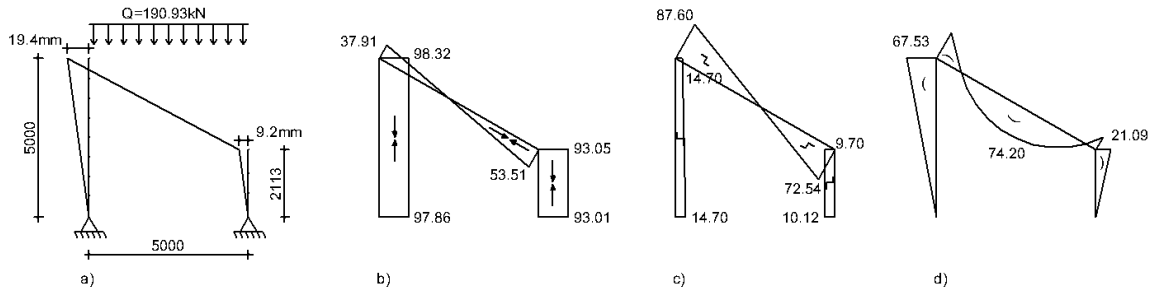



Figure F.5: a) Case 4 b) Axial force distribution in kN c) Shear force distribution in kN d) Bending moment distribution in kNm

Stability check for the columns according to section 6.3 of Eurocode 3:

$$\chi = \frac{1}{\Phi + \sqrt{\Phi^2 - \bar{\lambda}^2}} = \frac{1}{0,757 + \sqrt{0,757^2 - 0,612^2}} = 0,831$$

Where: $\Phi = 0,5 \cdot (1 + \alpha \cdot (\bar{\lambda} - 0,2) + \bar{\lambda}^2) = 0,5 \cdot (1 + 0,34 \cdot (0,612 - 0,2) + 0,612^2) = 0,757$

$$\bar{\lambda} = \sqrt{\frac{A \cdot f_y}{F_{cr}}} = \sqrt{\frac{4332 \cdot 235}{2718890}} = 0,612$$

M  $\psi \cdot M \quad C_{my} = 0,6 + 0,4 \cdot \psi = 0,6 + 0,4 \cdot 0 = 0,6$

Stability check using $C_{my} = 0,6$:

$$k_{yy} = C_{my} \cdot \left(1 + (\bar{\lambda}_y - 0,2) \cdot \frac{N_{Ed}}{\chi_y \cdot N_{Rk} / \gamma_{M1}} \right) \leq C_{my} \cdot \left(1 + 0,8 \cdot \frac{N_{Ed}}{\chi_y \cdot N_{Rk} / \gamma_{M1}} \right) =$$

$$0,6 \cdot \left(1 + (0,612 - 0,2) \cdot \frac{98090}{0,831 \cdot (235 \cdot 4332) / 1} \right) \leq 0,6 \cdot \left(1 + 0,8 \cdot \frac{98090}{0,831 \cdot (235 \cdot 4332) / 1} \right) = 0,629$$

$$\frac{N_{Ed}}{\chi_y \cdot N_{Rk}} + k_{yy} \cdot \frac{M_{y,Ed}}{M_{y,Rk}} = \frac{98090}{0,833 \cdot (235 \cdot 4332)} + 0,629 \cdot \frac{67530}{(235 \cdot 310821)} = 0,70 \leq 1,0$$

Stability check using $C_{my} = 0,9$:

$$k_{yy} = C_{my} \cdot \left(1 + (\bar{\lambda}_y - 0,2) \cdot \frac{N_{Ed}}{\chi_y \cdot N_{Rk} / \gamma_{M1}} \right) \leq C_{my} \cdot \left(1 + 0,8 \cdot \frac{N_{Ed}}{\chi_y \cdot N_{Rk} / \gamma_{M1}} \right) =$$

$$0,9 \cdot \left(1 + (0,612 - 0,2) \cdot \frac{98090}{0,831 \cdot (235 \cdot 4332) / 1} \right) \leq 0,9 \cdot \left(1 + 0,8 \cdot \frac{98090}{0,831 \cdot (235 \cdot 4332) / 1} \right) = 0,943$$

$$\frac{N_{Ed}}{\chi_y \cdot N_{Rk}} + k_{yy} \cdot \frac{M_{y,Ed}}{M_{y,Rk}} = \frac{98090}{0,833 \cdot (235 \cdot 4332)} + 0,943 \cdot \frac{67530}{(235 \cdot 310821)} = 0,99 \leq 1,0$$

Cross section resistance check for the columns

$$\frac{V_{Ed}}{V_{pl,Rd}} = \frac{11280}{139020} = 0,08 < 0,5 \quad \text{No reduction of the resistance for bending and axial force}$$

$$n = \frac{N_{Ed}}{N_{pl,Rd}} = \frac{98320}{1018020} = 0,0966$$

$$a = \frac{(A - 2 \cdot b \cdot t_f)}{A} = \frac{(4332 - 2 \cdot 180 \cdot 9,5)}{4332} = 0,2105$$

$$M_{N,Rd} = \frac{M_{pl,Rd} \cdot (1 - n)}{(1 - 0,5 \cdot a)} = \frac{73040 \cdot (1 - 0,0966)}{(1 - 0,5 \cdot 0,2105)} = 73749 \text{ Nm}$$

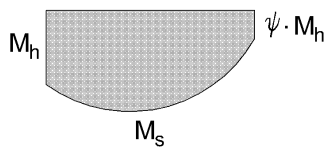
$$\frac{M_{Ed}}{M_{N,Rd}} = \frac{67530}{72618} = 0,92 \leq 1,0$$

Stability check for the beam according to section 6.3 of Eurocode 3:

$$\chi = \frac{1}{\Phi + \sqrt{\Phi^2 - \bar{\lambda}^2}} = \frac{1}{0,758 + \sqrt{0,758^2 - 0,613^2}} = 0,830$$

$$\text{Where:} \quad \Phi = 0,5 \cdot (1 + \alpha \cdot (\bar{\lambda} - 0,2) + \bar{\lambda}^2) = 0,5 \cdot (1 + 0,34 \cdot (0,613 - 0,2) + 0,613^2) = 0,758$$

$$\bar{\lambda} = \sqrt{\frac{A \cdot f_y}{F_{cr}}} = \sqrt{\frac{4332 \cdot 235}{2707860}} = 0,613$$



$$\alpha_h = M_h / M_s$$

$$C_{my} = 0,95 + 0,05 \cdot \alpha_h = 0,95 + 0,05 \cdot \frac{-67530}{74200} = 0,904 \text{ (see table 5.2)}$$

Stability check using $C_{my} = 0,904$:

$$k_{yy} = C_{my} \cdot \left(1 + (\bar{\lambda}_y - 0,2) \cdot \frac{N_{Ed}}{\chi_y \cdot N_{Rk} / \gamma_{M1}} \right) \leq C_{my} \cdot \left(1 + 0,8 \cdot \frac{N_{Ed}}{\chi_y \cdot N_{Rk} / \gamma_{M1}} \right) =$$

$$0,904 \cdot \left(1 + (0,613 - 0,2) \cdot \frac{7800}{0,830 \cdot (235 \cdot 4332) / 1} \right) \leq 0,904 \cdot \left(1 + 0,8 \cdot \frac{7800}{0,830 \cdot (235 \cdot 4332) / 1} \right) = 0,907$$

$$\frac{N_{Ed}}{\chi_y \cdot N_{Rk}} + k_{yy} \cdot \frac{M_{y,Ed}}{M_{y,Rk}} = \frac{7800}{0,830 \cdot (235 \cdot 4332)} + 0,907 \cdot \frac{74200}{(235 \cdot 310821)} = 0,93 \leq 1,0$$

Stability check using $C_{my} = 0,9$:

$$k_{yy} = C_{my} \cdot \left(1 + (\bar{\lambda}_y - 0,2) \cdot \frac{N_{Ed}}{\chi_y \cdot N_{Rk} / \gamma_{M1}} \right) \leq C_{my} \cdot \left(1 + 0,8 \cdot \frac{N_{Ed}}{\chi_y \cdot N_{Rk} / \gamma_{M1}} \right) =$$

$$0,9 \cdot \left(1 + (0,613 - 0,2) \cdot \frac{7800}{0,830 \cdot (235 \cdot 4332) / 1} \right) \leq 0,9 \cdot \left(1 + 0,8 \cdot \frac{7800}{0,830 \cdot (235 \cdot 4332) / 1} \right) = 0,903$$

$$\frac{N_{Ed}}{\chi_y \cdot N_{Rk}} + k_{yy} \cdot \frac{M_{y,Ed}}{M_{y,Rk}} = \frac{7800}{0,830 \cdot (235 \cdot 4332)} + 0,903 \cdot \frac{74200}{(235 \cdot 310821)} = 0,93 \leq 1,0$$

Cross section resistance check for the beam

$$\frac{V_{Ed}}{V_{pl,Rd}} = \frac{0}{139200} = 0,0 < 0,5 \quad \text{No reduction of the resistance for bending and axial force}$$

$$n = \frac{N_{Ed}}{N_{pl,Rd}} = \frac{13070}{1018020} = 0,0128$$

$$a = \frac{(A - 2 \cdot b \cdot t_f)}{A} = \frac{(4332 - 2 \cdot 180 \cdot 9,5)}{4332} = 0,2105$$

$$M_{N,Rd} = \frac{M_{pl,Rd} \cdot (1 - n)}{(1 - 0,5 \cdot a)} = \frac{73040 \cdot (1 - 0,0128)}{(1 - 0,5 \cdot 0,2105)} = 80585 \text{ Nm} \rightarrow \text{requirement: } M_{N,Rd} \leq M_{pl,Rd}$$

$$\frac{M_{Ed}}{M_{pl,Rd}} = \frac{74200}{73040} = 1,02 \geq 1,0$$